



5-2006

Adsorption of 2-Ketogluconate by Gibbsite, Goethite, and Kaolinite

Robert Maxwell Anderson III
University of Tennessee, Knoxville

Recommended Citation

Anderson, Robert Maxwell III, "Adsorption of 2-Ketogluconate by Gibbsite, Goethite, and Kaolinite." Master's Thesis, University of Tennessee, 2006.
https://trace.tennessee.edu/utk_gradthes/4525

This Thesis is brought to you for free and open access by the Graduate School at Trace: Tennessee Research and Creative Exchange. It has been accepted for inclusion in Masters Theses by an authorized administrator of Trace: Tennessee Research and Creative Exchange. For more information, please contact trace@utk.edu.

To the Graduate Council:

I am submitting herewith a thesis written by Robert Maxwell Anderson III entitled "Adsorption of 2-Ketogluconate by Gibbsite, Goethite, and Kaolinite." I have examined the final electronic copy of this thesis for form and content and recommend that it be accepted in partial fulfillment of the requirements for the degree of Master of Science, with a major in Environmental and Soil Sciences.

Michael E. Essington, Major Professor

We have read this thesis and recommend its acceptance:

Mark A. Radosevich, Neal S. Eash

Accepted for the Council:

Dixie L. Thompson

Vice Provost and Dean of the Graduate School

(Original signatures are on file with official student records.)

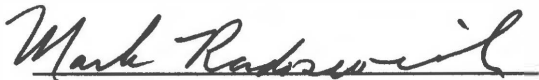
To the Graduate Council:

I am submitting herewith a thesis written by Robert Maxwell Anderson III entitled "Adsorption of 2-Ketogluconate by Gibbsite, Goethite, and Kaolinite." I have examined the final paper copy of this thesis for form and content and recommend that it be accepted in partial fulfillment of the requirements for the degree of Master of Science, with a major in Environmental Soil Science.

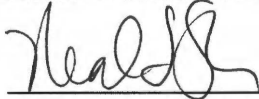


Michael E. Essington, Major Professor

We have read this thesis
and recommend it acceptance:



Mark A. Radosevich



Neal S. Eash

Accepted for the Council:



Vice Chancellor and
Dean of the Graduate Studies

AG-VET-MED.

Thesis
2006
.Ab3

Adsorption of 2-Ketogluconate by Gibbsite, Goethite, and

Kaolinite

A Thesis

Presented for the
Master of Science

Degree

The University of Tennessee, Knoxville

Robert Maxwell Anderson III

May 2006

Acknowledgements

First and foremost, I would like to acknowledge my Major Professor, Dr. Michael Essington, who taught me everything I know about soil chemistry. Thanks for everything Dr. Essington! I would also like to thank my other committee members, Dr. Neal Eash and Dr. Mark Radosevich, who had the time and patients to help with the final editing.

It is my pleasure to acknowledge my family, an unbelievable group of individuals: My grandfather and namesake Mac Anderson, who peacefully passed away during my time at The University of Tennessee; My grandmothers Dot Anderson and May Jones; My grandfather Ned Jones; My mom Jane Jones Pages; My dad Robert Anderson; My Brother Ned; My sisters Beth and Julie; and all of my cousins, uncles, aunts, step-family and in-laws.

Also, I must acknowledge my Knoxville crew, who shared with me their knowledge and love of The Great Smoky Mountains, and hundreds of miles of beautiful river. Thanks gentleman.

Dedication

I dedicate this Masters Thesis to my grandfather Neddo, Edward M. Jones, who taught me the value of family, of friends, of good food, and of wilderness and wildlife.

Abstract

In rhizosphere soil, the low-molecular mass organic acid (LMMOA) anions 2-ketogluconate (kG) is produced via microbial activity and exists in significant and sustained concentrations. One of the mechanisms in which this LMMOA anion may influence the chemistry of soil systems is through adsorption by constant-potential minerals. This study examines the adsorption of kG onto gibbsite, kaolinite and goethite in the presence or absence of phosphate (PO_4), arsenate (AsO_4) and sulfate (SO_4) as a function of pH and ionic strength. The adsorption of kG by gibbsite, goethite, and kaolinite is a function of solution pH and independent of solution ionic strength. The adsorption data supports the conclusion that kG is adsorbed by ligand exchange mechanisms. The adsorption of kG was decreased at all pH values in the presence of PO_4 and AsO_4 , and was not significantly affected by the presence of SO_4 at pH values above 6. The decrease in kG adsorption in the presence of AsO_4 and PO_4 is further evidence that kG is adsorbed via specific retention mechanisms. The addition of kG to gibbsite containing preadsorbed PO_4 did not result in PO_4 displacement, regardless of the concentration of kG. However, the addition of PO_4 to gibbsite containing preadsorbed kG resulted in the displacement of preadsorbed kG. These results indicate that kG is not held as strongly as PO_4 to gibbsite surfaces, and that the ability of PO_4 to displace adsorbed kG is greater than the ability of kG to displace adsorbed PO_4 . The adsorption of kG, PO_4 , AsO_4 , and SO_4 to gibbsite was modeled using the adsorption edge data and the CD-MUSIC surface complexation model. The kG adsorption data in both the 0.001 M and 0.01 M NaCl gibbsite systems were described by the formation of two monodentate-mononuclear inner-sphere complexes: $\equiv\text{AlkG}^{1/2-}$ and $\equiv\text{AlkGH}_1^{3/2-}$. Phosphate adsorption

by gibbsite was modeled by the formation of $\equiv\text{AlOPO}_3\text{H}^{3/2-}$ and $\equiv\text{AlOPO}_3\text{H}_2^{1/2-}$ in the low ionic strength systems (0.001 M NaCl), and by $\equiv\text{AlOPO}_3^{5/2-}$ and $\equiv\text{AlOPO}_3\text{H}_2^{1/2-}$ in the high ionic strength systems (0.01 M NaCl). Arsenate adsorption by gibbsite in both ionic strengths was modeled using the $\equiv\text{AlOAsO}_3^{5/2-}$ and $\equiv\text{AlOAsO}_3\text{H}_2^{1/2-}$ inner-sphere surface complexes. Sulfate adsorption was described by the formation of the outer-sphere $\equiv\text{AlOH}_2^{1/2+}\text{--SO}_4^{2-}$ species. The adsorption of kG by goethite in both the 0.001 M and 0.01 M NaCl systems was best described by the formation of the monodentate-mononuclear and bidentate-binuclear inner-sphere surface complexes: $\equiv\text{Fe}_2\text{kGH}_1^{1/2-}$ and $\equiv\text{Fe}_2\text{kGH}_1$. Both PO_4 and AsO_4 were completely adsorbed by goethite; therefore, chemical adsorption models could not be derived. However, SO_4 adsorption by goethite was described with the $\equiv\text{FeOH}_2^{1/2+}\text{--SO}_4^{2-}$ species. The chemical models and associated intrinsic equilibrium constants developed for ligand adsorption from the single ligand systems were employed to predict ligand retention in the kaolinite and binary ligand systems. In general, particularly at pH values greater than 7, the predicted adsorption behavior did not adequately predict the experimental adsorption data in the gibbsite or kaolinite systems. This finding suggests that the surface complexation reactions derived for pH >7 systems may have been incorrect. The adsorption behavior kG establishes the potential for this ligand to significantly impact rhizosphere chemistry. Ketogluconate is specifically retained by common soil minerals and may impact the phytoavailability of PO_4 and other specifically-retained ligands in the rhizosphere.

Table of Contents

Chapter	Page
I. Introduction	1
II. Material and Methods	26
Preparation of Solids	26
Preparation of Solutions	29
Adsorption Studies	29
Gibbsite Pretreated Ligand Adsorption Experiments	32
Data Analysis	33
Surface Complexation Modeling	34
III. Results and Discussion	40
Gibbsite	40
Effect of pH and Ionic Strength	40
Effects of Inorganic Ligands on 2-Ketogluconate Adsorption	47
Effect of 2-Ketogluconate on the Adsorption of Phosphate, Arsenate and Sulfate Adsorption	50
Effects of 2-Ketogluconate on Preadsorbed Phosphate	54
Effects of Phosphate on Preadsorbed 2-Ketogluconate	54
Surface Complexation Modeling	57
Predicting the Adsorption of Ligands in Binary Systems	69
Kaolinite	78
Effect of pH and Ionic Strength	78

Effects of Inorganic Ligands on 2-Ketogluconate Adsorption	83
Effect of 2-Ketogluconate on the Adsorption of Phosphate, Arsenate and Sulfate Adsorption	87
Surface Complexation Modeling	87
Goethite	102
Effect of pH and Ionic Strength	102
Effects of Inorganic Ligands on 2-Ketogluconate Adsorption	104
Surface Complexation Modeling	107
IV. Summary	112
V. Conclusions	119
References	120
VITA	131

List of Tables

Table	Page
1. Volumes and concentrations of HCl and NaOH pH adjustment solutions used to establish the adsorption edge of 2-keto-D-gluconate, phosphate, arsenate, and sulfate	31
2. Formation constants for aqueous species used to model kG, PO ₄ , AsO ₄ , and SO ₄ adsorption by gibbsite, kaolinite, and goethite in 0.001 and 0.01 M NaCl	35
3. CD-MUSIC model parameters used to develop chemical models of kG, PO ₄ , AsO ₄ , and SO ₄ adsorption by gibbsite, goethite and kaolinite surfaces	36
4. Surface protonation and counter ion retention reactions and associated equilibrium constants	37
5. Gibbsite surface complexation reactions, FITEQL-optimized intrinsic equilibrium constants (log K values), and associated goodness-of-fit parameters (WSOS/DF values)	60
6. Goodness-of-fit prediction values (WSOS/DF) for binary system adsorption to gibbsite	74
7. Goodness-of-fit parameters (WSOS/DF values) for ligand adsorption to kaolinite	90
8. Goethite surface complexation reactions, FITEQL-optimized intrinsic	

equilibrium constants (log K values), and associated goodness-of-fit
parameters (WSOS/DF values)

111

List of Figures

Figure	Page
1. Molecular structure of 2-keto-D-gluconate with numbered carbon atoms	7
2. The concentration of positive ($\equiv\text{AlOH}_2^{+0.5}$) and negative ($\equiv\text{AlOH}^{-0.5}$) charged surface sites on gibbsite as a function of pH	13
3. Representation of the singly- (Type A), doubly- (Type C), and triply-(Type B)coordinated surface functional groups on the goethite	16
4. A microscopic view of the solid-solution interface	20
5. Representation of the gibbsite surface that illustrates the Type A and Type C surface hydroxyls	22
6. Representation of the kaolinite surface that illustrates the Type A, Type C and Type B silanol and aluminol surface functional groups	23
7. The adsorption edge of 2-ketogluconate (kG) on gibbsite in 0.01 and 0.001 <i>M</i> NaCl	41
8. The adsorption edge of phosphate (PO_4) on gibbsite in 0.01 and 0.001 <i>M</i> NaCl	43
9. The adsorption edge of arsenate (AsO_4) on gibbsite in 0.01 and 0.001 <i>M</i> NaCl	44
10. The adsorption edge of sulfate (SO_4) on gibbsite in 0.01 and 0.001 <i>M</i> NaCl	46
11. The adsorption of ketogluconate (kG) to gibbsite in 0.001 <i>M</i> NaCl in the presence and absence of AsO_4 , PO_4 , and SO_4	48

12. The adsorption of ketogluconate (kG) to gibbsite in 0.01 <i>M</i> NaCl in the presence and absence of AsO ₄ , PO ₄ , and SO ₄	49
13. The effect of ketogluconate (kG) on the adsorption of AsO ₄ , PO ₄ , and SO ₄ to gibbsite in 0.01 <i>M</i> NaCl	51
14. The effect of ketogluconate (kG) on the adsorption of AsO ₄ , PO ₄ , and SO ₄ to gibbsite in 0.001 <i>M</i> NaCl	52
15. The effect of ketogluconate (kG) in the displacement of phosphate (PO ₄) from gibbsite in 0.01 <i>M</i> NaCl	55
16. The effect of phosphate (PO ₄) in the displacement of ketogluconate (kG) from gibbsite in 0.01 <i>M</i> NaCl	56
17. Ketogluconate surface complexes considered in the modeling and charge distribution at the solid-solution interface	58
18. The predicted and experimentally-determined adsorption of ketogluconate (kG) by gibbsite in 0.001 <i>M</i> NaCl	61
19. The predicted and experimentally-determined adsorption of ketogluconate (kG) by gibbsite in 0.01 <i>M</i> NaCl	62
20. The predicted and experimentally-determined adsorption of phosphate (PO ₄) by gibbsite in 0.001 <i>M</i> NaCl	64
21. Phosphate, arsenate, and sulfate modeled surface complexes and charge distribution at the solid-solution interface	65
22. The predicted and experimentally-determined adsorption of phosphate (PO ₄) by gibbsite in 0.01 <i>M</i> NaCl	66

23. The predicted and experimentally-determined adsorption of arsenate (AsO ₄) by gibbsite in 0.001 <i>M</i> NaCl	67
24. The predicted and experimentally-determined adsorption of arsenate (AsO ₄) by gibbsite in 0.01 <i>M</i> NaCl	68
25. The predicted and experimentally-determined adsorption of sulfate (SO ₄) by gibbsite in 0.001 <i>M</i> NaCl	70
26. The predicted and experimentally-determined adsorption of sulfate (SO ₄) by gibbsite in 0.01 <i>M</i> NaCl	71
27. The predicted and experimentally-determined adsorption of ketogluconate (kG) and phosphate (PO ₄) by gibbsite (binary system) in 0.001 <i>M</i> NaCl	73
28. The predicted and experimentally-determined adsorption of ketogluconate (kG) and phosphate (PO ₄) by gibbsite (binary system) in 0.01 <i>M</i> NaCl	75
29. The predicted and experimentally-determined adsorption of ketogluconate (kG) and sulfate (SO ₄) by gibbsite (binary system) in 0.001 <i>M</i> NaCl	76
30. The predicted and experimentally-determined adsorption of ketogluconate (kG) and sulfate (SO ₄) by gibbsite (binary system) in 0.01 <i>M</i> NaCl	77
31. The adsorption edge of 2-ketogluconate (kG) on kaolinite in 0.01 and 0.001 <i>M</i> NaCl	79
32. The adsorption edge of phosphate (PO ₄) on kaolinite in 0.01 and 0.001	

<i>M</i> NaCl	81
33. The adsorption edge of arsenate (AsO ₄) on kaolinite in 0.01 and 0.001 <i>M</i> NaCl	
<i>M</i> NaCl	82
34. The adsorption edge of sulfate (SO ₄) on kaolinite in 0.01 and 0.001 <i>M</i> NaCl	
NaCl	84
35. The adsorption of ketogluconate (kG) to kaolinite in 0.001 <i>M</i> NaCl in the presence and absence of AsO ₄ , PO ₄ , and SO ₄	85
36. The adsorption of ketogluconate (kG) to kaolinite in 0.01 <i>M</i> NaCl in the presence and absence of AsO ₄ , PO ₄ , and SO ₄	86
37. The effect of ketogluconate (kG) on the adsorption of AsO ₄ , PO ₄ , and SO ₄ to kaolinite in 0.01 <i>M</i> NaCl	88
38. The effect of ketogluconate (kG) on the adsorption of AsO ₄ , PO ₄ , and SO ₄ to kaolinite in 0.001 <i>M</i> NaCl	89
39. The predicted and experimentally-determined adsorption of ketogluconate (kG) by kaolinite in 0.01 <i>M</i> NaCl	92
40. The predicted and experimentally-determined adsorption of phosphate (PO ₄) by kaolinite in 0.001 <i>M</i> NaCl	93
41. The predicted and experimentally-determined adsorption of arsenate (AsO ₄) by kaolinite in 0.001 <i>M</i> NaCl	94
42. The predicted and experimentally-determined adsorption of arsenate (AsO ₄) by kaolinite in 0.01 <i>M</i> NaCl	95
43. The predicted and experimentally-determined adsorption of sulfate (SO ₄) by kaolinite in 0.001 <i>M</i> NaCl	97

44. The predicted and experimentally-determined adsorption of sulfate (SO ₄) by kaolinite in 0.01 <i>M</i> NaCl	98
45. The predicted and experimentally-determined adsorption of 2-ketogluconate (kG) and phosphate (PO ₄) by kaolinite in 0.001 <i>M</i> NaCl	99
46. The predicted and experimentally-determined adsorption of 2-ketogluconate (kG) and sulfate (SO ₄) by kaolinite in 0.001 <i>M</i> NaCl	100
47. The predicted and experimentally-determined adsorption of 2-ketogluconate (kG) and sulfate (SO ₄) by kaolinite in 0.01 <i>M</i> NaCl	101
48. The adsorption edge of 2-ketogluconate (kG) on goethite in 0.01 and 0.001 <i>M</i> NaCl	103
49. The adsorption of ketogluconate (kG) to goethite in 0.001 <i>M</i> NaCl in the presence and absence of AsO ₄ , PO ₄ , and SO ₄	105
50. The adsorption of ketogluconate (kG) to goethite in 0.01 <i>M</i> NaCl in the presence and absence of AsO ₄ , PO ₄ , and SO ₄	106
51. The predicted and experimentally-determined adsorption of ketogluconate (kG) by goethite in 0.001 <i>M</i> NaCl	108
52. The predicted and experimentally-determined adsorption of ketogluconate (kG) by goethite in 0.01 <i>M</i> NaCl	109

I. Introduction

In soils, low-molecular-mass-organic-acid (LMMOA) anions are comprised of a group of water-soluble non-humic substances with an arbitrary maximum molecular weight of approximately 300 to 500 D, and include oxalate, formate, citrate, acetate, malate, and succinate (Essington, 2003; Strobel, 2001; van Hees et al., 2003). These compounds are principally plant root and microbial exudates (and their derivatives), which are concentrated in the volume of soil immediately surrounding and adjacent to plant roots, (rhizosphere soil) and the microenvironment surrounding soil microbes. In the rhizosphere, LMMOA anions are constantly consumed and produced by numerous plant and microbial species. However, they may be found in significant and sustained concentrations (0.1-100 μ M) in these soil solutions (Jones, 1998). Organic acid anions have been hypothesized to play a major role in many soil processes, including soil mineral solubilization (Sulyok et al., 2005; Essington et al., 2005; Horányi, 2002; Filius et al., 1997), nutrient and metal mobility and bioavailability (Jones, 1998), metal detoxification (Jiang et al., 2005; Schwab et al., 2005; Sulyok et al., 2005; Jones et al., 2002; Sulyok et al., 2005), and in soil structural development (Jones et al., 2002; Sulyok et al., 2005).

Both plant roots and soil microbes are capable of exuding elevated concentrations of LMMOA anions, and at elevated rates, when stressed for specific mineral nutrients (e.g., phosphorus [P], iron [Fe], and manganese [Mn]), and when soil aluminum [Al] concentrations reach potentially phytotoxic levels (Sulyok et. al. 2005; Jones et. al. 2002;

Jones 1998). For example, in P deficient conditions, the rate of malate and citrate exudation from specific plant species (e.g., *Lupinus albus*, and *Brassica napus*) has been shown to increase significantly over that when P concentrations are within an optimal range for bioavailability, thus hastening P solubilization (Jones, 1998). Similarly, Jones (1998) noted that under conditions of Al toxicity, the roots of wheat, snapbean, and maize have been found to excrete elevated concentrations of malate or citrate into the rhizosphere. He suggested that the organic acids form stable aqueous complexes with Al, which renders the plant roots 5-20 times more resistant to the toxic effects of Al.

Organic acids released by plants and microbes can influence soil chemical processes via two principle mechanisms; metal complexation and competitive adsorption. The process of adsorption is a surficial process in which a dissolved substance (adsorptive) accumulates at reactive surface sites of a solid phase (adsorbent). Since all adsorption processes are also exchange processes, adsorption results in the displacement of an adsorbate (Essington, 2003). Adsorption can be represented quantitatively through both mechanistic and nonmechanistic approaches. Nonmechanistic approaches are often used to obtain compound-specific adsorption parameters that can be used to describe adsorption under specific environmental conditions (Essington, 2003). These approaches describe the mass distribution of an adsorbate between solid and solution phases at equilibrium. The distribution of a substance between soil solid and solution phases can be characterized by the distribution coefficient, K_d :

$$K_d = q/C_{eq} \quad [1]$$

where q is the mass of adsorbed substance per unit mass of adsorbent (in mmolkg^{-1}) and C_{eq} is the mass of adsorptive per unit volume in the equilibrium solution (in mmolL^{-1})

(Essington 2003). The variation of K_d with C_{eq} or q can be described mathematically to characterize the adsorption behavior of a substance through an adsorption isotherm model. Adsorption isotherms are commonly employed to delineate the relative affinity of a substance for a solid; however, no inferences as to mechanisms (i.e., the chemical reactions involved) can be made (Essington, 2003).

Experimental techniques to elucidate adsorption mechanisms typically involve the characterization of adsorption envelopes, where q is characterized as a function of solution pH and ionic strength. The q vs. pH adsorption envelopes may then be employed to develop a chemical model, which is a series of chemical reactions involving specific surface functional groups and specific aqueous species of the adsorbate. Each reaction may then be characterized by an equilibrium constant (Essington, 2003).

Ligands in the soil solution can adsorb to constant-potential mineral surface sites, through specific (inner-sphere or chemisorption) or non-specific (outer-sphere or physical adsorption) mechanisms. Constant potential minerals are those that generate charge deficit and/or excess at surface hydroxyl functional groups via protonation and deprotonation reactions, such as gibbsite, goethite, and kaolinite. Ligands that bond directly to a mineral through the displacement of surface bound H_2O or OH^- are said to be specifically adsorbed. This process is termed ligand exchange. Non-specifically-adsorbed ligands are those that are electrostatically adsorbed at protonated surface oxygens. This process is termed anion exchange. Generally speaking, ligands that can participate in ligand exchange processes (chemisorption) at mineral surfaces (e.g., AsO_4 and PO_4 species) are weak Lowry-Brönsted acid anions, and ligands that principally participate in anion exchange (physical adsorption) at mineral surfaces (e.g., SO_4^{2-} , NO_3^-

and Cl) are strong acid anions. Specifically-adsorbed substances may also participate in non-specific adsorption, while most non-specifically-adsorbed ligands do not form inner-sphere surface complexes.

The adsorption of LMMOA anions, such as citrate, malate, succinate, and oxalate by soil minerals has been investigated in a number of studies (Evanko and Dzombak, 1999; Filius et al., 1997; Horányi, 2002; Lackovic et al., 2003; Jones, 1998). It has been shown that these organic anions, and other di- and tri-carboxylates, participate in ligand exchange reactions on constant potential mineral surfaces. These organic ligands may effectively compete with other specifically adsorbed ligands (e.g., PO₄ species) and subsequently increase the phytoavailability of the displaced species (Huang et al., 2003; Haynes and Mokolobate, 2000; Jones, 1998).

The impact of LMMOA anions on soil properties can be attributed partly to the number, type, and position of reactive functional groups on the different carbon backbone structures (Evanko and Dzombak, 1998). For example, organic acid anions containing more than one carboxyl functional group, such as malate, citrate, and oxalate, have a higher affinity for trivalent metals and have a greater ability to complex metal cations than do anions with only one carboxyl group, such as lactate, formate, and acetate (Jones, 1998). The retention and mobility of organic acids in the soil environment is determined by the ionization of organic moieties and charge formation on mineral surfaces. Negative charge formation on organic acids allows for complexation of metal cations in solution (e.g., Al³⁺ or Fe³⁺), and for the displacement of adsorbed ligands, such as OH⁻, H₂O, and HPO₄²⁻ or H₂PO₄⁻.

Low-molecular-mass-organic-acid anions enhance mineral dissolution through aqueous chelation of metal cations (e.g., citrate). Complexation of metal cations by organic acids can alter metal adsorption behavior by forming soluble complexes, and enhance metal solubility and mineral dissolution rates (Jones, 1998; Blake and Walter, 1996). These complexes may be more or less attracted to mineral surfaces than the free metal cation (Essington, 2003). For example, citrate and malate have been found to mobilize significant amounts of P (Jones et al., 2002). Similar cases for organic acid mediated enhancement of metal mobilization and solubility has been established for Fe, Zn, and Cu (Jones et al., 2002). Wang et al. (2005) found that the rate of kaolinite dissolution was increased to the greatest degree by oxalate followed by citrate and malate. Increased soil solution concentrations of di- or tricarboxylate LMMOA anions have also been found to enhance phosphate dissolution, rendering a 10-1000-fold increase in soil solution P concentrations (Jones, 1998).

Competition for mineral surface sites between ligands with similar adsorption mechanisms influences both the composition of the surface sites and the soil solution. For example, citrate, oxalate, and malate adsorb to constant potential mineral surface sites through similar adsorption mechanisms. Further, they displace adsorbed PO_4 species and prevent the adsorption of added PO_4 (Jones, 1998). Hu et al. (2001), found that the adsorption of PO_4 species by constant-potential mineral surfaces was reduced when oxalate or citrate were present, resulting in an increase of PO_4 in solution relative to that found in the absence of the organic acids.

Numerous LMMOA anions are present in rhizosphere soils. Yet, only a small number have been examined relative to their impacts on soil chemical processes. 2-

Ketogluconate (kG) (Figure 1) is a LMMOA that is a microbial byproduct of glucose oxidation. It is produced by several species known to exist in soils, including *Klebsiella*, *Pseudomonas*, *Bacillus*, *Streptomyces*, *Aerobacter*, and *Acetobacter* (Klassen, 1992). Several kG producers have been isolated from the rhizosphere of common crops, including wheat, corn, and peas (Moghimi and Tate, 1978). Duff and Webley (1965) found kG in highest concentrations in agricultural soils, particularly in well-drained soils receiving heavy and recent manure applications. Neijssel and Tempest (1975) found that *Klebsiella aerogenes* converted glucose to kG at an increased rate when P was limiting. The increase in kG production rate also resulted in increased P solubilization.

The carboxyl-group of kG is a relatively strong weak acid ($pK_a=3.00$, Figure 1) (Nelson and Essington, 2005). It has also been suggested that the carbonyl on the number two carbon is sufficiently electronegative to promote the dissociation of the alcohol group on the number three carbon ($pK_a=11.98$) (Nelson and Essington, 2005). In typical soil solutions (pH 4 to 9 range), kG is predicted to predominately exist as a monovalent anion.

2-Ketogluconate has been shown to enhance the solubilities of calcium phosphate, gibbsite, and goethite. Halder and Chakrabarty (1993) found that the solubility of hydroxyapatite [$Ca_5(PO_4)_3OH$] was directly related to the solution concentration of kG. Duff and Webley (1959) suggested that kG was a strong chelating agent for the Ca^{2+} ion, promoting the dissolution of calcium phosphates. Moghimi and Tate (1978) also found that kG was effective in dissolving calcium phosphates, including hydroxyapatite, but much less effective than acetate, citrate, or the synthetic chelate EDTA (ethylenediaminetetraacetic acid). Moghimi and Tate (1978) postulated that the

2-Keto-D-gluconate

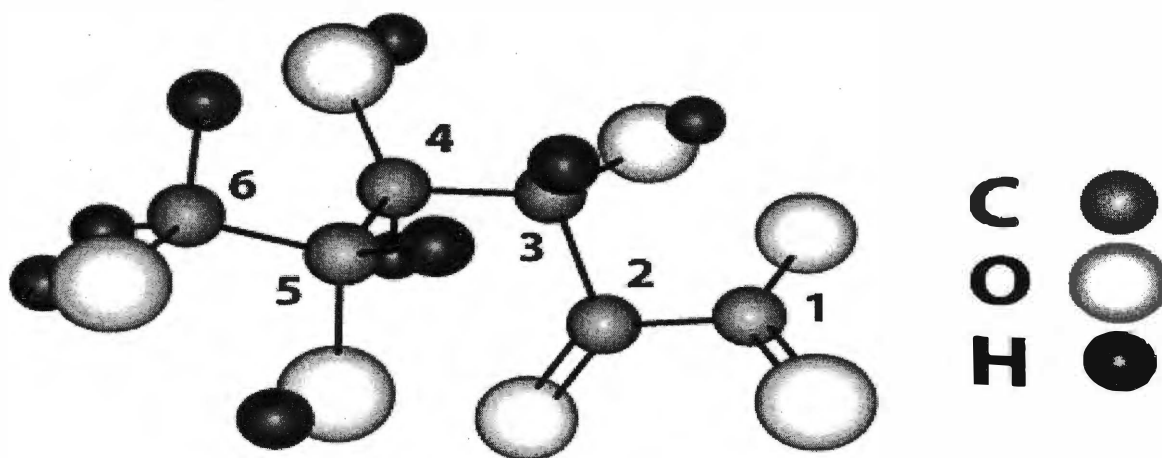


Figure 1. Molecular structure of 2-keto-D-gluconate with numbered carbon atoms.

dissolution of Ca-phosphate in the presence of kG was controlled by proton attack rather than through the chelation of Ca^{2+} ions. They were also the first to confirm kG to be one of the stronger monobasic carboxylic acids with a pK_a value of 2.8 at 25°C. Essington et al. (2005) found kG to have a significant and direct impact on the solubility of gibbsite $[\text{Al}(\text{OH})_3]$ and goethite $[\text{FeOOH}]$. They explained the increased solubility by predicting that Al^{3+} and Fe^{3+} form soluble complexes with kG. From the magnitude of the formation constants, Essington et al. (2005) suggested that kG forms bidentate aqueous complexes with both Al^{3+} and Fe^{3+} , while forming monodentate complexes with Al^{3+} only at $\text{pH} < 4.3$. The apparent formation of inner-sphere aqueous complexes of kG with Al^{3+} and Fe^{3+} may also indicate that kG adsorption to gibbsite $[\text{Al}(\text{OH})_3]$ and goethite $[\text{FeOOH}]$ involves inner-sphere mechanisms.

Citric acid, a well-documented chelate, has been shown in several studies to be capable of inner-sphere adsorption to constant potential mineral surfaces through ligand exchange (Lackovic et al., 2003; Evanko and Dzombak, 1999; Filius et al., 1997). Filius et al. (1997) found that the most important species in describing citrate, lactate, and malonate adsorption to goethite is the bidentate inner-sphere species through uncomplexed carboxylate groups. Indeed, the predicted bimolecular-bidentate adsorption nature of dicarboxylates to mineral surfaces is common to several organic acids (Filius et al., 1997; Evanko and Dzombak, 1999). Based on the predicted bidentate nature of aqueous Al^{3+} - and Fe^{3+} -kG complexes, the potential for kG to adsorb by similar mechanisms to gibbsite and goethite should also be considered. However, the adsorption of dicarboxylates (e.g., citrate) has also been modeled by assuming monodentate and

bidentate outer-sphere complexes (Filius et al., 1997; Lackovic et al., 2003), and monodentate inner-sphere species (Filius et al., 1997; Rosenqvist et al., 2003).

As mentioned previously, several LMMOA anions have been shown to specifically interact with constant potential mineral surfaces through ligand exchange. Knowledge of the chemical mechanisms behind the interactions of these organic anions with soil minerals has allowed researchers to examine rhizosphere processes that impact the phytoavailability of nutrients and toxins (Jones 1998). It has been shown that kG affects the solubility of calcium phosphates, as well as gibbsite and goethite, via aqueous metal complexation reactions. Determination of adsorption mechanisms of kG, as well as its ability to compete with other ligands for mineral surface sites, is also required in order to understand and predict the impact of this ligand on rhizosphere processes.

The adsorption behavior of kG in the presence of arsenate (AsO_4), phosphate (PO_4), and sulfate (SO_4) may be used to infer the adsorption mechanisms of kG. It has been well established that PO_4 and AsO_4 are specifically adsorbed by Al, Fe, and Mn hydrous oxides, hydroxides, and oxyhydroxides (collectively termed hydrous oxides) (Violante and Pigna, 2002). In contrast, SO_4 has been shown to principally participate in non-specific adsorption to hydrous oxide surfaces (He et al., 1997; Wijnja et al., 2000). Comparisons of kG adsorption behavior in the presence and absence of the PO_4 , AsO_4 , and SO_4 oxyanions may provide evidence for determining if the kG adsorption mechanism is principally chemisorption or physical adsorption, and further to provide the data necessary to develop chemical models of surface complexation.

The fate and mobility of PO_4 and AsO_4 , as well as the effect of LMMOA anions on their adsorption to hydrous oxide surfaces, is pertinent to maintaining and protecting

soil-water-plant systems (Violante and Pigna, 2002; Wijnja et al., 2000; Wijnja et al., 2002). For instance, arsenic is a ubiquitous contaminant and is highly toxic to humans, animals, and plants (Chen et al., 2004; Violante and Pigna, 2002). The fate and mobility of AsO_4 in the environment has become of increasing concern as their occurrence in soil-water-plant systems has increased and has proven to be problematic (Chen et al., 2004; He and Zhu, 1998; Weerasooriya et al., 2003). The interactions of LMMOA anions with AsO_4 may impact the retention and mobility of this pollutant in soil and water systems and, therefore, warrants investigation.

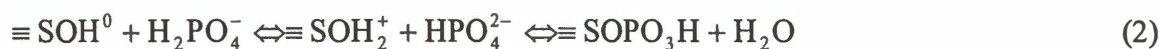
One of the common limitations in crop production is low phytoavailable P. In general, bioavailable soil P levels must be elevated through fertilizer additions to exceed P retention and to achieve maximum crop yield potentials (Haynes and Mokolobate, 2001). Low P availability can be attributed to both the low solubility of phosphate minerals, as well as to the high adsorption capacity of hydrous oxide minerals. The specific adsorption of organic acids that are exuded by plant roots and microbes in the rhizosphere may act to increase the phytoavailability of P (Haynes and Mokolobate, 2001). Analysis of the competitive adsorption behavior of kG in the presence or absence of PO_4 , as well as that of PO_4 in the presence or absence of kG, is critical for determining the retention mechanisms of kG, as well as in determining the impact of kG on PO_4 behavior.

The capacity of LMMOA anions to influence mineral dissolution and adsorbed phase composition can be attributed to the ability of organic anions to complex metal cations (Kwong and Huang, 1979; Essington, 2003). The mechanisms of interaction of a ligand with a mineral surface may be inferred through experimental observation. Two

master variables that affect ligand retention to mineral surfaces are the solution pH and ionic strength. The pH dictates the ionization of mineral surfaces and ligand dissociation, both of which are processes that influence ligand retention. For instance, the nonspecific (outer-sphere) adsorption of a SO_4^{2-} ion to gibbsite and kaolinite is a direct result of positive charge formation on the mineral surfaces (Essington, 2003). The adsorption of SO_4^{2-} decreases with the concomitant increase in pH and negative surface charge (He et al., 1997).

The background electrolyte used in an adsorption study also influences charge formation and ligand adsorption on mineral surface sites. Changing the concentration of the background electrolyte (ionic strength) affects the activity of the adsorbing species, and the competition of the background electrolyte and adsorbate anions for available surface sites (Hayes et al., 1988). Outer-sphere adsorbed ions are expected to be more sensitive to ionic strength variation than inner-sphere adsorbed ions since electrolyte ions and outer-sphere adsorbed ions compete in the same adsorption plane on constant potential mineral surfaces (Hayes et al., 1988). Background electrolytes that are known to participate entirely in outer-sphere adsorption (such as NaCl), contribute to charge formation only on outer-sphere surface sites. Thus, increasing the ionic strength of NaCl will affect the adsorption of ligands that participate in outer-sphere adsorption mechanisms. Therefore, adsorbates that display adsorption envelopes (q vs. pH) that are independent of ionic strength are interpreted to indicate relatively strongly bonded surface complexes and specific (nonelectrostatic) adsorption mechanisms (Hayes et al., 1988; Essington, 2003). Also, ligand adsorption that exceeds the net positive charge created by the mineral surface, an adsorption maximum or an inflection in the adsorption

envelope that occurs when the pH is close to the pK_a of the ligand adsorbate, and adsorption that is influenced by other specifically adsorbed species are all indicators of specific surface interactions (Essington, 2003). The adsorption of polyprotic acid anions (e.g., AsO_4 and PO_4 species) is at a maximum at low pH values, and an inflection in the adsorption envelope is observed when the pH approaches the pK_a of a deprotonation reaction. For example, the reaction $H_2PO_4^- = HPO_4^{2-} + H^+$ has a pK_{a2} of 7.1. The dissociation of $H_2PO_4^-$ releases protons that form H_2O on the mineral surface, which is then displaced by HPO_4^{2-} , as described by the reactions:



At pH values above the pK_{a2} , the HPO_4^{2-} species dominates and can not provide protons to promote H_2O formation on the surface. Thus, adsorption decreases with further increases in pH above pK_{a2} and an inflection in the adsorption envelope is observed at approximately pH 7.1. The decrease in PO_4 adsorption occurs at pH values above pK_{a2} also occurs due to a decrease in the concentration of positively charged surface sites (Figure 2).

Ligand adsorption that is influenced by the presence of other specifically adsorbed species is strong evidence that the ligand participates in specific adsorption mechanisms. For example, AsO_4 and PO_4 have similar chemical properties (e.g., they are both group V elements) and have both been shown to adsorb specifically to constant potential mineral surface sites (Gao and Mucci, 2001; Violante and Pigna, 2002). Gao and Mucci (2001) found that the adsorption of AsO_4 was decreased in proportion to the amount of PO_4 present (the opposite was also true, but to a lesser extent). The

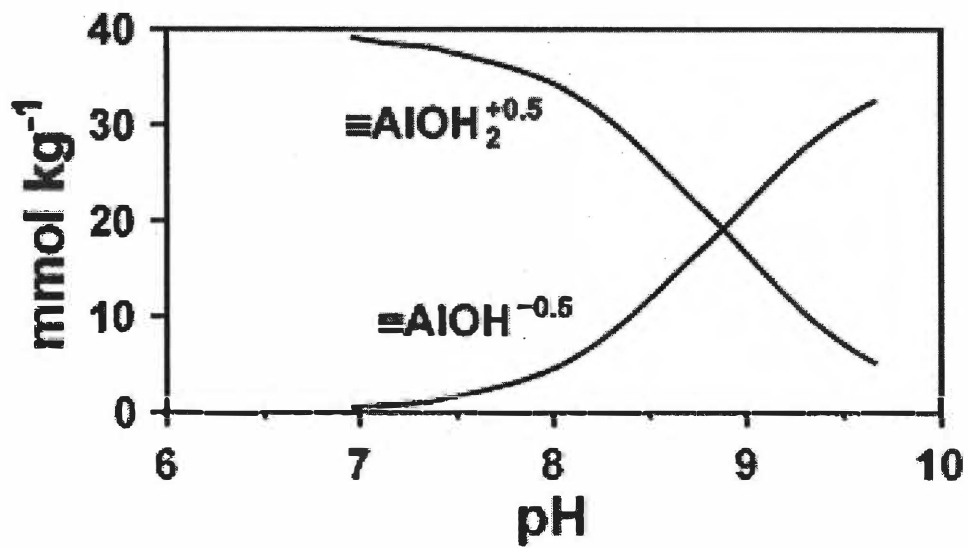


Figure 2. The concentration of positive ($\equiv\text{AlOH}_2^{+0.5}$) and negative ($\equiv\text{AlOH}^{-0.5}$) charged surface sites on gibbsite as a function of pH (From Essington, 2003.)

reversibility of adsorption (desorption) can also indicate adsorption mechanisms. Outer-sphere, electrostatic retention of a substance is easily reversible; whereas, inner-sphere adsorption is apparently irreversible, suggesting a high degree of metal-ligand interaction and covalent bonding (Hayes et al, 1988)

Adsorption is a complex process that involves physical, chemical, and electrostatic interactions at adsorbent surfaces. The complexity of adsorption processes at the solid-solution interface has necessitated the creation and application of several physical models that simplify the solid-solution interface in an attempt to explain and predict adsorption behavior (Sakar et al., 2000). These models are generally termed surface complexation models (SCMs) and can be used to interpret adsorption envelopes and predict the chemical reactions that result in adsorption. Surface complexation models are mechanistic models that vary according to how they conceptualize charge distribution and surface potentials, and the location of adsorbed species in the solid-solution interface (the transition zone between mineral phase and bulk solution) (Goldberg, 1992).

In order to successfully develop and employ SCMs, knowledge of the properties of the mineral surfaces, aqueous speciation, and the specific chemical reactions that are responsible for compound adsorption must be stipulated. A chemical model of the system is represented by several mass-balance and mass-action expressions to include all species in the system. Surface complexation models all share a set of assumptions and common characteristics that describe the solid-solution interface (Goldberg, 1992). First, mineral surfaces are assumed to contain one or more well-defined surface functional groups. It is at these specific surface sites that ligands can specifically adsorb to the mineral by

binding to one or more of the mineral's structural metals. Singly-, doubly-, and triply-coordinated surface functional groups may occur, and are defined by the number of structural metals attached to a single surface ligand (Figure 3). Another common attribute of SCMs is that the site density can be found for each type of surface functional group, and the total concentration of sites can be computed. Thirdly, mechanistic models consider the free energy change of adsorption (ΔG°_{ads}) to be composed of intrinsic (chemical) and coulombic (electrostatic) free energy terms. This can be represented by

$$\Delta G^{\circ}_{ad} = \Delta G^{\circ}_{int} + \Delta G^{\circ}_{coul} \quad [3]$$

The right side of the Eq. [3] illustrates the dependence of adsorption on the composition of the environment in which adsorption occurs (Tadanier and Eick, 2002). The intrinsic free energy term (ΔG°_{int}) is the chemical component that represents the chemical energy change that occurs as a result of the adsorption reaction. The coulombic term (ΔG°_{coul}) represents the electrostatic work associated with the movement of ions from bulk solution to the mineral surface:

$$\Delta G^{\circ}_{coul} = F\Delta Z\psi_0 \quad [4]$$

where G is in units of kJ mol^{-1} , F is the Faraday constant ($96,485 \text{ C mol}^{-1}$), ΔZ is the net change in surface charge due to adsorption, and ψ_0 (in V) is the relative surface potential (Goldberg, 1992; Tadanier and Eick, 2002). For each adsorption reaction, a conditional adsorption constant (varies with ionic strength and the composition of the adsorbed phase) K_{ads} can be found that describes the reaction. The K_{ads} is a product of the intrinsic (K_{int}) and coulombic (K_{coul}) constants:

$$K_{ads} = K_{int} K_{coul} \quad [5]$$

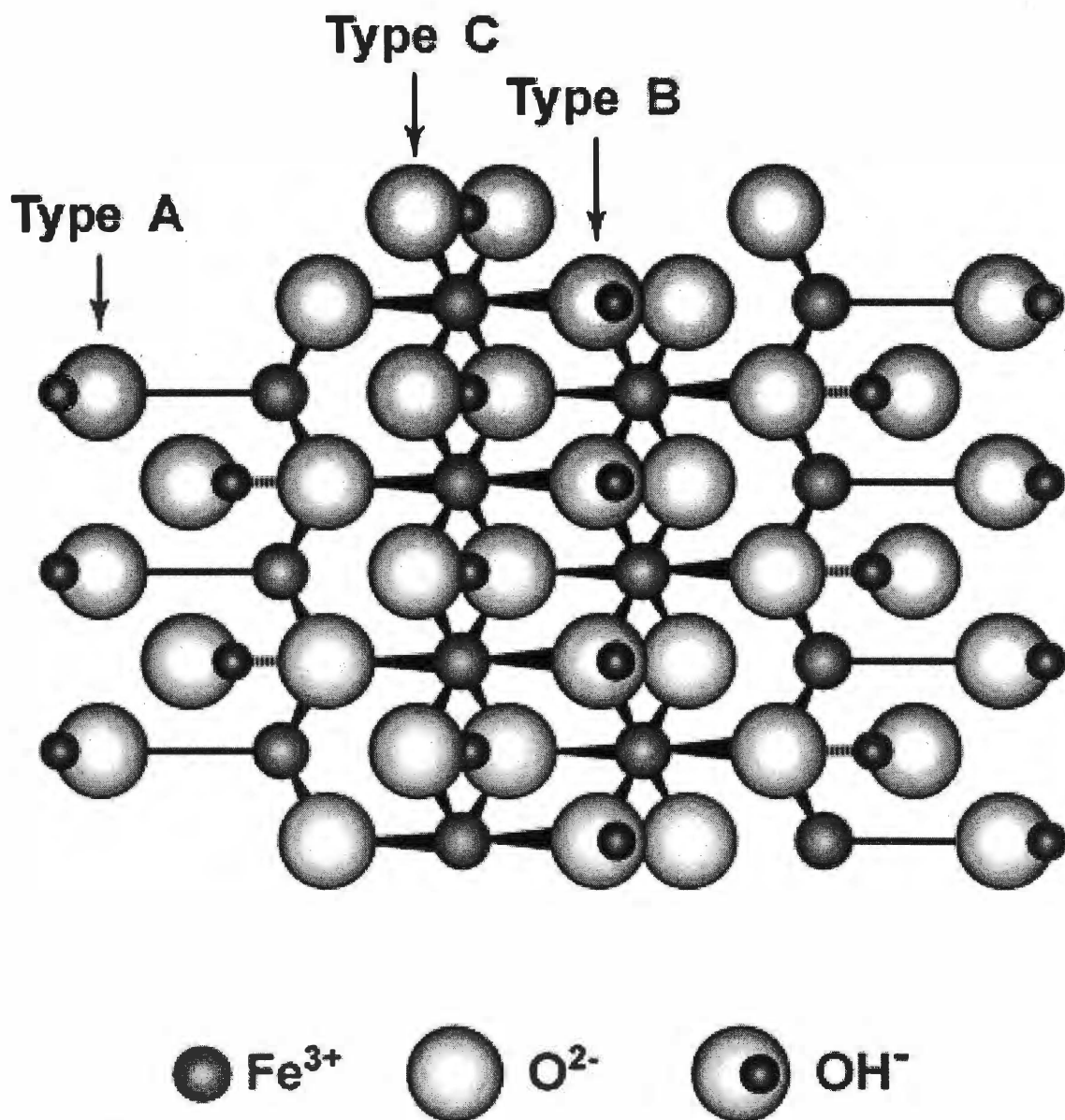


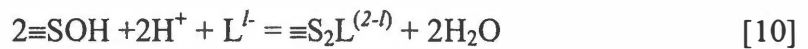
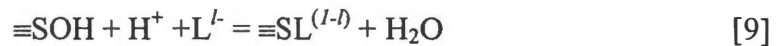
Figure 3. Representation of the singly- (Type A), doubly- (Type C), and triply- (Type B) coordinated surface functional groups on the goethite (From Essington, 2003).

where each constant is related to ΔG° by:

$$K = \exp(-\Delta G^\circ / RT). \quad [6]$$

where ΔG° is in kJ mol^{-1} , R is the universal gas constant ($8.3143 \cdot 10^{-3} \text{ kJ K}^{-1} \text{ mol}^{-1}$), and T is the temperature expressed in Kelvin.

The intrinsic equilibrium constant K_{int} is a true constant at a fixed ionic strength and is independent of the adsorbed phase composition (Essington, 2003). The stoichiometry of each model adsorption reaction and values for both the intrinsic and coulombic equilibrium constants are required to describe adsorption. The following reactions represent a generalized chemical model that would be considered in a SCM:



where $\equiv\text{SOH}$ represents the surface functional group, L is the ligand, and $l-$ is the charge on the ligand (Goldberg, 1992). The intrinsic equilibrium constants (K_{int}) are derived by rearranging Eq. [5]:

$$K_{int} = \frac{K_{ads}}{K_{coul}} \quad [11]$$

Using the reaction in Eq. [7] as an example

$$K_{ads} = \frac{[\equiv\text{SOH}_2^+]}{[\equiv\text{SOH}][\text{H}^+]} \quad [12]$$

and

$$K_{\text{coul}} = \exp(F(+1)\psi_0) \quad [13]$$

Substituting Eqs. [12] and [13] into Eq. [11] yields

$$K_{+(int)} = \left\{ \frac{[\equiv \text{SOH}_2^+]}{[\equiv \text{SOH}][\text{H}^+]} \right\} \exp\left[-\frac{F\psi_0}{RT}\right] \quad [14]$$

The intrinsic constants for the remaining surface processes (Eqs. [8] to [10]) are similarly determined:

$$K_{-(int)} = \left\{ \frac{[\equiv \text{SO}^-][\text{H}^+]}{[\equiv \text{SOH}]} \right\} \exp\left[\frac{F\psi_0}{RT}\right] \quad [15]$$

$$K_{L(int)}^1 = \left\{ \frac{[\equiv \text{SL}^{(1-l)}]}{[\equiv \text{SOH}][\text{L}^{l-}][\text{H}^+]} \right\} \exp\left[-\frac{(1-l)F\psi_0}{RT}\right] \quad [16]$$

$$K_{L(int)}^2 = \left\{ \frac{[\equiv \text{S}_2\text{L}^{(2-l)}]}{[\equiv \text{SOH}]^2[\text{L}^{l-}][\text{H}^+]} \right\} \exp\left[-\frac{(2-l)F\psi_0}{RT}\right] \quad [17]$$

where brackets indicate molar concentrations. Through charge balance and mass balance equations, and using q vs. pH data, intrinsic equilibrium constants (K_{int}) for each adsorption reaction can be determined from equations [7] to [17] using the mathematical approach outlined by Westall (1980).

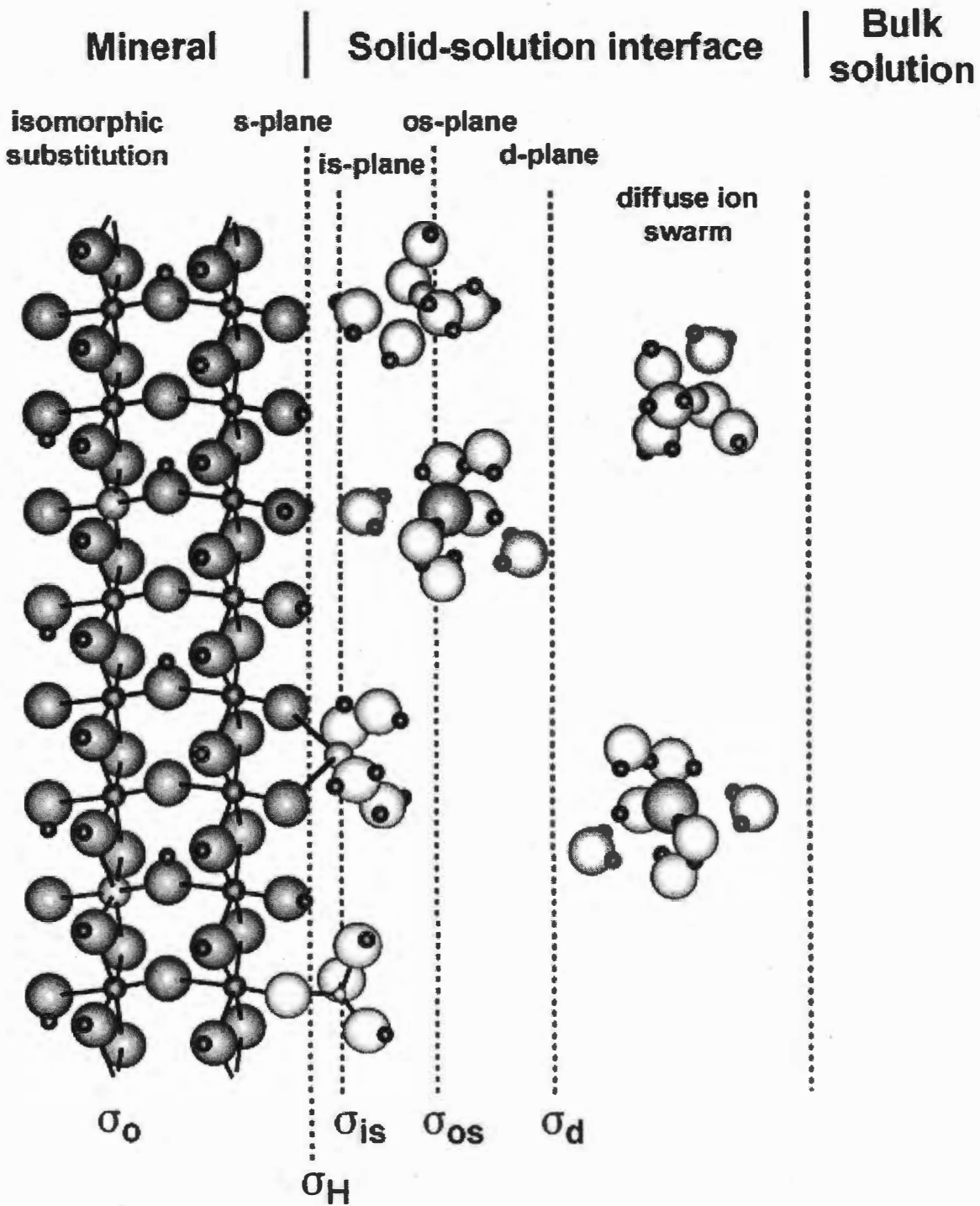
Several unique SCMs have been successfully employed to describe organic ligand adsorption to hydrous oxides (Goldberg, 1992). As previously mentioned, models vary according to how they conceptualize the solid-solution interface. The location and magnitude of charge development (negative or positive) at the interface, as well as the location of adsorbed species are SCM-specific parameters. In general, surface charge development occurs at specific sites through protonation and deprotonation reactions, as well as through the adsorption of metals and ligands (Goldberg 1992). The resulting

surface charge necessitates the retention of oppositely charged ions (counter ions) from solution, to balance surface charge.

Surface complexation models mainly differ by how they conceptualize the layers of surface charge development in the solid-solution interface, employing one or more electrostatic planes to describe adsorption. The charge distribution multi-site complexation model (CD-MUSIC, Hiemstra and Van Riemsdijk, 1999) which is a recent adaptation of the triple layer model (TLM, modified by Hayes and Leckie, 1987), has been used to describe inorganic and organic ligand adsorption to hydrous metal oxides (Filius et al., 1997, Filius et al., 2001; Weerasooriya et al., 2003). The CD-MUSIC model allows for metal and ligand adsorption by both inner-sphere and outer-sphere mechanisms. In the CD-MUSIC model there are two surface planes where adsorption occurs. In the *is*-plane, protons and specifically adsorbed metals and ligands are retained. The charge density associated with the *is*-plane (σ_{in}) is a result of the charge density of the adsorbed proton (σ_H) plus the charge density of inner-sphere metal and ligand complexes (σ_{is}) ($\sigma_{in} = \sigma_{is} + \sigma_H$). In the *os*-plane, outer-sphere adsorption occurs, and the outer-sphere surface charge density is designated σ_{os} . The total surface charge density that results from proton, metal, and ligand retention is balanced by the charge density of counterions (σ_d) such that $\sigma_{in} + \sigma_{os} = -\sigma_d$ (Essington, 2003) (Figure 4).

Within the CD-MUSIC, two types of surface-charging models can be applied: 1- pK_a or 2- pK_a . The 2- pK_a approach is illustrated in Eqs. [7] and [8]. The 1- pK_a approach can be illustrated by:





Surface charge density components

Figure 4. A microscopic view of the solid-solution interface (From Essington, 2003).

In the 1-pK_a approach, the distribution of surface charge is dictated by Pauling's electrostatic valence principle. For instance, the structural Al⁺³ in gibbsite [Al(OH)₃] is in octahedral coordination with hydroxyl anions (surrounded by 6 OH⁻ ions) (Hiemstra et al., 1999). Within a gibbsite structure, each bond radiating from Al⁺³ in octahedral coordination has strength of +1/2 which is satisfied by a -1/2 charge from a doubly coordinated OH⁻ group (each OH⁻ group in the gibbsite structure is attached to two Al⁺³ ions) (Essington, 2003). Based on this analyses, a singly-coordinated surface hydroxyl (an OH⁻ group bonded to one structural Al⁺³) will bear -1/2, if ≡Al-OH, or +1/2, if ≡Al-OH₂. Thus, the adsorption of a proton and the distribution of surface charge at the surface OH⁻ group is described by a single pK_a for the reaction $\equiv\text{Al-OH}^{-1/2} + \text{H}^+ \leftrightarrow \equiv\text{Al-OH}_2^{+1/2}$.

As previously mentioned, hydrous metal oxide systems (e.g. gibbsite) contain one or more predominant surface functional groups that serve as sites for ligand adsorption. The gibbsite edge surface consists of equal amounts of doubly- and singly-coordinated hydroxyl groups ($\equiv\text{Al}_2\text{OH}^0$ and $\equiv\text{AlOH}^{-1/2}$), and only doubly coordinated hydroxyl groups on the planar surface (Figure 5) (Dietzel and Böhme, 2005). Kaolinite also contains $\equiv\text{Al}_2\text{OH}^0$ and $\equiv\text{AlOH}^{-1/2}$ sites existing on the edges (Figure 6) (Adri, et. al., 2001). The singly coordinated hydroxyl groups ($\equiv\text{AlOH}^{-1/2}$) on the edges of gibbsite and kaolinite surfaces are the only sites that may participate in ligand exchange within the environmental pH range. Goethite [FeOOH] contains singly- ($\equiv\text{FeOH}^{-1/2}$), doubly- (Fe_2OH^0), and triply- ($\equiv\text{Fe}_3\text{O}^{-1/2}$) coordinated surface hydroxyl groups; however, the doubly coordinated groups are considered to be non-reactive and only the singly-coordinated group will participate in ligand exchange (Figure 3)(Filius et al., 1997;

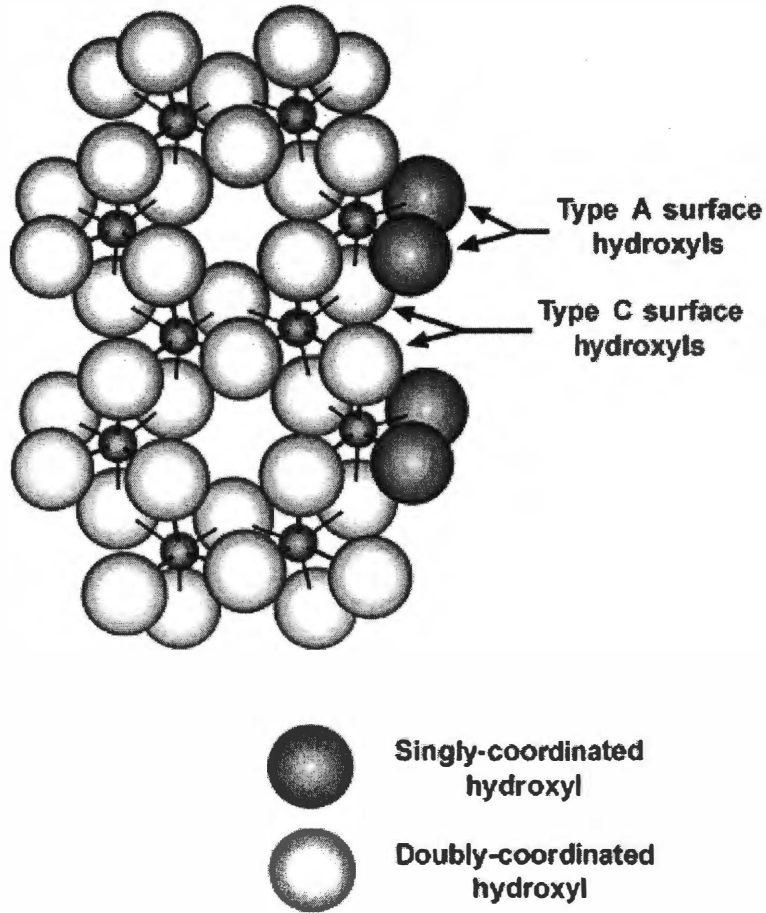


Figure 5. Representation of the gibbsite surface that illustrates the Type A and Type C surface hydroxyls (from Essington, 2003).

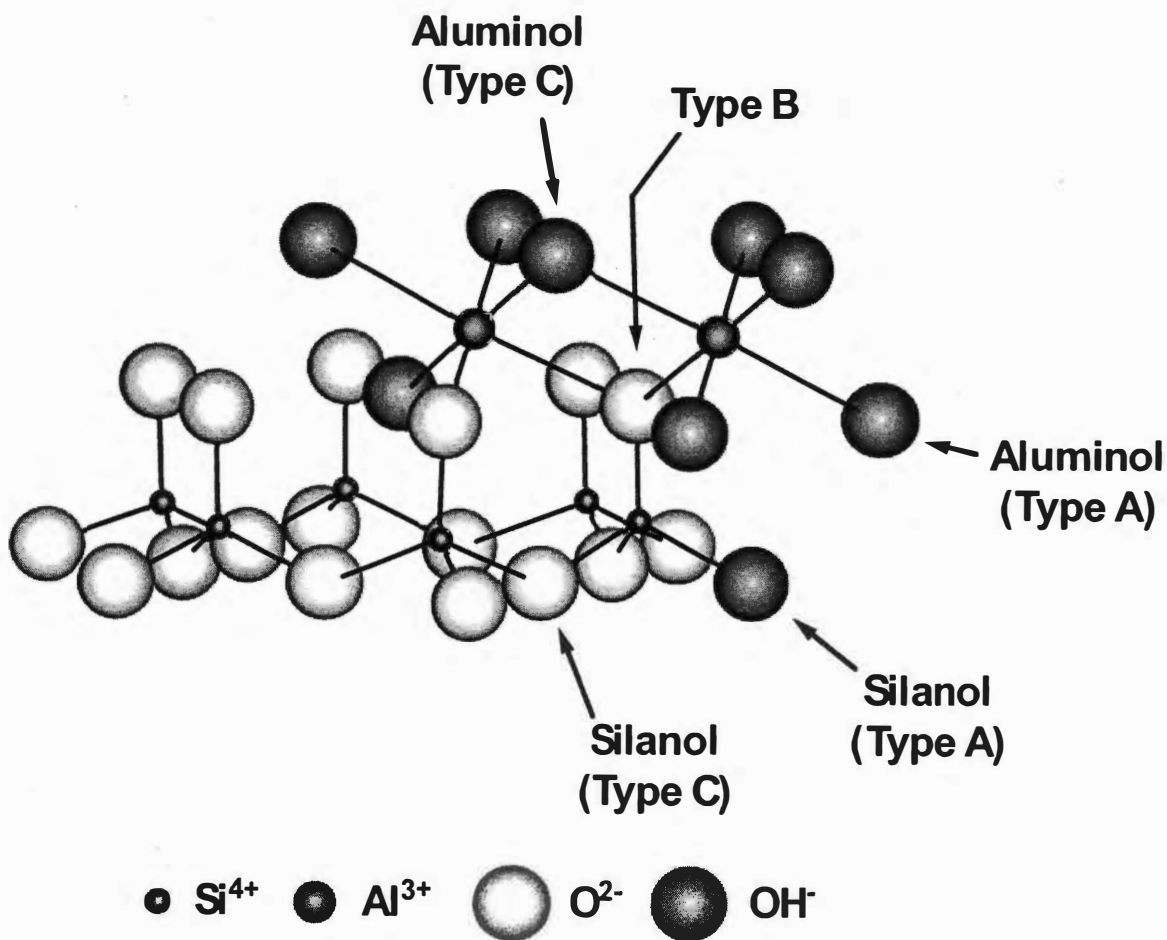


Figure 6. Representation of the kaolinite surface that illustrates the Type A, Type C and Type B silanol and aluminol surface functional groups.

Antelo et. el., 2005). Kaolinite [$\text{Al}_2\text{Si}_2\text{O}_5(\text{OH})_4$] and gibbsite contain the same reactive functional group ($\equiv\text{AlOH}^{-1/2}$), and therefore, it is anticipated that an adsorbate would adsorb to the two surfaces in a similar manner. Thus, optimized K_{int} values for ligand adsorption on gibbsite Type A sites may also be used to predict ligand adsorption on kaolinite. Such an approach is similar to that performed by Sarkar et al. 2000. They showed that the adsorption of mercury by kaolinite could be predicted using chemical models derived for mercury adsorption by quartz and gibbsite.

The interactions of LMMOA anions with soil mineral phases may influence the retention and mobility of organic and inorganic constituents in the soil environment via several different mechanisms. Primary and secondary aluminosilicates and their weathering products (e.g., hydrous metal oxides) are ubiquitous in mineral soils (Essington, 2003). Hydrous metal oxides, particularly those that are poorly or microcrystalline, bear extensive and highly reactive surfaces that can participate in chemisorption. Three of the more common minerals that occur in soils include gibbsite, goethite, and kaolinite. The determination of adsorption mechanisms of kG to these minerals will provide a better understanding of the effects of kG on the fate and mobility of soil nutrients and toxins in the environment.

The hypothesis of this study was that kG is specifically adsorbed by constant potential mineral surfaces, affecting surface charge characteristics and the retention of other specifically adsorbed ligands.

The objectives of this study were to: (i) examine the adsorption of 2-ketogluconate by gibbsite, kaolinite, and goethite as a function of solution pH, ionic strength, and the presence of SO_4 , PO_4 , and AsO_4 ; (ii) use the CD-MUSIC surface

complexation model to examine and predict the potential adsorption mechanisms; and to
(iii) apply the predicted chemical adsorption models to complex chemical systems.

II. Materials and Methods

All reagents were of analytical grade and used without purification, unless noted otherwise. All experiments were conducted in CO₂-free systems and under a blanket of N₂ gas. All solutions were prepared using Type-I deionized water (18Ω).

Preparation of Solids

Hydrated alumina (SF-4) was obtained from Alcan Chemicals (Beachwood, OH) and was shown by x-ray diffraction to be composed of synthetic gibbsite, without detectable impurities. Two-gram samples of gibbsite were placed into 50-mL polypropylene centrifuge tubes. The solid was treated with 20 mL of 0.01 *M* NaOH for 30 min to remove poorly crystallized Al(OH)₃ coatings (Bloom and Weaver, 1982). The solid was then centrifuge-washed four consecutive times with NaCl background electrolyte (either 0.01 *M* or 0.001 *M* NaCl). Following the last washing, the suspension were combined and brought to a solid-to-solution ratio of 50 g L⁻¹. The suspension was stored at ambient temperature (20°C -22°C) until needed.

Synthetic goethite was obtained from Kraemer Pigments (New York, NY) and was shown by x-ray diffraction to be composed of synthetic goethite. Four 12.5-g samples of dry goethite were placed into separate 250-mL centrifuge bottles. The solid was treated with 150 mL of 0.4 *M* HCl for 30 min to remove poorly crystalline materials (Essington et al., 2005). The solid was then centrifuge-washed four consecutive times with 200 mL volumes of NaCl background electrolyte (0.01 *M* or 0.001 *M* NaCl). The goethite suspension (in 200 mL NaCl solution) was then brought to pH 7 by dropwise addition of 0.1 *M* NaOH. The suspensions from each centrifuge bottle were combined in a 1L volumetric cylinder and brought to volume with either 0.01 *M* or 0.001 *M* NaCl so

that the solid-to-solution ratio was 50 g L⁻¹. The suspension was transferred to a 1L plastic Nalgene bottle and stored at ambient temperature (20°C -22°C) until needed.

A well-crystallized Georgia kaolinite (KGa-1) was obtained from the Source Clays Repository of the Clay Mineralogy Society, and was treated according to the procedure of Sarkar et al. (2000). A 100 g sample of kaolinite was dispersed and disaggregated in a commercial-grade blender with 500 mL Type I water for 45 min. The suspension was then brought to pH 9.5 by dropwise addition of 0.1 M NaOH in order to facilitate dispersion and to remove poorly crystalline materials. The < 2.0- μ m size fraction was isolated using Stoke's Law centrifugal sedimentation. The < 2.0- μ m suspension was then centrifuge-washed with 1 M NaCl and then brought to pH 3 with 0.1 M HCl to aid flocculation. The kaolinite was centrifuge-washed with NaCl background electrolyte (0.01 M or 0.001 M NaCl) until the pH of the suspension was approximately 6. The solid-to-solution ratio was brought to 50 g L⁻¹ with 0.01 M or 0.001 M NaCl and stored at ambient temperature (20°C -22°C) until needed.

The total concentration of surface sites is an important parameter used for interpreting and predicting adsorption mechanisms. Site concentrations can be determined using the formula:

$$S_T = (n_s) (10^{18})(a)(S_A) / A_N \quad [19]$$

where S_T has units of mol L⁻¹, n_s is the site density (nm⁻²), 10^{18} is a conversion factor, a is the concentration of the solid in a suspension (g L⁻¹), S_A is the specific surface area of the solid (m²g⁻¹), and A_N is Avagadro's number (6.022 X 10²³ mol⁻¹) (Essington, 2003).

Gibbsite consists of equal numbers of singly-coordinated (Type A) (\equiv AlOH^{1/2-}) and

doubly-coordinated (Type C) ($\equiv\text{Al}_2\text{OH}^0$) surface hydroxyls on the edge surfaces, and only Type C hydroxyls on the planar surfaces (Figure 5) (Hiemstra et al., 1999). The specific surface area of the SF-4 gibbsite was found to be $78 \text{ m}^2\text{g}^{-1}$ by the ethylene glycol mono ethyl ether (EGME) method (Quirk and Murray, 1999), and composed of 8.0 nm^{-2} singly-coordinated $\equiv\text{AlOH}^{1/2-}$ surface functional groups located on the edge surfaces (n_s) (Sarkar et al., 1999). The concentration of gibbsite in the adsorption study suspensions (a) was 10 g L^{-1} . According to the pK_a approach (described below), the surface acidity of gibbsite is assumed to be controlled by the protonation of the singly coordinated $\equiv\text{AlOH}^{1/2-}$ group as described by the reaction in Eq. [18]. Therefore, the singly coordinated $\equiv\text{AlOH}^{1/2-}$ is the only surface functional group considered in describing ligand adsorption, and the computed concentration of sites is $2.07 \times 10^{-3} \text{ M}$.

The surface area (S_A) of the Kga-1 kaolinite was reported to be $10.05 \text{ m}^2\text{g}^{-1}$ (Van Olphen and Fripiat, 1979). The site density was assumed to be a sum of equal concentrations of aluminol ($\equiv\text{AlOH}$) and silanol ($\equiv\text{SiOH}$) functional groups (Sarkar et al., 2000). The silanol groups do not participate in ligand exchange. However, the surface acidity of kaolinite is a function of both silanol and aluminol groups. The computed concentration of Type A aluminol sites in the kaolinite adsorption study suspensions is $5.0 \times 10^{-4} \text{ M}$.

The surface area of the goethite was found to be $198 \text{ m}^2\text{g}^{-1}$ by EGME. The goethite surface consists of singly-, doubly-, and triply-coordinated surface hydroxyl groups (Figure 3). The pK_a value for the doubly-coordinated hydroxyl groups ($\equiv\text{Fe}_2\text{OH}^0$) lie outside of the pH range in this study (pH 3 to 10), and the triply-coordinated groups do not participate in ligand exchange. Therefore, these groups are not considered in the

modeling (Tadanier and Eick, 2002). However, the surface acidity of goethite is controlled by the protonation of singly-coordinated ($\equiv\text{FeOH}^{-1/2}$) and triply-coordinated groups ($\equiv\text{Fe}_3\text{O}^{-1/2}$) (Tadanier and Eick, 2002). The computed concentrations of Type A surface functional groups in goethite adsorption suspensions is $1.134 \times 10^{-2} M$.

Preparation of Solutions

A 0.1 M $\text{Ca}_{0.5}\text{kG}$ solution was prepared from the hemi-calcium salt, $\text{Ca}_{0.5}\text{-C}_6\text{H}_9\text{O}_7 \cdot 2\text{H}_2\text{O}$. A stock solution of 0.1 M Na-2-keto-D-gluconate (NakG) was prepared by a passing the $\text{Ca}_{0.5}\text{kG}$ solution through Na-saturated ion exchange resin (DOWEX HCR-W2). Stock solutions of 0.1 M AsO_4 , 0.1 M HPO_4 , and 0.1 M SO_4 , were prepared in CO_2 -free Type I water from their sodium salts ($\text{Na}_2\text{HAsO}_4 \cdot 7\text{H}_2\text{O}$, $\text{Na}_2\text{HPO}_4 \cdot 7\text{H}_2\text{O}$, and Na_2SO_4). These 0.1 M stock solutions were then diluted to 4 mM working solutions with Type I water. Also, combined ligand working solutions of 4mM kG and 4mM AsO_4 , 4mM kG and 4mM PO_4 , and 4mM kG and 4mM SO_4 were prepared from the 0.1 M stock solutions. The background electrolyte solutions were 0.01 M and 0.001 M NaCl prepared from solid NaCl. Solutions of 0.1 M and 0.01 M HCl and 0.1 M and 0.01 M NaOH were prepared from J.T. Baker DILUT-IT™ analytical concentrates and CO_2 -free Type I water.

Adsorption Studies

Batch adsorption studies were performed in 50-mL polypropylene centrifuge tubes. For the adsorption experiments, the 50 g L^{-1} solid suspension of gibbsite, goethite, or kaolinite was vigorously shaken and then a 4 mL aliquot was transferred by volumetric

pipette to each reaction vessel. To this was added 15.5 mL of NaCl background electrolyte, followed by additions of HCl or NaOH to bring each solution to the desired pH as described in Table 1. The reaction vessels were then capped, vortexed, and 0.5 mL of the 4 mM absorptive working solution was added by volumetric pipette. This resulted in a 10 g L⁻¹ solid-to-solution ratio and a 0.1 mM initial concentration of adsorptive. For the control systems, no solid suspension was used, and 19.5 ml of the NaCl background electrolyte was added to each reaction vessel in addition to the 0.5 mL of adsorptive solution and pH adjustments. The reaction vessels were again vortexed and placed onto an *Innova 2100* platform shaker and shaken continuously for 72 h at ambient temperature (20°C -22°C). The 72 h equilibration time was determined from preliminary kinetic studies. After equilibration, the liquid and solid phases were separated by centrifugation at 1000 x g for 20 min. A 5-mL aliquot of the supernatant was withdrawn by pipette for ligand analysis, and the remaining supernatant was used for pH determinations.

Ketogluconate, PO₄, AsO₄, and SO₄ concentrations were determined using ion chromatography (DIONEX DX-100, Sunnyvale, CA) with Dionex Ion-Pac AS4A-SC analytical and guard columns, and suppressed conductivity detection. A 1.8 mM Na₂CO₃-1.7 mM NaHCO₃ eluent was used with a flow rate of 1.5 mL min⁻¹ and an injection volume of 25 μL. The retention times for the analytes were 1.15 min for kG, 3.85 min for PO₄, 5.88 min for SO₄, and 6.4 min for AsO₄. The method detection limit (MDL) for all analytes was 1.0 μM. The pH measurements were performed under a blanket of N₂ using a Thermo Orion Ross series combination pH electrode calibrated

Table 1. Volumes and concentrations of HCl and NaOH pH adjustment solutions used to establish the adsorption edge of 2-keto-D-gluconate, phosphate, arsenate, and sulfate.

Sample	Gibbsite		Goethite		Kaolinite			
	0.1M HCl	0.1M NaOH	0.01M HCl	0.01M NaOH	0.001 M NaCl		0.01 M NaCl	
					0.01M HCl	0.01M NaOH	0.01M HCl	0.01M NaOH
	-	-	-	mL	-	-	-	-
1	0.1	0	1.5	0	1	0	1	0
2	0.05	0	1	0	0.25	0	0.5	0
3	0.025	0	0.5	0	0	0	0.25	0
4	0.01	0	0	0	0	0.1	0.1	0
5	0	0	0	0.5	0	0.25	0	0
6	0	0.01	0	0.75	0	0.5	0	0.1
7	0	0.025	0	1	0	0.6	0	0.25
8	0	0.05	0	1.5	0	0.8	0	0.5
9	0	0.1	0	2	0	1	0	0.8

using pH 4, 7, and 10 commercial buffer solutions. The pH readings were recorded when a $< 0.1 \text{ mV min}^{-1}$ drift was observed.

Fourteen separate adsorption experiments were performed for each mineral: kG alone, SO_4 alone, PO_4 alone, AsO_4 alone, kG with SO_4 , kG with PO_4 , and kG with AsO_4 , each under two ionic strength conditions (0.01 *M* and 0.001 *M* NaCl). For each adsorption experiment, ligand retention at nine different pH values in the 3 to 10 range (in triplicate) was characterized. Also, nine control systems (without solids) were prepared in duplicate. Each adsorption experiment resulted in 45 total reaction vessels.

Gibbsite Pretreated Ligand Adsorption Experiments

To investigate the ability of kG to displace adsorbed PO_4 , kG was added to gibbsite systems containing preadsorbed PO_4 . For each adsorption experiment, nine equilibrium solutions containing gibbsite were prepared in triplicate, and as described above, to adsorb PO_4 and SO_4 as a function of pH. Following equilibration, 0.5 mL of 4 mM kG was added to each tube. The tubes were then vortexed, placed on a platform shaker, and equilibrated for an additional 72 h period. After equilibration, the supernatant liquid and gibbsite were separated by centrifugation, and kG, or PO_4 and pH were determined as described above.

To investigate the influence of kG concentration on adsorbed PO_4 by gibbsite, increasing concentrations of kG were added to the pretreated PO_4 systems. Again, this involved the equilibration of 0.2 g gibbsite in 19.5 mL 0.01 *M* NaCl with 0.5 mL of the 4 mM PO_4 solution as a function of pH. After equilibration, aliquots of 0.5 mL of 8 mM or 16 mM kG were added to each system and equilibrated for an additional 72 h period. The

separation of solid and liquid phases, and the chemical characterizations of the equilibrium solution were performed as previously described.

Data Analysis

Initial concentrations (C_{in} , μM) of each ligand in the adsorption systems were determined through the analyses of the control systems. Equilibrium solution concentrations of each adsorptive (C_{eq} , μM) were determined through the analyses of equilibrium supernatant solutions from the adsorption systems. The concentration of adsorbed ligand, or surface excess (q , $\mu mol\ kg^{-1}$), was determined by difference:

$$q = V_l(C_{in} - C_{eq}) / m_s \quad [20]$$

where V_l is the volume of solution in the system (0.02 L) and m_s is the mass of solid (2×10^{-4} kg).

Adsorption edges (plots of q vs. pH) were constructed for all systems using the mean pH and q data from the triplicate adsorption systems. The mean pH values were determined according to the expression:

$$\text{mean pH} = -\log\{10^{-pH/3}\} \quad [21]$$

The standard error (SE) values for pH and q were also computed and illustrated by error bars on the adsorption edge plots. The SE values were computed by

$$SE = \frac{\sigma}{\sqrt{n}} \quad [22]$$

where, σ is the standard deviation of the q or pH mean and n is the number of replications ($n = 3$).

Surface Complexation Modeling

The q vs. pH adsorption data were employed to develop chemical models that describe ligand (kG, PO₄, AsO₄, and SO₄) adsorption. The CD-MUSIC SCM computations were conducted using FITEQL 4.0 software (Herbelin and Westall, 1999). The CD-MUSIC model requires values for surface parameters of the adsorbent (e.g., surface hydrolysis and electrolyte adsorption constants), formation constants for all aqueous species, and intrinsic equilibrium constants for all surface complexes considered in the chemical model (Sarkar et al., 1999). Formation constants for aqueous species were obtained from the literature and adjusted for ionic strength using the Davies equation (Table 2). Parameters describing the chemical processes at the solid-solution interface, including surface hydrolysis and counterion complexation reactions for the 0.001 and 0.01 M NaCl systems were also obtained from literature sources (Tables 3 and 4).

Adsorption data (q vs. pH) were used by FITEQL 4.0 and the CD-MUSIC SCM to optimize the intrinsic equilibrium constants for the ligand adsorption reactions. FITEQL optimizes the intrinsic equilibrium constants for user-defined surface complexation reactions by combining a non-linear least squares routine with the chemical model which describes solid-solution interface speciation, mineral surface parameters, aqueous speciation, and mass and charge balance constraints (Sarkar et al., 1999). A goodness-of-fit parameter calculated by FITEQL, defined as the weighted sum of squares

Table 2. Formation constants for aqueous species used to model kG, PO₄, AsO₄, and SO₄ adsorption by gibbsite, kaolinite, and goethite in 0.001 and 0.01 M NaCl. †

Reactions	log °K	
	0.001 M NaCl	0.01 M NaCl
$\text{H}_2\text{O} \Leftrightarrow \text{H}^+ + \text{OH}^-$ ‡	-13.97	-13.91
$\text{kG}^- + \text{H}^+ \Leftrightarrow \text{HkG}^0$ §	2.90	2.84
$\text{kG}^- \Leftrightarrow \text{H}_{-1}\text{kG} + \text{H}^+$ §	-11.95	-11.92
$\text{PO}_4^{3-} + \text{H}^+ \Leftrightarrow \text{HPO}_4^{2-}$	12.28	12.01
$\text{PO}_4^{3-} + 2\text{H}^+ \Leftrightarrow \text{H}_2\text{PO}_4^-$	19.57	19.10
$\text{PO}_4^{3-} + 3\text{H}^+ \Leftrightarrow \text{H}_3\text{PO}_4$	21.3	20.86
$\text{AsO}_4^{3-} + \text{H}^+ \Leftrightarrow \text{HAsO}_4^{2-}$	11.32	11.46
$\text{AsO}_4^{3-} + 2\text{H}^+ \Leftrightarrow \text{H}_2\text{AsO}_4^-$	18.10	18.34
$\text{AsO}_4^{3-} + 3\text{H}^+ \Leftrightarrow \text{H}_3\text{AsO}_4^0$	20.29	20.56
$\text{SO}_4^{2-} + \text{H}^+ \Leftrightarrow \text{HSO}_4^-$	1.88	1.76

† Values were obtained from Martell et al., (2004) unless noted otherwise, and modified for ionic strength using Davies equation.

‡ Baes and Mesmer (1986)

§ Nelson and Essington (2005)

Table 3. CD-MUSIC model parameters used to develop chemical models of kG, PO₄, AsO₄, and SO₄ adsorption by gibbsite, goethite and kaolinite surfaces.

Property	Gibbsite	Goethite	Kaolinite
Surface area, m ² g ⁻¹	78	198	10.05
Site density Type A sites nm ⁻² (aluminol for kaolinite)	8.0 [†]	3.45 [‡]	3.0 [§]
Site density silanol sites nm ⁻²	-	-	3.0
Site density Type B sites nm ⁻²	-	2.7 [‡]	-
Type A sites, ×10 ⁻⁴ mol L ⁻¹ (aluminol for kaolinite)	20.7	113.4	5.0
Silanol sites, ×10 ⁻⁴ mol L ⁻¹	-	-	5.0
Type B sites, ×10 ⁻⁴ mol L ⁻¹	-	90.0	
Inner-layer capacitance, F m ⁻²	0.9	1.2 [¶]	0.9
Outer-layer capacitance, F m ⁻²	0.2	0.2 [¶]	0.2
Suspension density, g L ⁻¹	10.0	10.0	10.0

[†]Sakar et al., 1999

[‡]Tadanier and Eick, 2002

[§]Sarkar et al., 2000

[¶]Goldberg, 2005

Table 4. Surface protonation and counter ion retention reactions and associated equilibrium constants.

Reaction [†]	log K		
	Gibbsite	Goethite	Kaolinite
Surface Protonation Reactions			
$\equiv \text{SOH}^{1/2-} + \text{H}^+ \leftrightarrow \equiv \text{SOH}_2^{1/2+}$	8.8 [¶]	9.2 [‡]	8.8 [¶]
$\equiv \text{Si} - \text{OH}^0 + \text{H}^+ \leftrightarrow \equiv \text{SiOH}_2^+$	-	-	2.77 [§]
$\equiv \text{Si} - \text{OH}^0 \leftrightarrow \equiv \text{SiO}^- + \text{H}^+$	-	-	-6.77 [§]
$\equiv \text{Fe}_3\text{O}^{1/2-} + \text{H}^+ \leftrightarrow \equiv \text{Fe}_3\text{OH}^{1/2+}$	-	9.2 [‡]	-
Electrolyte Ion-Pair Formation Reactions			
$\equiv \text{SOH}^{1/2-} + \text{Na}^+ \leftrightarrow \equiv \text{SOH}^{1/2-} - \text{Na}$	-0.1	-1.0 [‡]	-0.1
$\equiv \text{SOH}^{1/2-} + \text{Cl}^- + \text{H}^+ \leftrightarrow \equiv \text{SOH}_2^{1/2+} - \text{Cl}^-$	8.7	8.2 [‡]	8.7
$\equiv \text{Fe}_3\text{O}^{1/2-} + \text{Cl}^- + \text{H}^+ \leftrightarrow \equiv \text{FeOH} - \text{Cl}^{1/2-}$	-	8.2 [‡]	-
$\equiv \text{Fe}_3\text{O}^{1/2-} + \text{Na}^+ \leftrightarrow \equiv \text{Fe}_3\text{OH} - \text{Na}^{1/2+}$	-	-1.0 [‡]	-

[†] S is Al for gibbsite and kaolinite, and Fe for goethite

[‡]Tadanier and Eick, 2002

[¶]Sarkar et al., 1999

[§]Sarkar et al., 2000.

of residuals divided by the degrees of freedom (WSOS/DF), is a measure of the overall variance associated with the model predictions (Evanko and Dzombak, 1999). Values of WSOS/DF between 0.1 and 20 generally indicate that the user-defined chemical model adequately describes the ligand adsorption data (Evanko and Dzombak, 1999).

The chemical model and the FITEQL-optimized intrinsic constants that describe the adsorption of kG, PO₄, AsO₄, and SO₄ to gibbsite (single ligand adsorption) were used to predict adsorption of kG in the presence of PO₄, AsO₄, or SO₄ to gibbsite (multi-ligand adsorption), as well as to predict individual and multi-ligand adsorption to kaolinite. In these systems, the goodness-of-fit parameter generated by FITEQL (WSOS/DF), is an indication of the accuracy of the chemical models to predict adsorption in multi-ligand systems (or the kaolinite systems). The goal of the modeling was to find a chemical model with the least number of surface species (simplest model), that generates the lowest values of WSOS/DF (Evanko and Dzombak, 1999), and that was applicable to both ionic strength conditions. For example, surface species used to model PO₄ adsorption to gibbsite in 0.01 M NaCl must also be capable of modeling PO₄ adsorption to gibbsite in 0.001 M NaCl, as well as to model PO₄ adsorption to gibbsite in the presence of kG.

For gibbsite, goethite, and kaolinite, it was assumed that the Type A, singly-coordinated surface functional groups were the only reactive functional groups relative to ligand exchange on the solid surfaces (Evanko and Dzombak, 1999). The triply-coordinated groups on goethite surfaces have been shown to participate only in outer sphere adsorption. The doubly-coordinated surface functional groups on gibbsite and the

silanol groups on kaolinite are also considered non-reactive relative to ligand exchange. However, the triply-coordinated ($\text{Fe}_3\text{O}^{1/2-}$) groups on goethite surfaces and the singly-coordinated ($\equiv\text{SiOH}^0$) silanol groups on kaolinite contribute to the surface acidity of the minerals and were considered in the modeling. The site density (n_s) of singly-coordinated $\equiv\text{SOH}^{1/2-}$ groups (Table 3), and thus the concentration of reactive surface sites for each solid, were taken from the literature. Following Tadanier and Eick (2002), the site density of the singly-coordinated and triply coordinated sites was 3.45 and 2.7 nm^{-2} . For gibbsite, it was assumed that 20% of the total surface area consisted of edge surfaces (Hiemstra et al., 1999), and so 1.6 nm^{-2} (20% of 8.0 nm^{-2}) was used as the site density. The site density of kaolinite was assumed to consist of 3.0 nm^{-2} aluminol sites and 3.0 nm^{-2} silanol sites (Sarkar et al., 2000).

III. Results and Discussion

Gibbsite

Effects of pH and Ionic Strength

The adsorption of kG by gibbsite is a function of solution pH (Figure 7).

Adsorption is at a maximum at pH values below approximately pH 5. Above pH 5, adsorption decreases with increasing pH, irrespective of ionic strength conditions. In the 0.01 M NaCl systems, an adsorption maximum of 7.2 mmolkg⁻¹ occurs in the pH 3 to 5 range and a minimum adsorption of approximately 2.4 mmolkg⁻¹ occurs at the highest pH studied. In the 0.001 M NaCl systems, a maximum adsorption of 7.1 mmolkg⁻¹ occurs in the pH 3 to 5 range and a minimum adsorption of 2.1 mmolkg⁻¹ occurs at highest pH value. The pH₅₀ values, the pH at which 50% of q_{\max} is achieved, is approximately 9 for both the 0.01 and 0.001 M NaCl systems. These kG adsorption edges are similar to those of oxalate and citrate on allophanes, two compounds known to adsorb via inner-sphere and multidentate mechanisms (Jara et al., 2006). The observed kG adsorption edge may be interpreted to describe two independent processes: anion exchange or ligand exchange. In general, the kG adsorption appears to mirror the expected reduction in $\equiv\text{AlOH}_2^{1/2+}$ concentration with increasing pH. This finding suggests that kG retention is electrostatic through the anion exchange process:



The observation that the pH₅₀ approximates the pK_a for $\equiv\text{AlOH}_2^{1/2+}$ dissociation (Table 4) may also be interpreted to support an anion exchange process. However, ligand exchange

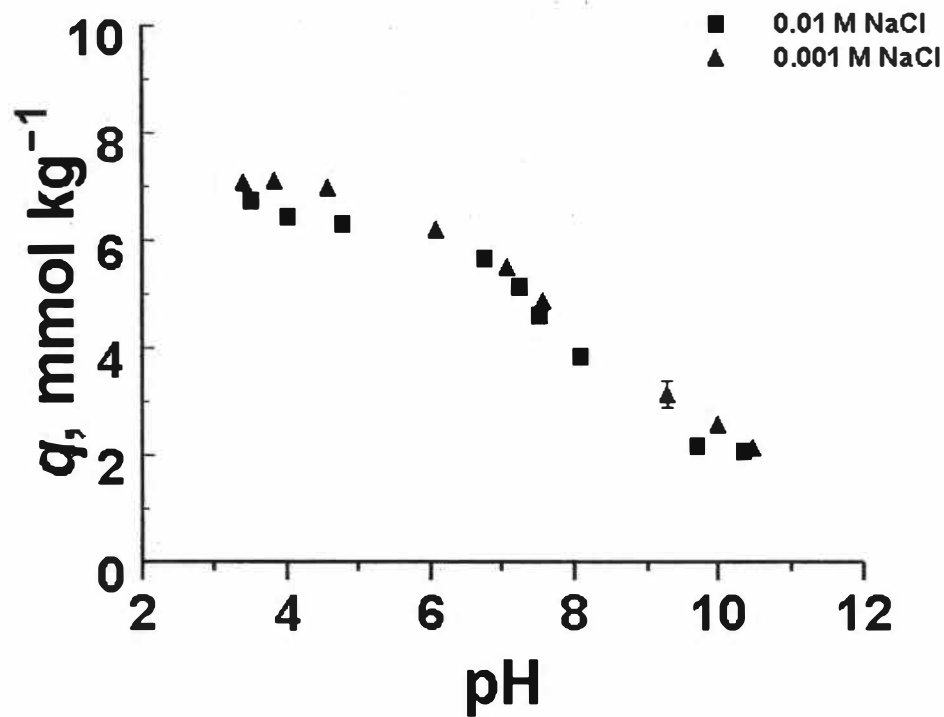


Figure 7. The adsorption edge of 2-ketogluconate (kG) on gibbsite in 0.01 and 0.001 *M* NaCl. Error bars represent the standard error (Eq. [22]) of q . Where error bars cannot be seen, they are within the range of the marker.

according to the reaction:



is also supported by the adsorption edge data. As pH increases, the concentration of Al-coordinated surface H₂O decreases, with a corresponding increase in surface OH⁻. Being a weaker ligand, H₂O may participate in a ligand exchange process with kG⁻; whereas, kG⁻ may not have sufficient base strength to displace OH⁻. Correspondingly, the observation that pH₅₀ for kG⁻ is approximately equal to the pK_a of $\equiv\text{AlOH}_2^{1/2+}$ also supports a ligand exchange mechanism.

Although the adsorption edged data can be interpreted to support either anion or ligand exchange, the ligand exchange mechanism is directly supported by the observation that kG adsorption by gibbsite is not influenced by ionic strength. The ten-fold increase in ionic strength and Cl⁻ ions did not cause a concomitant decrease in the adsorption of kG⁻ (Figure 7). The ten-fold increase in non-specifically adsorbed Cl⁻ ions would result in greater competition among other non-specifically adsorbed ions for outer-sphere gibbsite surface sites, while not significantly affecting inner-sphere adsorption. The fact that kG retention is not influenced by ionic strength is direct evidence that kG adsorbs to gibbsite surface sites via inner-sphere mechanisms.

The adsorption of PO₄ and AsO₄ was also a function of pH (Figures 8 and 9). A maximum adsorption plateau of approximately 9 mmol kg⁻¹ occurred at pH values below 5. Phosphate and AsO₄ adsorption then decreased with increasing pH. Adsorption of PO₄

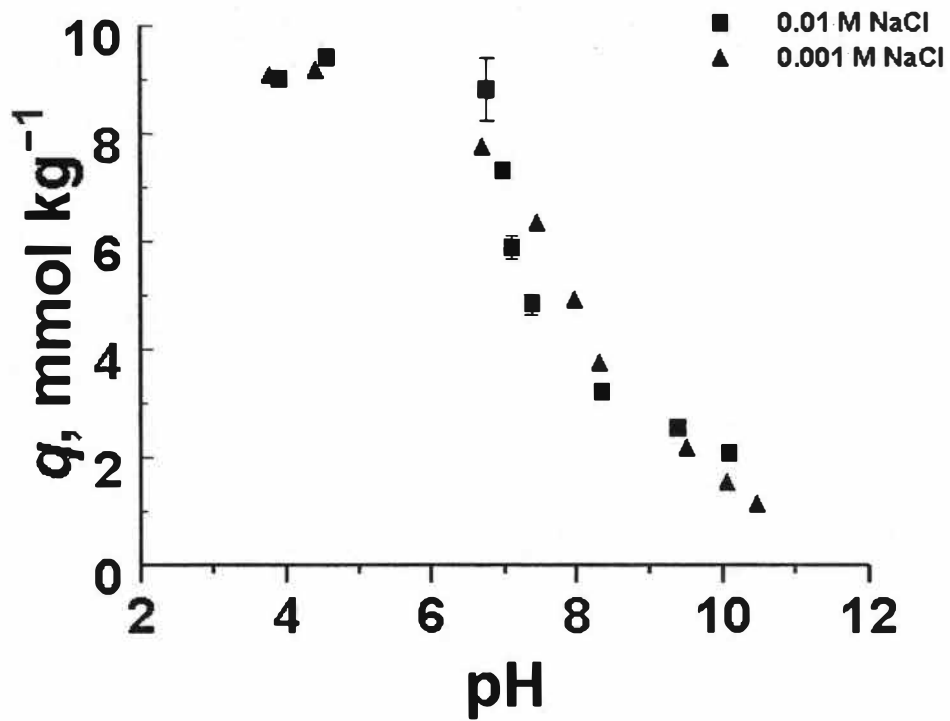


Figure 8. The adsorption edge of phosphate (PO_4) on gibbsite in 0.01 and 0.001 M NaCl. Error bars represent the standard error (Eq. [22]) of q . Where error bars cannot be seen, they are within the range of the marker.

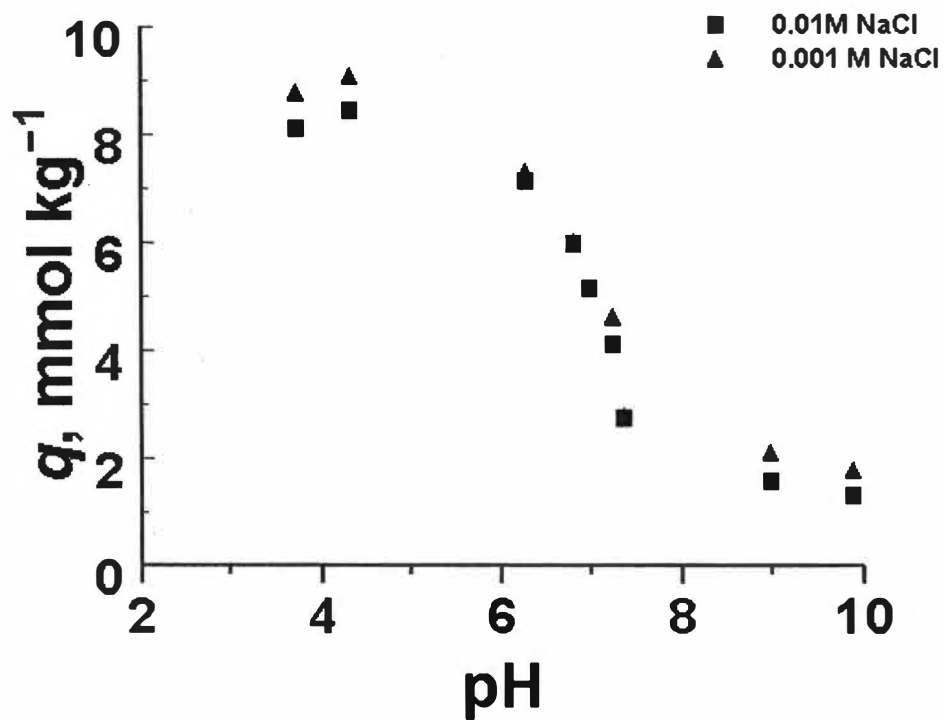


Figure 9. The adsorption edge of arsenate (AsO_4) on gibbsite in 0.01 and 0.001 M NaCl. Error bars represent the standard error (Eq. [22]) of q . Where error bars cannot be seen, they are within the range of the marker.

and AsO_4 was very similar in both the 0.01 and 0.001 *M* NaCl systems. The pH_{50} value occurred in the pH 7 to 8 range. As was noted for kG adsorption, ionic strength had little impact on the adsorption of AsO_4 or PO_4 . These findings are consistent with the well-established conclusion that AsO_4 and PO_4 are adsorbed to gibbsite via specific, inner-sphere mechanisms (Violante and Pigna, 2002; He et al, 1997; Goldberg and Sposito, 1984). Again, the similarities between AsO_4 , PO_4 , and kG^- adsorption envelopes support the conclusion that kG is retained via inner-sphere mechanisms.

The SO_4 adsorption envelope to gibbsite differed from AsO_4 , PO_4 , and kG (Figure 10). Most notably, SO_4 adsorption was less than that observed for AsO_4 , PO_4 , and kG, and was a function of the ionic strength. Maximum SO_4 adsorption occurred at low pH values (pH 3-5) in both systems, but was lower in the higher ionic strength system: approximately 3 mmol kg^{-1} in 0.01 *M* NaCl vs. 4.9 mmol kg^{-1} in 0.001 *M* NaCl. Adsorption of SO_4 decreased with increasing pH in both systems and approached a minimum near pH 8. A pH_{50} value occurred at a pH of approximately 7 in both cases. Several studies have concluded that SO_4 adsorption by constant potential mineral surfaces occurs via outer-sphere mechanisms, a finding that is also supported by the adsorption edge data in Figure 10. However, studies have suggested that SO_4 may participate in specific ligand exchange reactions at pH values below 6 (Sposito, 1989; He et al., 1997; Rahnemaie et al., 2005; Jara et al., 2006).

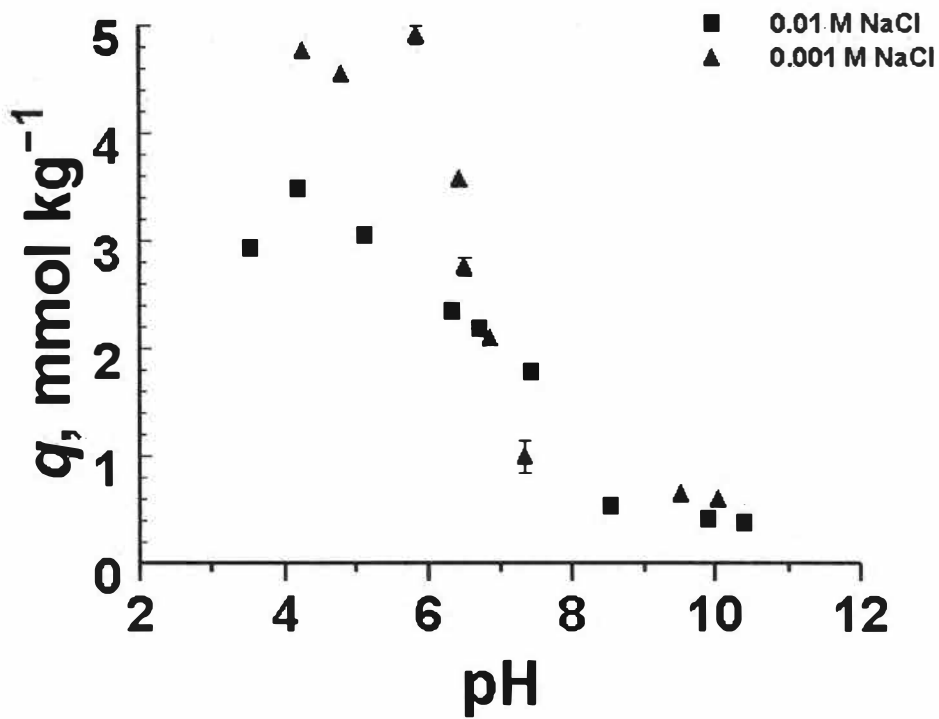


Figure 10. The adsorption edge of sulfate (SO_4) on gibbsite in 0.01 and 0.001 M NaCl. Error bars represent the standard error (Eq. [22]) of q . Where error bars cannot be seen, they are within the range of the marker.

Effects of Inorganic Ligands on 2-Ketogluconate Adsorption

The adsorption of kG was decreased in the presence of specifically adsorbed ligands (PO_4 and AsO_4), and was not significantly affected by the presence of the non-specifically adsorbed ligand (SO_4) at pH values above 6 (Figures 11 and 12). In most cases and at lower pH values (3 to 7), the adsorption of kG was decreased 50% or more in the presence of specifically adsorbed ligands, while the difference in adsorption becomes minimal at pH values in the 7 to 10 range. In the 0.001 M NaCl systems, all ligands affected kG retention at pH values less than 6. Phosphate had the greatest impact on kG adsorption, decreasing kG retention from 7 mmol kg^{-1} to less than 2 mmol kg^{-1} in the pH 3 to 5 range. Arsenate decreased kG adsorption to approximately 4.2 mmol kg^{-1} , and SO_4 decreased adsorption to 5.3 mmol kg^{-1} . The influence of PO_4 and AsO_4 on kG retention is also seen at higher pH values. The impact of PO_4 and SO_4 on kG adsorption is similar to the observed impact of PO_4 and SO_4 on oxalate and citrate adsorption by synthetic and natural allophanes (Jara et al., 2006). In the 0.01 M NaCl systems, a reduction in adsorbed kG in the presence of AsO_4 and PO_4 was observed into the alkaline pH range, even though the degree of the effect was not as substantial as was seen in the 0.001 M systems. The impact of SO_4 on kG adsorption is minimal and restricted to the pH 3 to 4 range, which corresponds to the pH conditions where SO_4 may be specifically retained; thus, competing with specifically retained kG. The observation that kG adsorption was decreased to a greater degree in the presence of PO_4 than to AsO_4 is in accordance with other studies that have shown PO_4 to be adsorbed to a greater extent than AsO_4 to gibbsite surfaces (Violante and Pigna, 2002). The decrease in kG adsorption in the

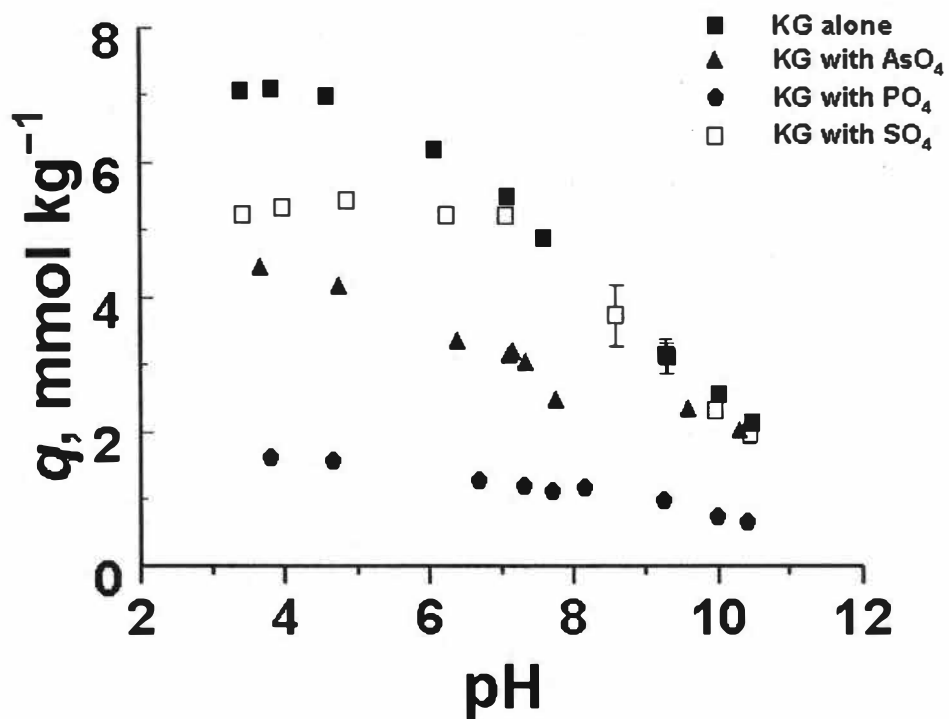


Figure 11. The adsorption of ketogluconate (kG) to gibbsite in 0.001 M NaCl in the presence and absence of AsO₄, PO₄, and SO₄. Error bars represent the standard error (Eq. [22]) of q . Where error bars cannot be seen, they are within the range of the marker.

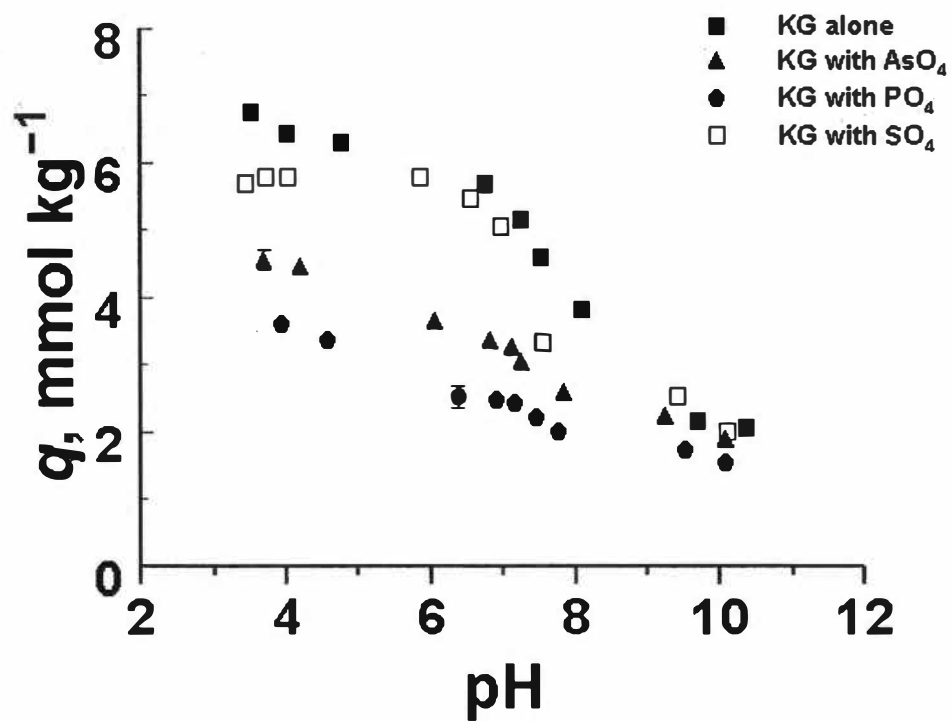


Figure 12. The adsorption of ketogluconate (kG) to gibbsite in 0.01 M NaCl in the presence and absence of AsO₄, PO₄, and SO₄. Error bars represent the standard error (Eq. [22]) of q . Where error bars cannot be seen, they are within the range of the marker.

presence of the specifically adsorbed ligands, particularly AsO_4 and PO_4 , is further direct evidence that kG is adsorbed via specific mechanisms.

Effect of 2-Ketogluconate on the Adsorption of Phosphate, Arsenate and Sulfate

Adsorption

The adsorption of PO_4 , AsO_4 and SO_4 was affected by the presence of kG under both ionic strength conditions (Figure 13 and 14). Arsenate and SO_4 retention was reduced by about 50%, while PO_4 retention was reduced by about 20%. Arsenate adsorption in the high ionic strength systems (0.01 M NaCl) (Figure 13) was decreased from a maximum adsorption of about 8.2 mmol kg^{-1} in the absence of kG, to a maximum adsorption of 4.9 when kG was present (approximately a 40% reduction). As pH increases (in the pH 6 to 7 range), the impact of kG on AsO_4 in adsorption decreases. At pH values of 7 and above, there is no difference between the amount of AsO_4 retained in the presence or absence of kG. Adsorption of PO_4 in 0.01 M was decreased from a maximum of 9.2 mmol kg^{-1} in the absence of kG, to 7.1 mmol kg^{-1} when kG was present (a 23% reduction). The difference in PO_4 adsorption in the presence and absence of kG decreased with increasing pH, up to about pH 7. From pH 7 and above, PO_4 adsorption was consistently 1 mmol kg^{-1} less in the presence of kG, relative to the absence of kG. The decrease in AsO_4 and PO_4 adsorption in the presence of kG is evidence that kG is effectively competing with these two ligands for gibbsite surface sites. This further supports the conclusion that kG adsorbs to gibbsite via inner-sphere mechanisms. In the SO_4 systems, in 0.01M NaCl, the maximum adsorption of SO_4 drops from 3.6 mmol kg^{-1}

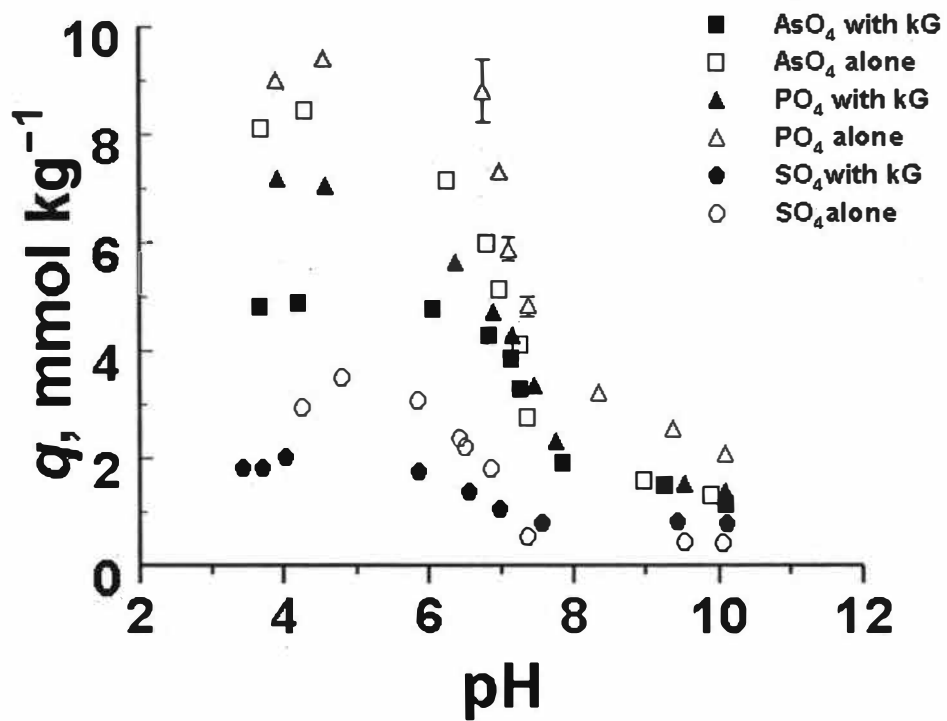


Figure 13. The effect of ketogluconate (kG) on the adsorption of AsO_4 , PO_4 , and SO_4 to gibbsite in 0.01 M NaCl. Error bars represent the standard error (Eq. [22]) of q . Where error bars cannot be seen, they are within the range of the marker.

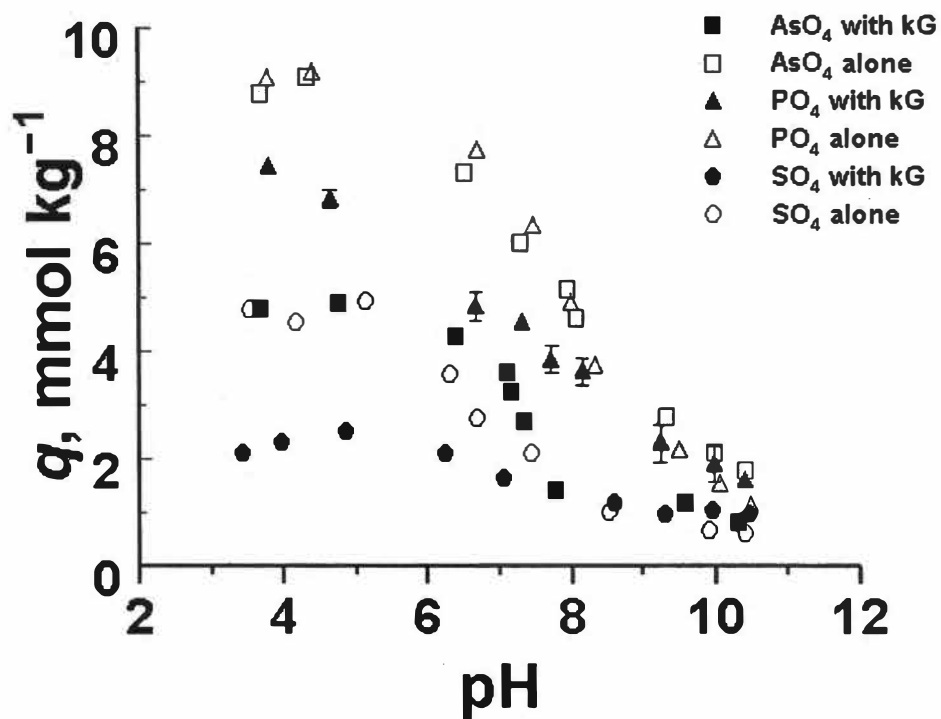


Figure 14. The effect of ketogluconate (kG) on the adsorption of AsO_4 , PO_4 , and SO_4 to gibbsite in 0.001 M NaCl . Error bars represent the standard error (Eq. [22]) of q . Where error bars cannot be seen, they are within the range of the marker.

in the absence of kG, to 2.0 mmol kg⁻¹ when kG is present (a 44% reduction). At pH values above 7, SO₄ retention is negligible in both the presence and absence of kG.

In general, the effect of kG on the adsorption of PO₄, AsO₄ and SO₄ at the low ionic strength (0.001 M NaCl) (Figure 14) was similar to that of the high ionic strength systems. Arsenate adsorption in the low ionic strength systems was decreased from a maximum adsorption of 9.0 mmol kg⁻¹ in the absence of kG, to a maximum adsorption of 4.9 when kG was present (a 46% reduction). The difference in the amount of AsO₄ absorbed in the presence and absence of kG decreases with increasing pH. However, unlike the low ionic strength systems, the difference in AsO₄ adsorption does not approach zero near neutral pH values. Adsorption of PO₄ at the low ionic strength was decreased from a maximum of about 9.2 mmol kg⁻¹ in the absence of kG, to about 7.1 mmol kg⁻¹ when kG was present (a 23% decrease). Like AsO₄, kG reduces PO₄ adsorption throughout the pH range examined. As in the high ionic strength systems, the decrease in AsO₄ and PO₄ adsorption in the presence of kG is evidence that kG is effectively competing with these two ligands for gibbsite surface sites, which is supporting evidence that kG adsorbs to gibbsite via inner-sphere mechanisms. In the SO₄ systems, at the low ionic strength, the maximum adsorption of SO₄ drops from about 5.0 mmol kg⁻¹ in the absence of kG to 2.4 mmol kg⁻¹ when kG is present (a 52% reduction). In the pH 6 to 8 range, the difference in the amount of SO₄ retained in the two systems decreases with increasing pH. However, at pH values above 8, SO₄ adsorption is not influence by kG.

Effects of 2-Ketogluconate on Preadsorbed Phosphate

The adsorption edge experiments that were performed by adding equal concentrations of PO₄ and kG simultaneously resulted in lower adsorption of PO₄ compared to PO₄ adsorption in the absence kG (Figures 13 and 14). The addition of kG to gibbsite containing preadsorbed PO₄ did not result in PO₄ desorption (Figure 15), regardless of the concentration of kG (up to 0.4 mmol L⁻¹ kG). This can be explained by examining the covalent and possibly bidentate nature of the inner-sphere bonding of PO₄. Unlike exchangeable anions (outer-sphere complexes), which are held by Coulombic forces, specifically adsorbed ligands (inner-sphere complexes) form bonds with covalent character through the sharing of electrons between the metal and ligand (Essington, 2003). Covalently-bonded ligands do not readily exchange, or desorb, from mineral surfaces. This can be observed through adsorption hysteresis of adsorption isotherms, where an adsorbed ligand will not desorb, as would an electrostatically adsorbed ligand. In the present case, preadsorbed PO₄ has formed stable bonds with the gibbsite surface, and the addition of kG at the concentrations examined can not displace adsorbed PO₄ species. These conclusions suggest that kG, a microbial byproduct in rhizosphere soils that contain low phytoavailable P concentrations, may not have the ability to displace adsorbed PO₄ species from gibbsite surfaces.

Effects of Phosphate on Preadsorbed 2-Ketogluconate

The addition of PO₄ to gibbsite containing preadsorbed kG resulted in the displacement of approximately 45% of the preadsorbed kG in pH 3 to 7 range (Figure 16). As pH increases above pH 7, the effect of PO₄ on the adsorption of preadsorbed kG

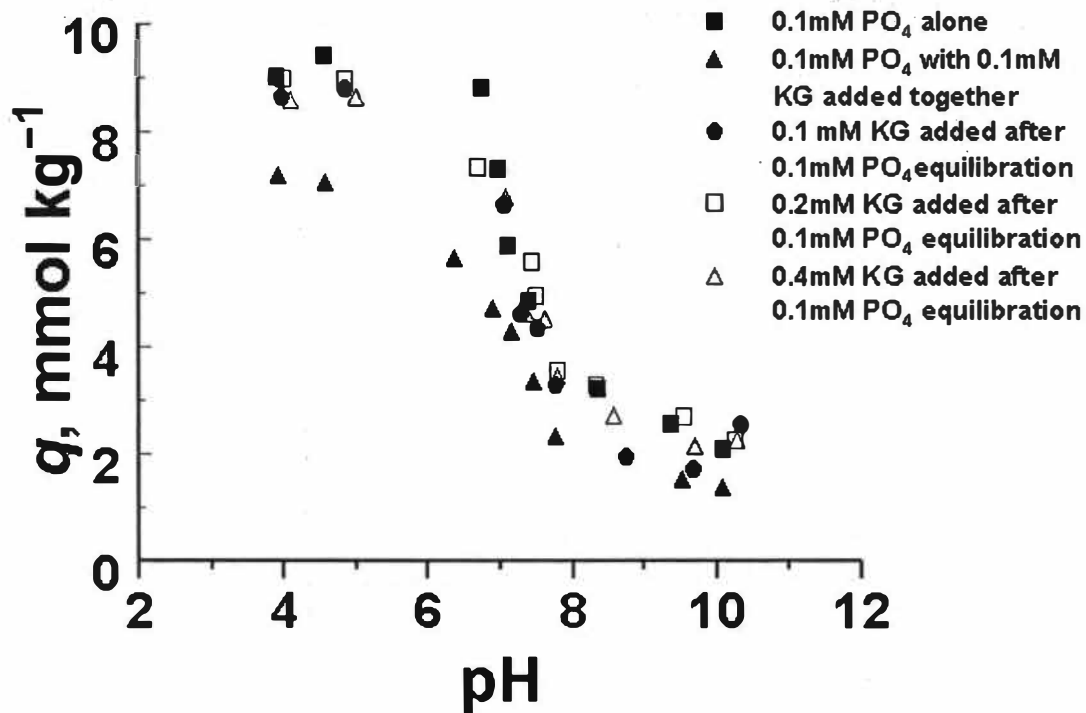


Figure 15. The effect of ketogluconate (kG) in the displacement of phosphate (PO₄) from gibbsite in 0.01 M NaCl. Error bars represent the standard error (Eq. [22]) of q . Where error bars cannot be seen, they are within the range of the marker.

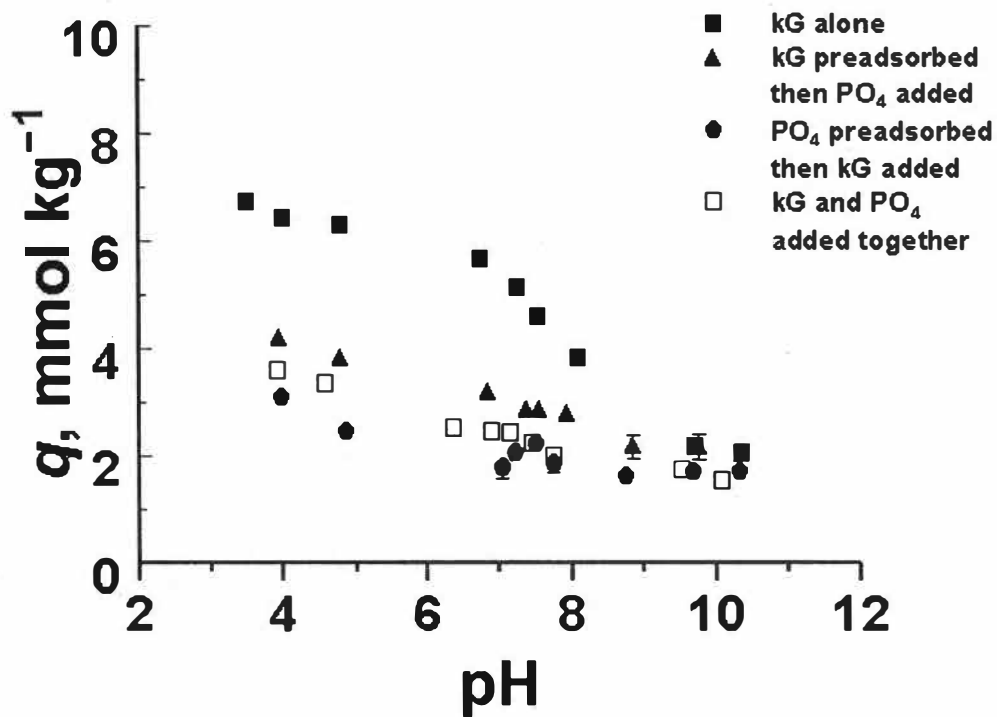


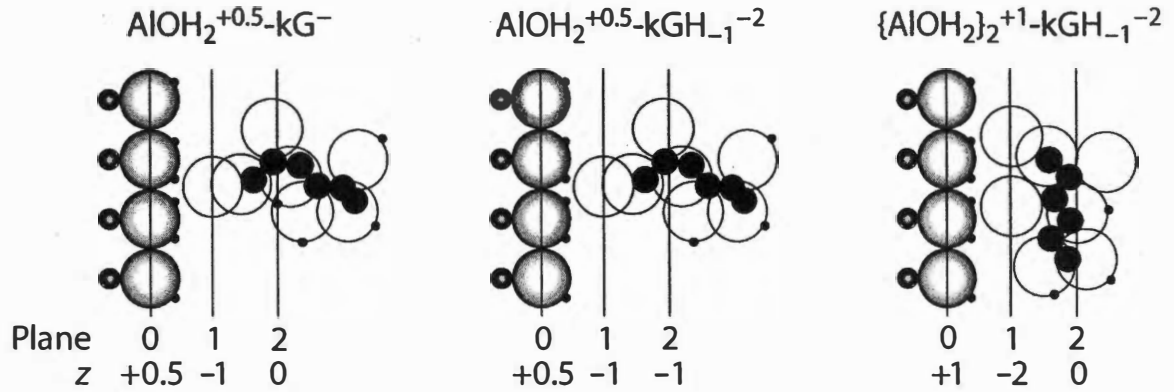
Figure 16. The effect of phosphate (PO_4) in the displacement of ketogluconate (kG) from gibbsite in 0.01 M NaCl. Error bars represent the standard error (Eq. [22]) of q . Where error bars cannot be seen, they are within the range of the marker.

becomes minimal as adsorption approaches 2 mmol kg^{-1} in both adsorption edges (kG alone and kG preadsorbed with PO_4 added). As seen in Figure 16, the adsorption of preadsorbed kG when PO_4 is added is greater than the adsorption of kG when added simultaneously with PO_4 . The effectiveness of the presence of PO_4 in displacing preadsorbed kG was different than that of the reverse (Figure 15), where kG did not cause the displacement of preadsorbed PO_4 . These results indicate that kG is not held as strongly as PO_4 to gibbsite surfaces. Also seen in Figure 16, is the adsorption of kG when added to a preadsorbed PO_4 system, which is slightly less than the adsorption of kG when added simultaneously with PO_4 . These results indicate that that ability of PO_4 to displace adsorbed kG is greater than the ability of kG to displace adsorbed PO_4 .

Surface Complexation Modeling

The adsorption of kG by constant potential mineral surfaces may be visualized to occur via a number of non-specific and specific mechanisms (Figure 17). Although the experiment adsorption edge data supports the hypothesis that kG is retained via inner-sphere mechanism, the application of surface complexation models (SCMs) can be used to provide additional supporting evidence by identifying the specific chemical reactions responsible for adsorption. Ligand adsorption to gibbsite was examined with the CD-MUSIC SCM model in conjunction with the FITEQL 4.0 computer code. Although numerous surface complexes were considered (Figure 17), the kG adsorption data in both the 0.001 M and 0.01 M NaCl systems were best described by assuming that kG forms two monodentate-mononuclear inner-sphere complexes according to the reactions:

Outer-Sphere Surface Complexes



Inner-Sphere Surface Complexes

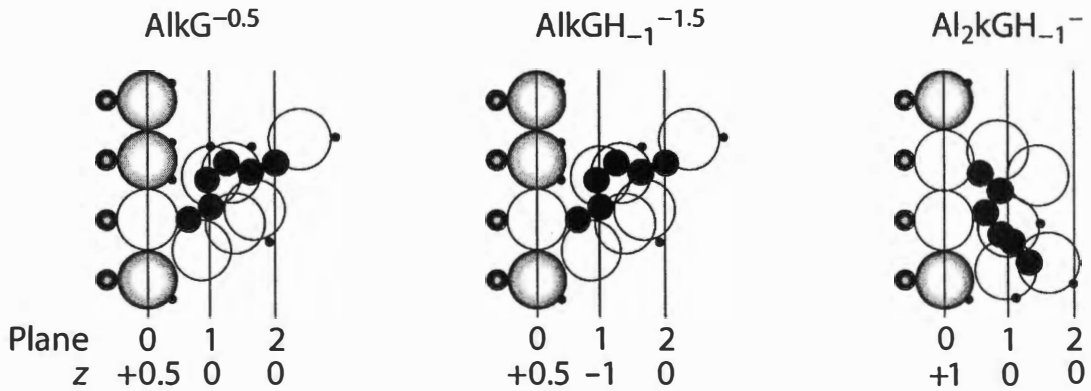


Figure 17. Ketogluconate surface complexes considered in the modeling and charge distribution at the solid-solution interface.



These two surface species and the distribution of charge at the solid-solution interface are shown in Figure 17. The optimized adsorption constants and goodness-of-fit parameters (WSOS/DF) are shown in Table 5. At pH values that are less than the pK_a of $\equiv\text{AlOH}_2^{1/2+}$, the $\equiv\text{AlkG}^{1/2-}$ species predominates as a result of Eq. [25] (Figure 18 and 19). As H_2O disappears from the gibbsite surface through the dissociation of $\equiv\text{AlOH}_2^{1/2+}$, the specific retention of kG is facilitated through the dissociation of the kG hydroxyl that is adjacent to the carbonyl group (Nelson and Essington, 2005). The dissociated proton then protonates $\equiv\text{AlOH}^{1/2-}$ sites to create H_2O on the surface (forming $\equiv\text{AlOH}_2^{1/2+}$), which then undergoes ligand exchange with the H_1kG^{2-} species to form $\equiv\text{AlkGH}_1^{3/2-}$ (Eq. [26]). Key to the formation of the $\equiv\text{AlkG}_1^{3/2-}$ surface species is the dissociation of the hydroxyl moiety on the number 3 carbon of kG . However, the pK_a for this dissociation is approximately 12, which is a substantially greater pH value than the pH at which the $\equiv\text{AlkG}_1^{3/2-}$ species is predicted to occur. The surface-induced deprotonation of the kG hydroxyl at pH values that are less than the pK_a can be envisioned to occur in a manner similar to that of the citrate hydroxyl. The citrate hydroxyl has a pK_a that reportedly ranges from ~ 11 to ~ 13.8 ; yet, metal-citrate complexation occurs through the citrate hydroxyl even into the acidic pH range (Essington, 2006)

The adsorption of PO_4 , AsO_4 , and SO_4 were also modeled using the adsorption edge data and the CD-MUSIC SCM. The model that best described PO_4 adsorption to

Table 5. Gibbsite surface complexation reactions, FITEQL-optimized intrinsic equilibrium constants (log K values), and associated goodness of fit parameters (WSOS/DF values).

Reaction	Log K		WSOS/DF	
	0.001M	0.01M	0.001M	0.01M
	NaCl	NaCl	NaCl	NaCl
$kG^- + \equiv AlOH^{1/2-} + H^+ \Leftrightarrow AlkG^{1/2-} + H_2O$	12.49	12.33	12.80	13.64
$kG^- + \equiv AlOH^{1/2-} \Leftrightarrow AlH_{-1}kG^{3/2-} + H_2O$	4.49	4.26		
$AsO_4^{3-} + \equiv AlOH^{1/2-} + H^+ \Leftrightarrow AlOAsO_3^{5/2-} + H_2O$	16.94	16.05	11.76	48.32
$AsO_4^{3-} + \equiv AlOH^{1/2-} + 3H^+ \Leftrightarrow AlOAsO_3H_2^{1/2-} + H_2O$	31.70	31.07		
$PO_4^{3-} + \equiv AlOH^{1/2-} + 3H^+ \Leftrightarrow AlOPO_3H^{3/2-} + H_2O$	26.37	NA		
$PO_4^{3-} + \equiv AlOH^{1/2-} + 3H^+ \Leftrightarrow AlOPO_3H_2^{1/2-} + H_2O$	33.14	32.42	34.67	24.26
$PO_4^{3-} + \equiv AlOH^{1/2-} + H^+ \Leftrightarrow AlOPO_3^{5/2-} + H_2O$	NA	17.65		
$SO_4^{2-} + \equiv AlOH^{1/2-} + H^+ \Leftrightarrow AlOH_2^{1/2+} - SO_4^{2-}$	12.36	9.57	69.48	6.61

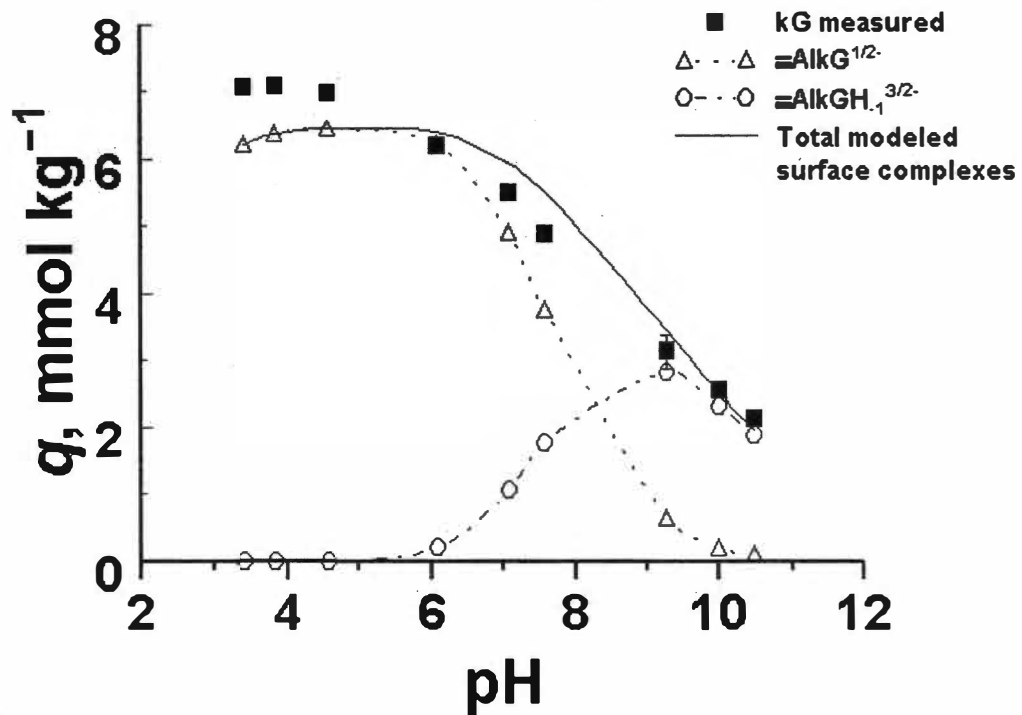


Figure 18. The predicted and experimentally-determined adsorption of ketogluconate (kG) by gibbsite in 0.001 M NaCl. The closed squares represent the experimental data; diamonds represent the predicted formation of $\equiv\text{AlkG}^{1/2-}$ and open circles represent the predicted formation of $\equiv\text{AlkGH}_1^{3/2-}$. Error bars represent the standard error (Eq. [22]) of q . Where error bars cannot be seen, they are within the range of the marker.

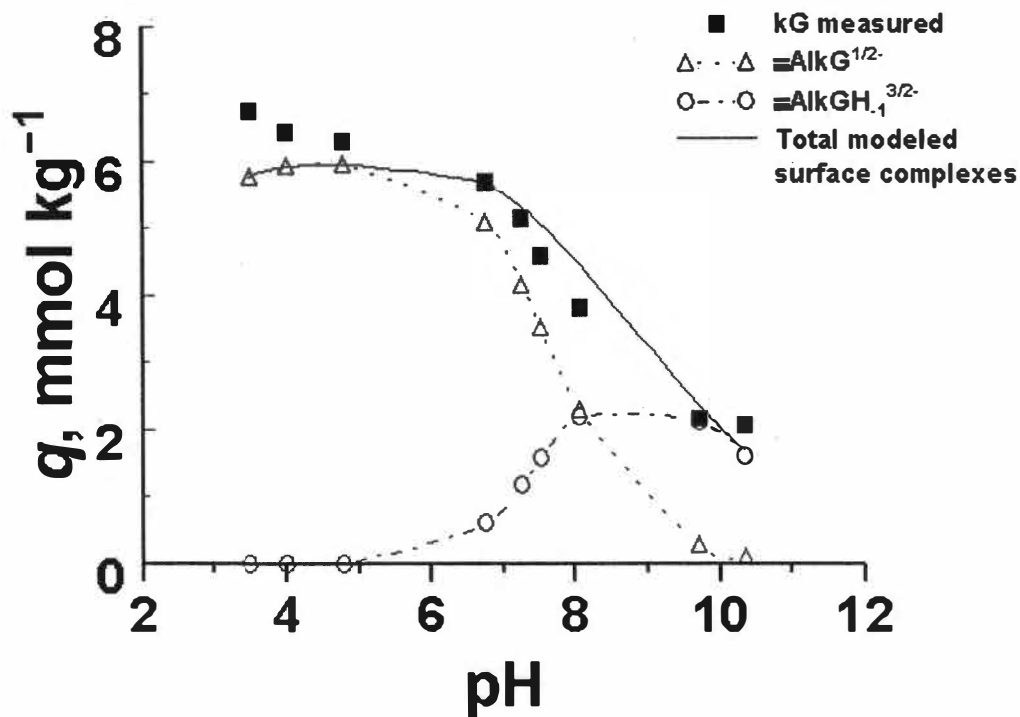
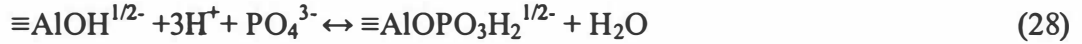
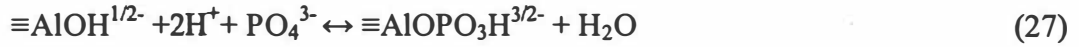


Figure 19. The predicted and experimentally-determined adsorption of ketogluconate (kG) by gibbsite in 0.01 M NaCl. The closed squares represent the experimental data; diamonds represent the predicted formation of $\equiv\text{AlkG}^{1/2-}$; and open circles represent the predicted formation of $\equiv\text{AlkGH}_{1.1}^{3/2-}$. Error bars represent the standard error (Eq. [22]) of q . Where error bars cannot be seen, they are within the range of the marker.

gibbsite was a function of ionic strength. In the low ionic strength systems (0.001 M NaCl), the adsorption data was modeled using the two inner-sphere complexes:

$\equiv\text{AlOPO}_3\text{H}^{3/2-}$, and $\equiv\text{AlOPO}_3\text{H}_2^{1/2-}$ as described by the reactions (Figure 20):

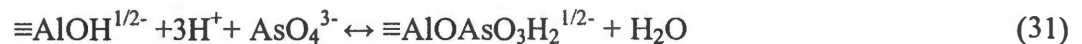
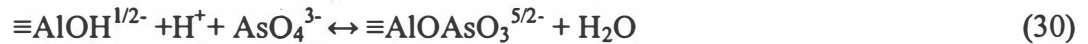


The adsorbed PO_4 surface species and charge distribution at the solid-solution interface are shown in Figure 21. Under the high ionic strength conditions (0.01 M NaCl), the PO_4 adsorption data was modeled using the two inner-sphere complexes: $\equiv\text{AlOPO}_3^{5/2-}$ and $\equiv\text{AlOPO}_3\text{H}_2^{1/2-}$, as described by the reaction in Eq. [28], and the reaction (Figure 22):



These PO_4 surface species, and the charge distribution at the solid-solution interface are shown in Figure 21. All associated adsorption constants (optimized by FITEQL) are shown in Table 5.

Arsenate adsorption data at both ionic strengths were modeled using the $\equiv\text{AlOAsO}_3^{5/2-}$ and $\equiv\text{AlOAsO}_3\text{H}_2^{1/2-}$ inner-sphere surface complexes (Figure, 21, 23 and 24). The formation of these surface species is described by the reactions:



Adsorption is well predicted in the low ionic strength system as indicated by the relatively low WSOS/DF values (Table 5). However, adsorption was under-predicted in

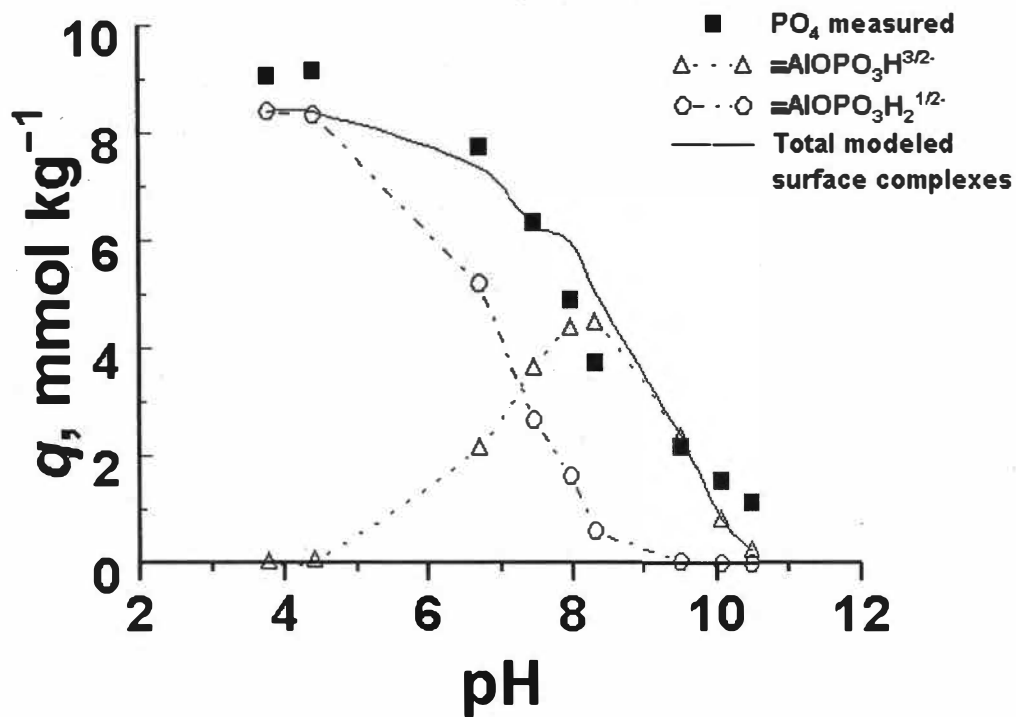
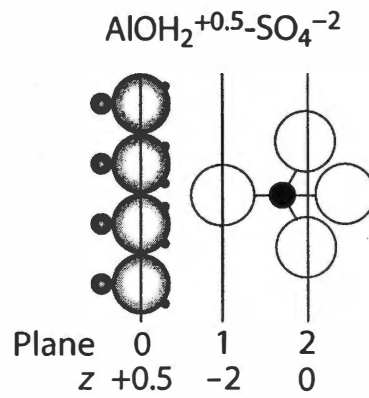


Figure 20. The predicted and experimentally-determined adsorption of phosphate (PO_4) by gibbsite in 0.001 M NaCl . The closed squares represent the experimental data; diamonds represent the predicted formation of $\equiv\text{AlOPO}_3\text{H}^{3/2-}$; and open circles represent the predicted formation of $\equiv\text{AlOPO}_3\text{H}_2^{1/2-}$. Error bars represent the standard error (Eq. [22]) of q . Where error bars cannot be seen, they are within the range of the marker.

Outer-Sphere Surface Complexes



Inner-Sphere Surface Complexes

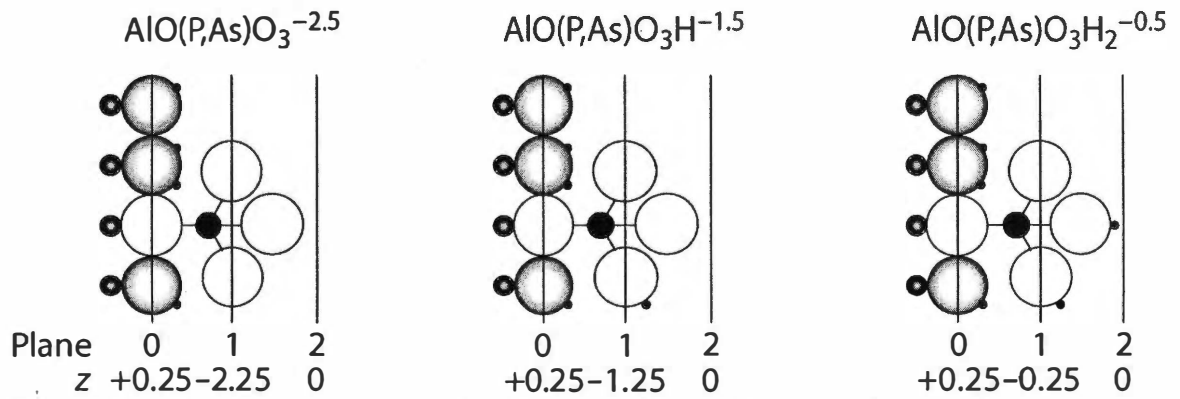


Figure 21. Phosphate, arsenate, and sulfate modeled surface complexes and charge

distribution at the solid-solution interface.

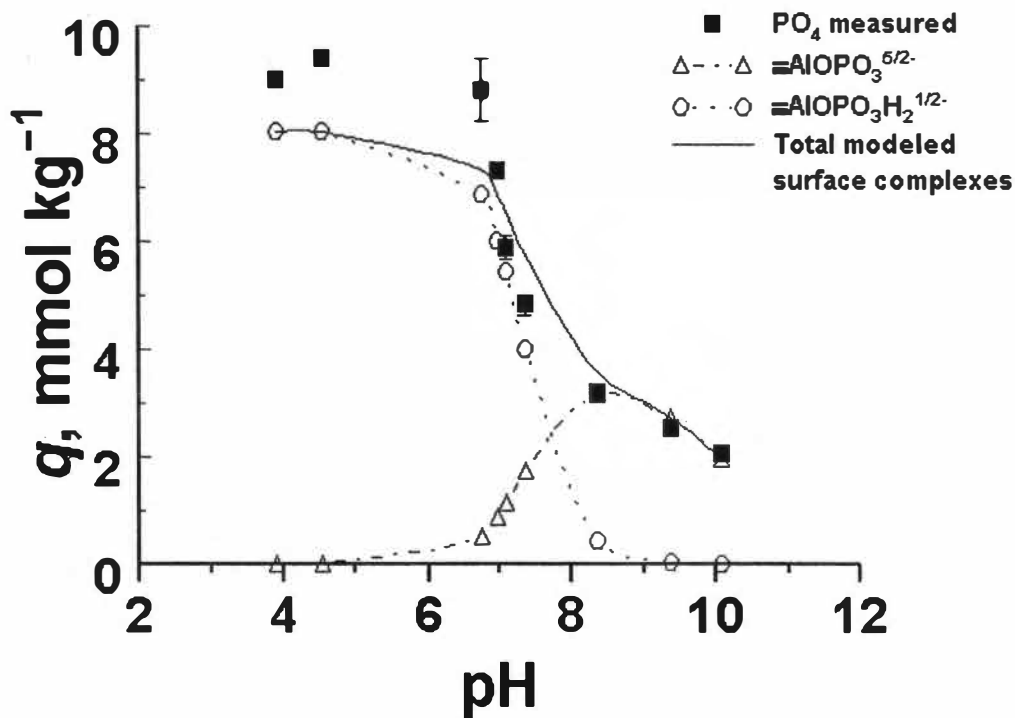


Figure 22. The predicted and experimentally-determined adsorption of phosphate (PO_4) by gibbsite in 0.01 M NaCl . The closed squares represent the experimental data; diamonds represent the predicted formation of $\equiv\text{AlOPO}_3^{5/2-}$; and open circles represent the predicted formation of $\equiv\text{AlOPO}_3\text{H}_2^{1/2-}$. Error bars represent the standard error (Eq. [22]) of q . Where error bars cannot be seen, they are within the range of the marker.

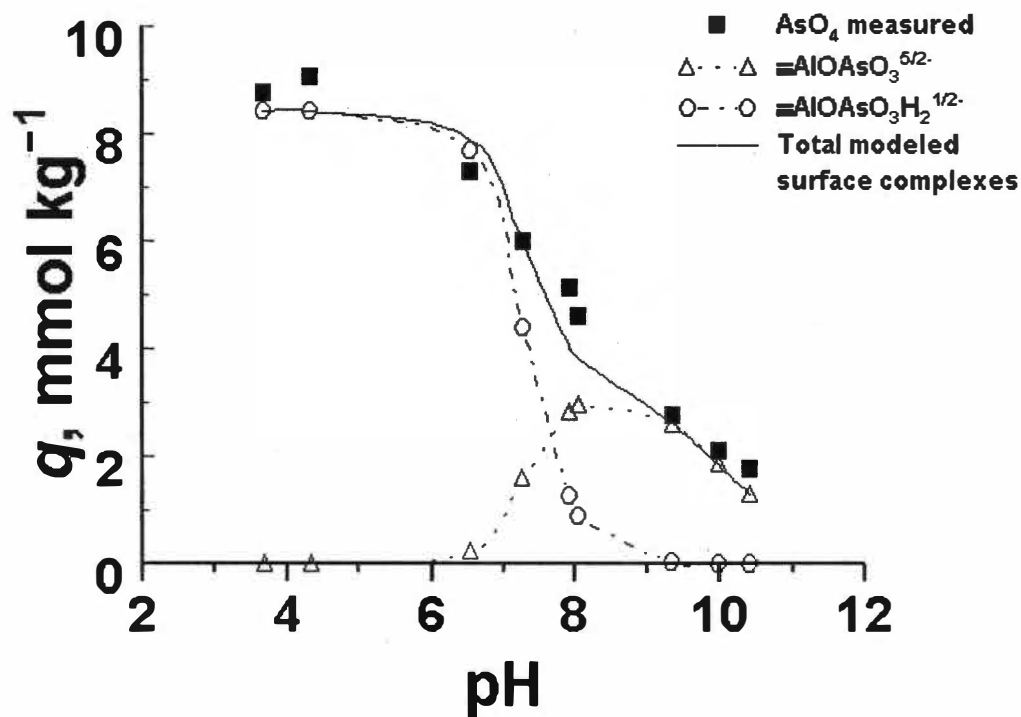


Figure 23. The predicted and experimentally-determined adsorption of arsenate (AsO_4) by gibbsite in 0.001 M NaCl . The closed squares represent the experimental data; diamonds represent the predicted formation of $\equiv\text{AlOAsO}_3^{5/2-}$; and open circles represent the predicted formation of $\equiv\text{AlOAsO}_3\text{H}_2^{1/2-}$. Error bars represent the standard error (Eq. [22]) of q . Where error bars cannot be seen, they are within the range of the marker.

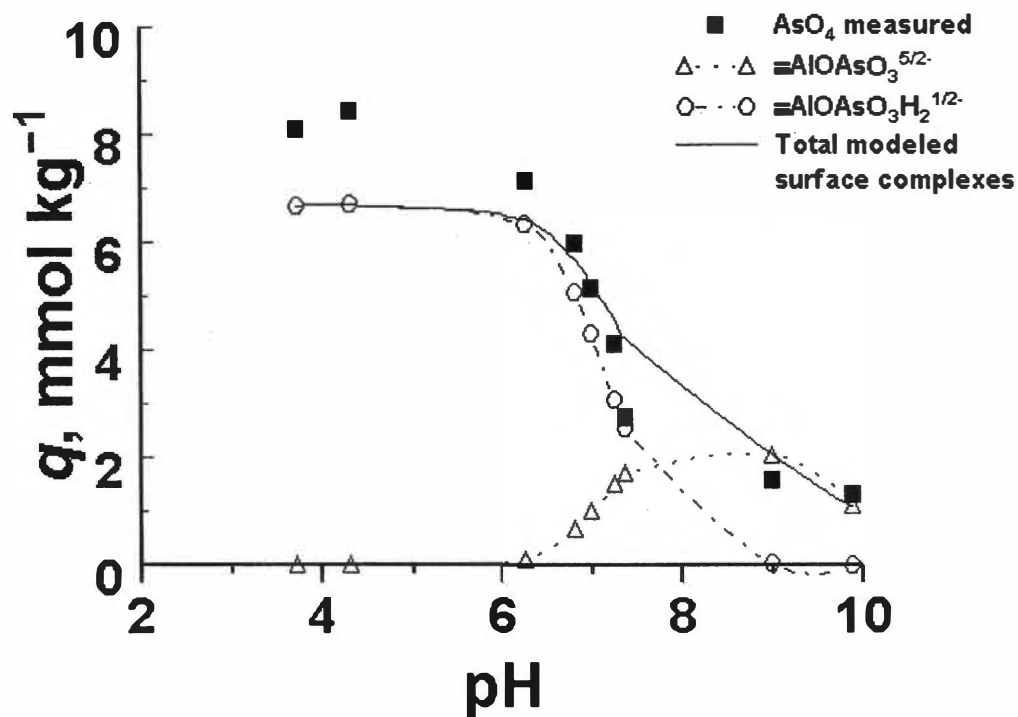


Figure 24. The predicted and experimentally-determined adsorption of arsenate (AsO_4) by gibbsite in 0.01 M NaCl . The closed squares represent the experimental data; diamonds represent the predicted formation of $\equiv\text{AlOAsO}_3^{5/2-}$; and open circles represent the predicted formation of $\equiv\text{AlOAsO}_3\text{H}_2^{1/2-}$. Error bars represent the standard error (Eq. [22]) of q . Where error bars cannot be seen, they are within the range of the marker.

the high ionic strength system. Other studies have also observed this under-predicted AsO₄ retention (Weesooriya et al., 2004). Adsorption constants are presented in Table 5, and the surface species and charge distribution at the solid-solution interface is shown in Figure 21. Sulfate adsorption data at both ionic strength conditions were described using the outer-sphere $\equiv\text{AlOH}_2^{1/2+}\text{--SO}_4^{2-}$ species (Figures 25 and 26):



Adsorption constants are presented in Table 5, and the surface species and charge distribution at the solid-solution interface is shown in Figure 21.

Predicting the Adsorption of Ligands in Binary Systems

The equilibrium adsorption constants (Table 5) for the reactions that describe the retention of kG, PO₄, AsO₄, and SO₄ were optimized using adsorption data from the single ligand systems. These reactions and constants were used as non-adjustable parameters to predict ligand adsorption in the binary systems. The adsorption of kG in both ionic strength systems was modeled by two monodentate-mononuclear inner-sphere complexes (Figures 17 and 18) as described by the reactions in Eqs. [25] and [26]. For PO₄ adsorption in the low ionic strength systems (0.001 M NaCl) (Figure 20), the adsorption data was modeled using the two inner-sphere complexes as described by the reactions in Eqs. [27] and [28]. To predict kG and PO₄ adsorption in the low ionic strength binary systems, the reactions in Eqs. [25] to [28] and associated optimized adsorption constants (Table 5) were used to predict adsorption. Measured values

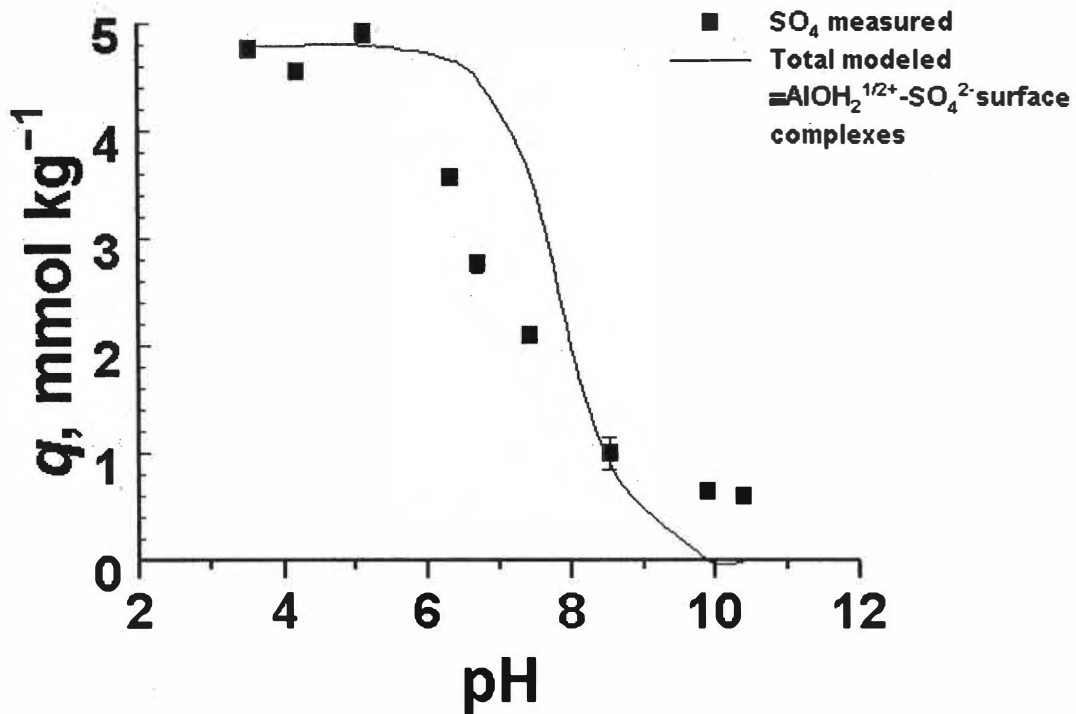


Figure 25. The predicted and experimentally-determined adsorption of sulfate (SO_4) by gibbsite in 0.001 M NaCl . The closed squares represent the experimental data; the solid line represent the predicted formation of $\equiv\text{AlOH}_2^{1/2+}\text{-SO}_4^{2-}$. Error bars represent the standard error (Eq. [22]) of q . Where error bars cannot be seen, they are within the range of the marker.

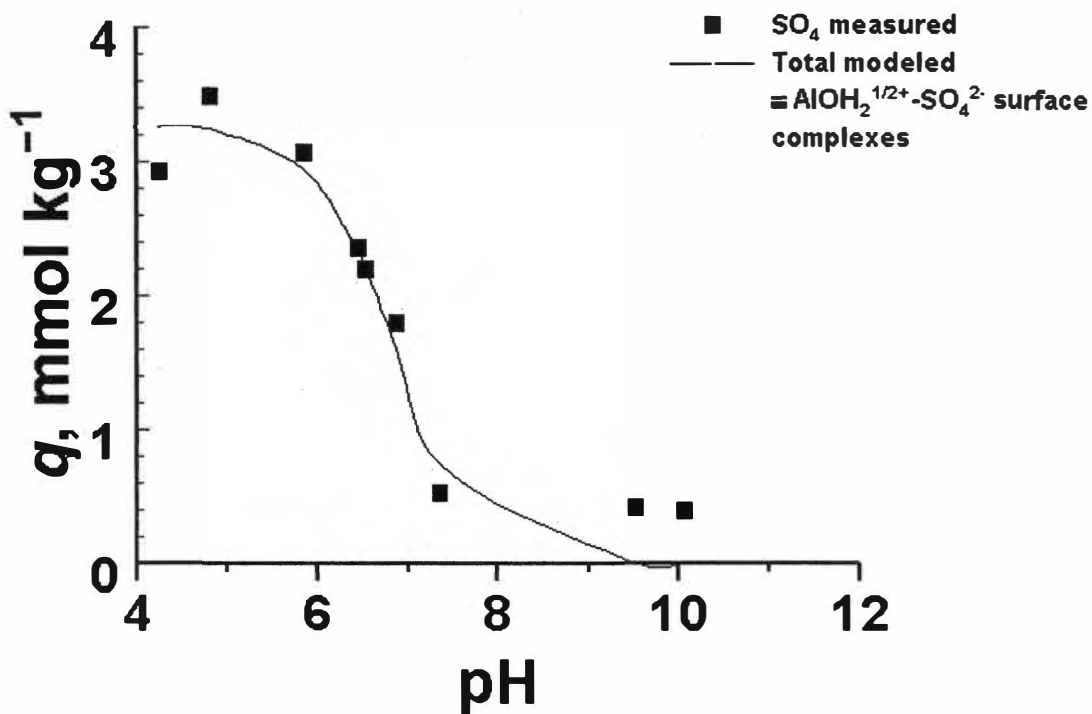


Figure 26. The predicted and experimentally-determined adsorption of sulfate (SO_4) by gibbsite in 0.01 M NaCl . The closed squares represent the experimental data; the solid line represent the predicted formation of $\equiv\text{AlOH}_2^{1/2+}\text{-SO}_4^{2-}$. Error bars represent the standard error (Eq. [22]) of q . Where error bars cannot be seen, they are within the range of the marker.

were then compared with predicted values (Figure 27). The WSOS/DF values for these predictions are presented in Table 6. As seen in Figure 27, both kG and PO₄ adsorption in the 0.001 M NaCl and binary systems were well predicted. For kG and PO₄ adsorption in the high ionic strength (0.01 M NaCl) systems, the reactions in Eqs. [25], [26], [28], and [29] and associated optimized adsorption constants (Table 5) were used to predict adsorption (Figure 28). As seen in Figure 28, the adsorption models describe the adsorption of PO₄ at pH values less than 7. However, PO₄ adsorption above pH 7 and kG adsorption throughout the entire pH range was not well- predicted. For the kG and AsO₄ systems at both ionic strengths FITEQL did not converge. For the kG and SO₄ systems at both ionic strengths, the reactions in Eqs. [25], [26], and [32] and associated optimized adsorption constants (Table 5) were used to predict adsorption (Figures 29 and 30). For the low ionic strength (0.001 M NaCl) system (Figure 29) kG adsorption in the presence of SO₄ was well predicted. However, SO₄ adsorption in the presence of kG was under-predicted by the model at pH values greater than 8. As expected, the model predicts a decrease in adsorbed SO₄ with increasing pH as a result of the loss of positively charged surface functional groups. In the high ionic strength (0.01 M NaCl) (Figure 30) systems, kG adsorption in the presence of SO₄ was accurately described. However, the adsorption of SO₄ in the presence of kG was under-predicted by the model.

The binary modeling efforts are summarized in Table 6. In the case that the FITEQL program converged on the binary system data using optimized intrinsic equilibrium constants from the single ligand systems with relatively low WSOS/DF

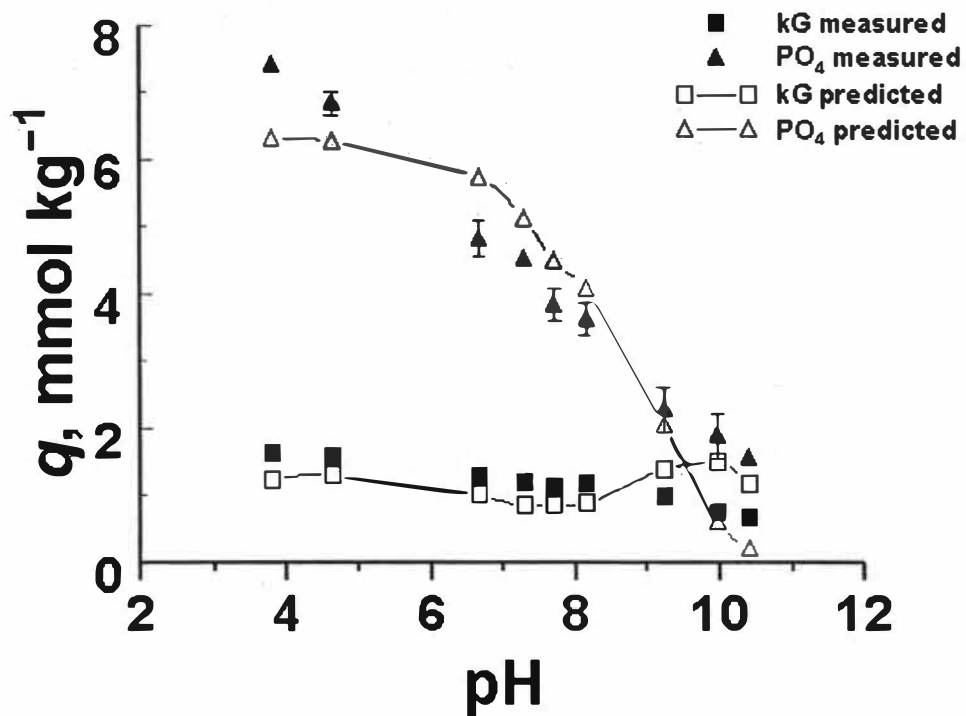


Figure 27. The predicted and experimentally-determined adsorption of ketogluconate (kG) and phosphate (PO₄) by gibbsite (binary system) in 0.001 M NaCl. The closed markers represent the experimental data; the solid lines with open markers represent the predicted adsorption. Error bars represent the standard error (Eq. [22]) of q . Where error bars cannot be seen, they are within the range of the marker.

Table 6. Goodness-of-fit prediction values (WSOS/DF) for binary system adsorption to gibbsite.

Binary system	WSOS/DF value	
	0.001 M NaCl	0.01 M NaCl
kG and PO ₄	30.21	78.29
kG and AsO ₄	No Convergence	No Convergence
kG and SO ₄	43.87	81.6

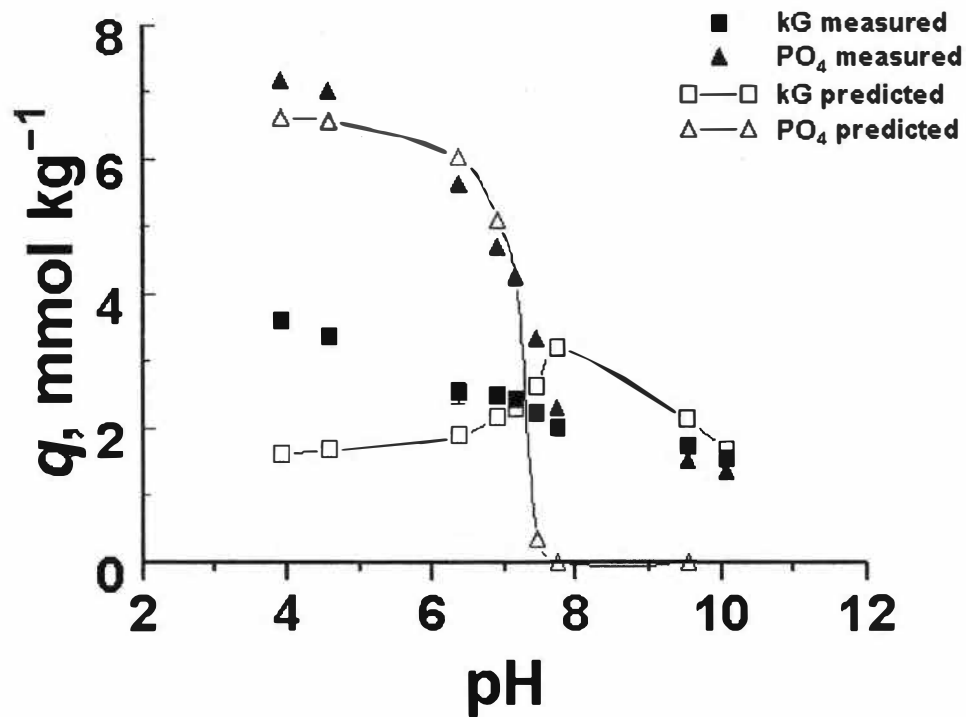


Figure 28. The predicted and experimentally-determined adsorption of ketogluconate (kG) and phosphate (PO₄) by gibbsite (binary system) in 0.01 M NaCl. The closed markers represent the experimental data; the solid lines with open markers represent the predicted adsorption. Error bars represent the standard error (Eq. [22]) of q . Where error bars cannot be seen, they are within the range of the marker.

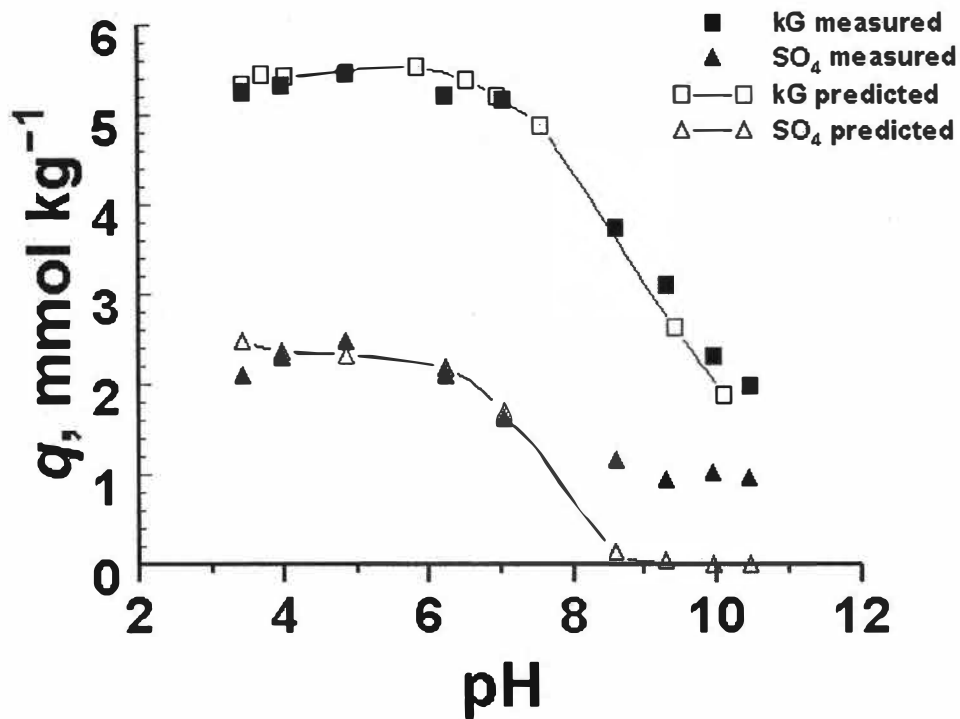


Figure 29. The predicted and experimentally-determined adsorption of ketogluconate (kG) and sulfate (SO₄) by gibbsite (binary system) in 0.001 M NaCl. The closed markers represent the experimental data; the solid lines with open markers represent the predicted adsorption. Error bars represent the standard error (Eq. [22]) of q . Where error bars cannot be seen, they are within the range of the marker.

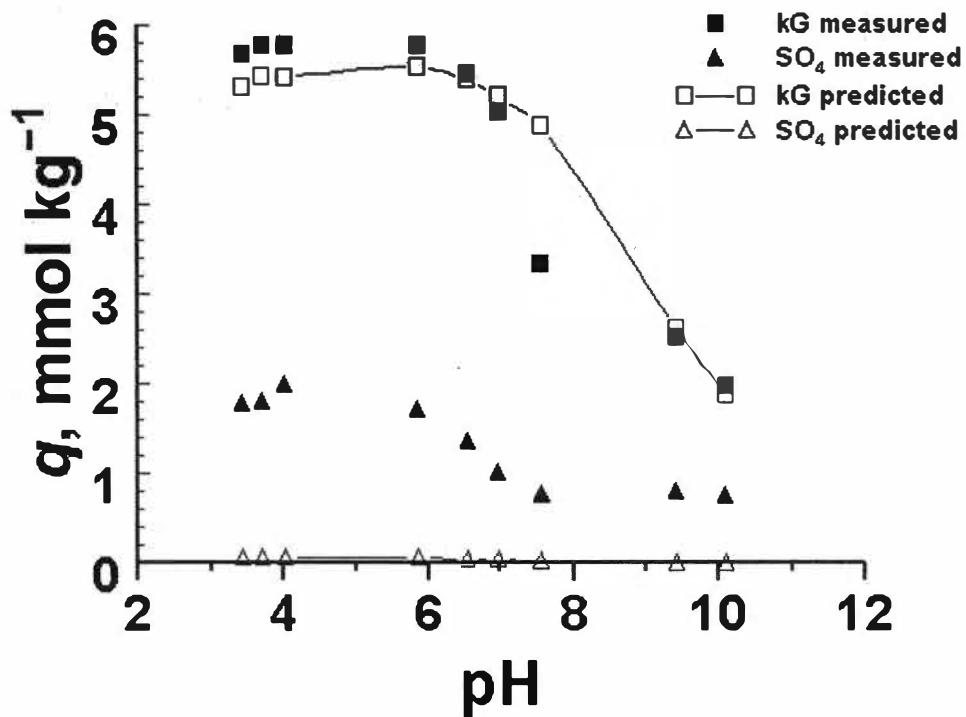


Figure 30. The predicted and experimentally-determined adsorption of ketogluconate (kG) and sulfate (SO₄) by gibbsite (binary system) in 0.01 M NaCl. The closed markers represent the experimental data; the solid lines with open markers represent the predicted adsorption. Error bars represent the standard error (Eq. [22]) of q . Where error bars cannot be seen, they are within the range of the marker.

values it can be concluded that the chemical model accurately described adsorption in both single and binary systems. In the case that the predicted models did not converge with the experimental data, this is an indication that the models used to describe adsorption in the single ligand systems are not accurate. The intrinsic equilibrium constants optimized for in the single ligand systems should theoretically describe adsorption in the binary systems, as all other variables in the experiment (pH and ionic strength conditions) were held constant. Different chemical models may better describe the adsorption data in the systems with relatively high WSOS/DF values, and when the FITEQL program did not converge. In the binary systems where the FITEQL program converged with relatively low WSOS/DF values, it can be concluded that the chemical model used to describe those systems may be used to accurately predict adsorption in more chemically complex systems.

Kaolinite

Effects of pH and Ionic Strength

The adsorption of kG, PO₄ and AsO₄ to kaolinite was similar to that of gibbsite in that retention is at a maximum at low pH values, then decreases with increasing pH. In all cases, less of each ligand adsorbed to kaolinite than to gibbsite at maximum adsorption. However, this may be due to the lower surface area of kaolinite, as well as to the lower concentrations of ≡AlOH functional groups of kaolinite relative to gibbsite. The adsorption of kG by kaolinite is nearly a linear function of solution pH and is independent of ionic strength (Figure 31). In both ionic strength conditions, an adsorption maximum of 4.5 mmolkg⁻¹ occurs near pH 3.5. At the high ionic strength, kG minimum adsorption of approximately 1.0 mmolkg⁻¹ occurs at the highest pH studied. At the low

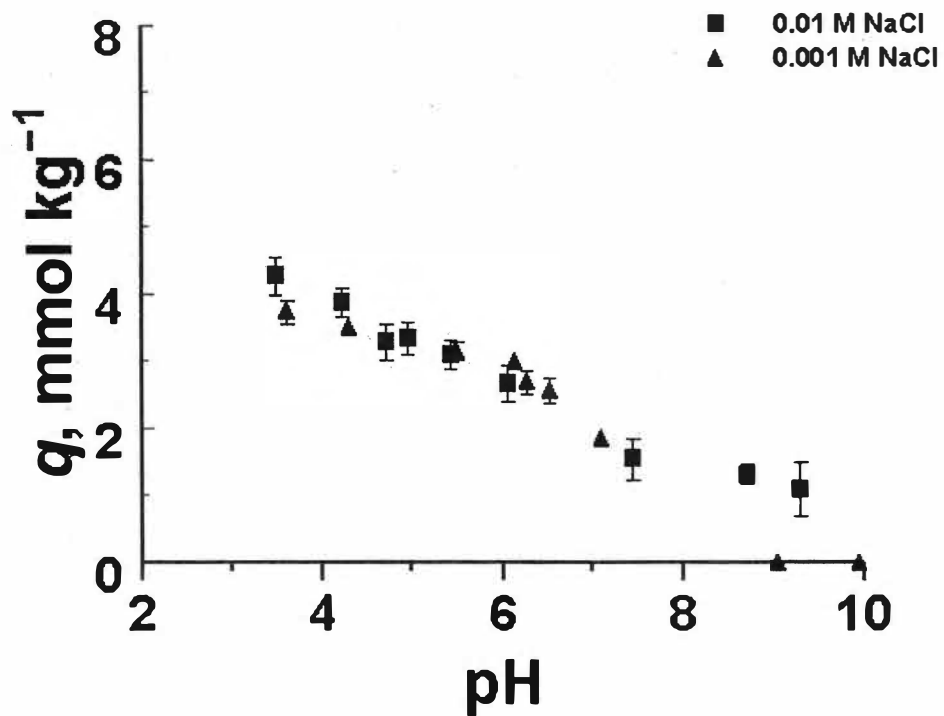


Figure 31. The adsorption edge of 2-ketogluconate (kG) on kaolinite in 0.01 and 0.001 M NaCl. Error bars represent the standard error (Eq. [22]) of q . Where error bars cannot be seen, they are within the range of the marker.

ionic strength, kG adsorption is too low to detect at pH values above 9. The pH_{50} values, the pH at which 50% of q_{max} is achieved, occurs at approximately pH 7 for both the 0.01 and 0.001 M NaCl systems. As was noted for gibbsite, the observation that ionic strength did not impact kG retention is direct evidence that inner-sphere surface complexation reactions are responsible for kG adsorption. This stands to reason, as both gibbsite and kaolinite bear the reactive $\equiv AlOH$ functional group.

The adsorption of PO_4 was also a function of pH (Figures 32). In the high ionic strength (0.01 M NaCl) systems a plateau of maximum adsorption of approximately 7 $mmol\ kg^{-1}$ was observed in the pH 3 to 5 range. Adsorption then decreased with increasing pH to a minimum adsorption of approximately 2 $mmol\ kg^{-1}$ at pH 9. At the low ionic strength (0.001 M NaCl) a maximum adsorption of approximately 5 $mmol\ kg^{-1}$ occurred at pH values below 6, and decreased with increasing pH to a minimum adsorption of approximately 0.5 $mmol\ kg^{-1}$ at pH 10. The pH_{50} values occurred near pH 8 in both systems. Ionic strength appeared to impact PO_4 adsorption to kaolinite to a greater degree than to gibbsite. This was not expected. Phosphate adsorption should not be impacted by ionic strength, or PO_4 retention should be greater in the lower ionic strength systems. The observed retention behavior of PO_4 as a function of ionic strength could not be explained.

The adsorption of AsO_4 to kaolinite was a function of pH (Figure 33) and was similar to that of PO_4 . In the high ionic strength (0.01 M NaCl) system, adsorption in the pH 3 to 6 range was approximately 6 $mmol\ kg^{-1}$, and then decreased with increasing pH to a minimum adsorption of 1.8 $mmol\ kg^{-1}$ at pH 9. The pH_{50} value occurs at approximately 8. In the low ionic strength (0.001 M NaCl) system, a plateau of

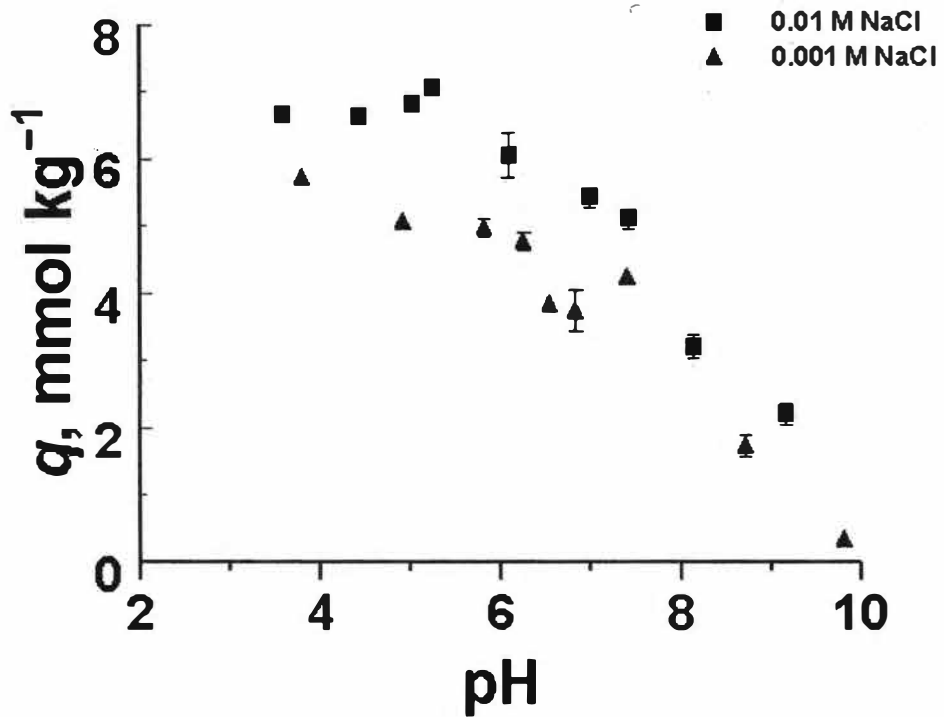


Figure 32. The adsorption edge of phosphate (PO_4) on kaolinite in 0.01 and 0.001 M NaCl. Error bars represent the standard error (Eq. [22]) of q . Where error bars cannot be seen, they are within the range of the marker.

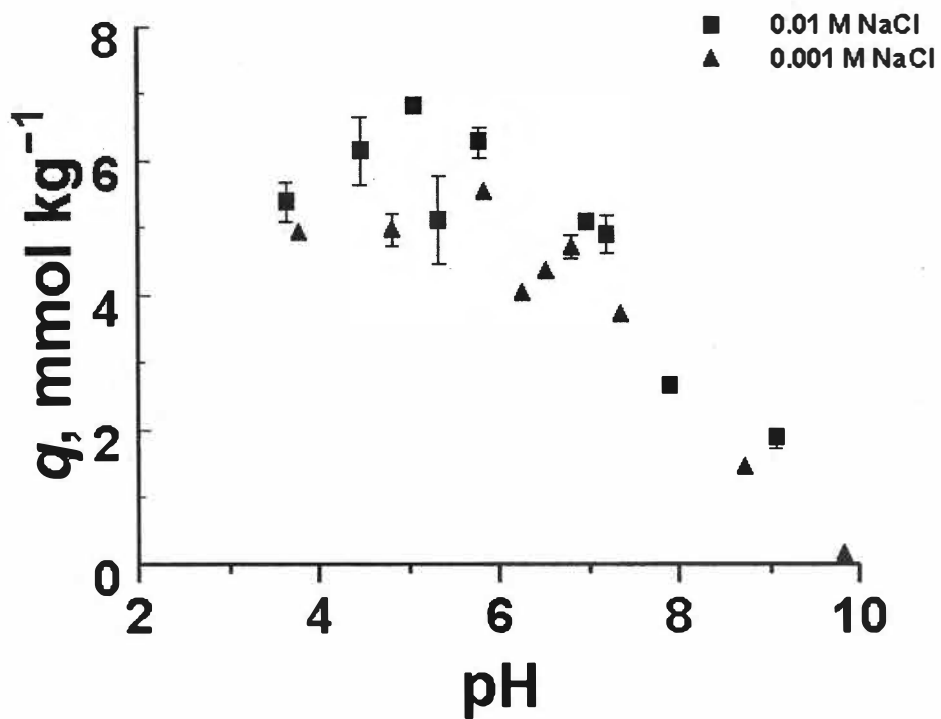


Figure 33. The adsorption edge of arsenate (AsO_4) on kaolinite in 0.01 and 0.001 M NaCl. Error bars represent the standard error (Eq. [22]) of q . Where error bars cannot be seen, they are within the range of the marker.

maximum adsorption of approximately 5 mmol kg^{-1} occurs in the pH 3.5 to 6.0 range, and adsorption decreases with increasing pH. Adsorption approaches zero near pH 10. As in the PO_4 systems, AsO_4 adsorption maximum is greater at the higher ionic strength than observed in the low ionic strength system. Again, this is contrary to what is expected.

The adsorption of SO_4 by kaolinite ranged between approximately 0 and 1.0 mmol kg^{-1} throughout the pH range studied (Figure 34). Ionic strength had little apparent impact on SO_4 adsorption, as SO_4 adsorption was minimal.

Effects of Inorganic Ligands on 2-Ketogluconate Adsorption

The effect of inorganic ligands on the adsorption on kG by kaolinite was very similar to that of gibbsite (Figure 35 and 36). The adsorption of kG was decreased in the presence of specifically adsorbed ligands (PO_4 and AsO_4) and was not significantly affected by the presence of the non-specifically adsorbed SO_4 ligand at pH values above 6. At low pH values ($\text{pH} < 7$), kG adsorption was decreased by approximately 50% in the presence of PO_4 and AsO_4 . Further, kG adsorption becomes minimal at higher pH values (pH 7 to 10). In the low ionic strength system (0.001 M NaCl), the kG adsorption maximum in the presence of PO_4 and AsO_4 was decreased by approximately 47% from that in the absence of these ligands at pH 3.5. At pH 5, kG adsorption in the presence of PO_4 was decreased by approximately 85% from kG adsorption in the absence of PO_4 . The difference in adsorption between kG alone and kG in the presence of PO_4 or AsO_4 gradually decreases with increasing pH, and approaches zero near pH 10. As was noted for the gibbsite systems, the decrease in kG adsorption in the presence of the specifically

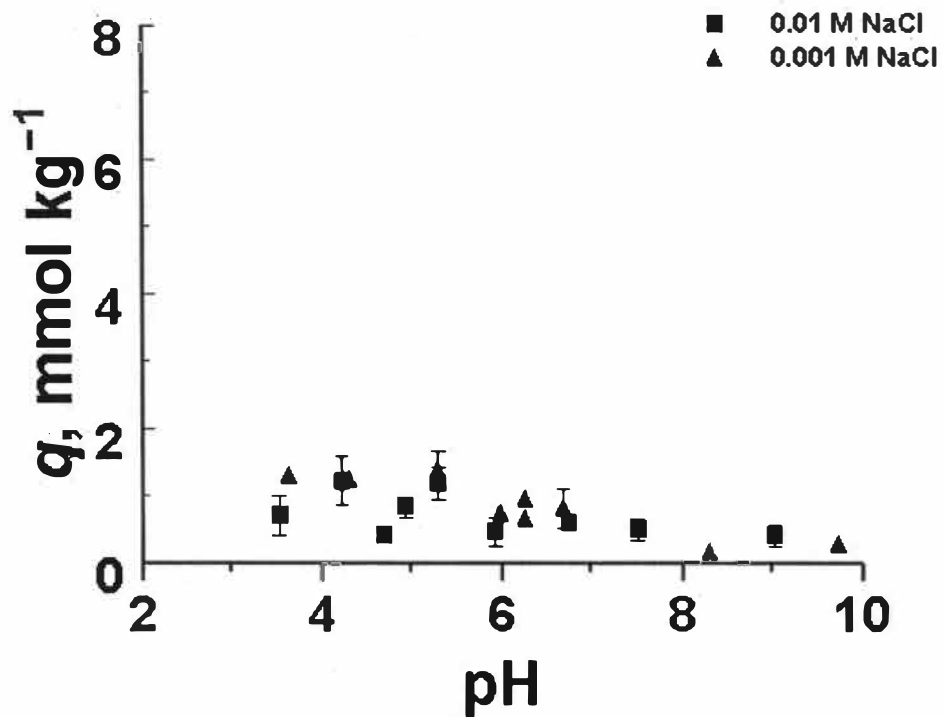


Figure 34. The adsorption edge of sulfate (SO_4) on kaolinite in 0.01 and 0.001 M NaCl. Error bars represent the standard error (Eq. [22]) of q . Where error bars cannot be seen, they are within the range of the marker.

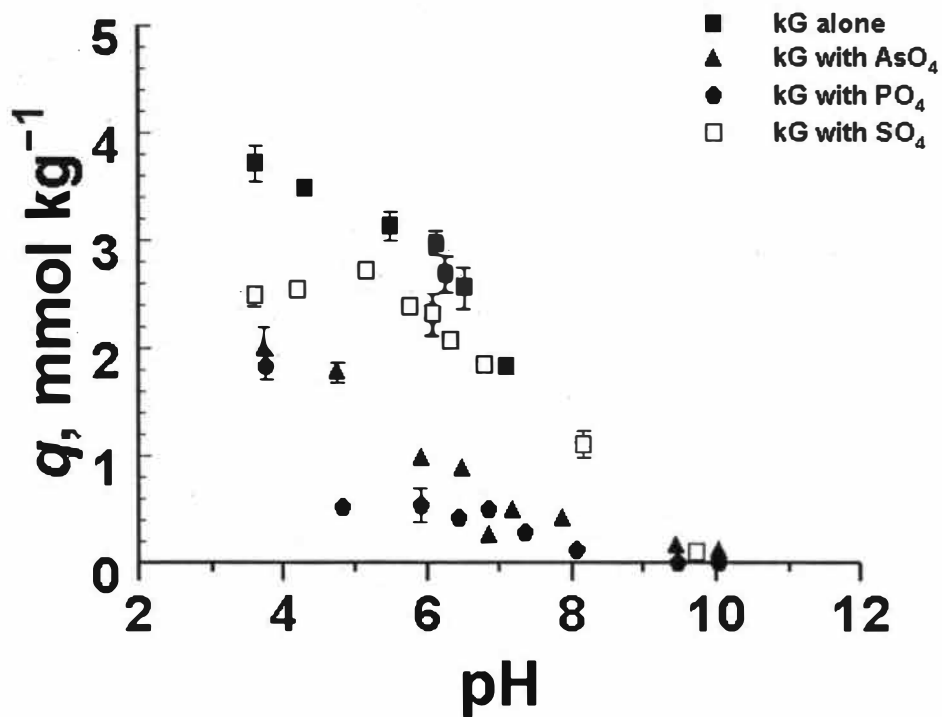


Figure 35. The adsorption of ketogluconate (kG) to kaolinite in 0.001 M NaCl in the presence and absence of AsO_4 , PO_4 , and SO_4 . Error bars represent the standard error (Eq. [22]) of q . Where error bars cannot be seen, they are within the range of the marker.

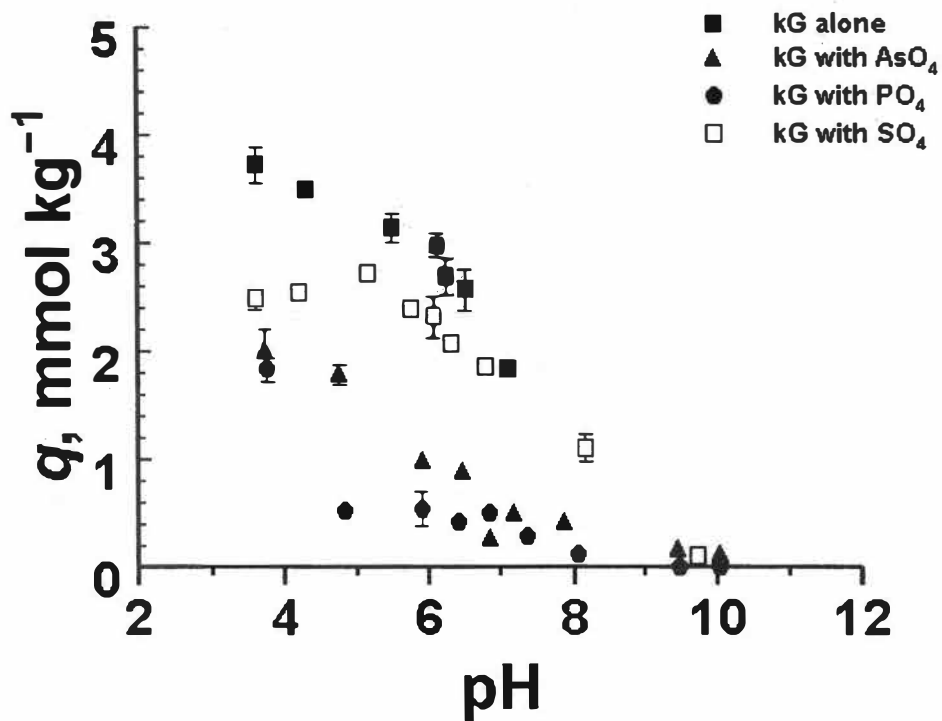


Figure 36. The adsorption of ketogluconate (kG) to kaolinite in 0.01 M NaCl in the presence and absence of AsO₄, PO₄, and SO₄. Error bars represent the standard error (Eq. [22]) of q . Where error bars cannot be seen, they are within the range of the marker.

adsorbed ligands compared to that in the absence of these ligands is evidence that kG adsorbs to kaolinite via inner-sphere mechanisms. The kG adsorption maximum (in pH<5 solutions) is decreased by about 32% in the presence of SO₄ relative to kG adsorption in the absence of SO₄. Above pH 5 SO₄ does not impact kG adsorption behavior. This effect was also observed in the binary gibbsite systems, and supports the hypothesis of previous research that SO₄ may participate in inner-sphere adsorption pH values less than 6 (He et al., 1997; Rahnemaie et al., 2005; Jara et al., 2006).

Effects of 2-Ketogluconate on the Adsorption of Phosphate, Arsenate, and Sulfate

The adsorption of PO₄ and AsO₄ was affected by the presence of kG in both 0.001 and 0.001 M NaCl, while SO₄ adsorption was not influenced by kG (Figures 37 and 38). In the high ionic strength system, the AsO₄ adsorption maximum was reduced by 50%, while the PO₄ adsorption maximum was not affected by kG. The adsorption of AsO₄ at the high ionic strength is significantly reduced in the presence of kG at all pH values studied, while kG had no impact on PO₄ adsorption throughout the pH range studied. In the low ionic strength system (0.001 M NaCl), the impact of kG on PO₄ and AsO₄ was pronounced, reducing the AsO₄ adsorption maximum by 40% and that of PO₄ by 33%. However, only AsO₄ retention was influenced by kG at pH values greater than 6.

Surface Complexation Modeling

The ligand surface complexation models established using the gibbsite single-ligand systems (Table 5) were used as non-adjustable parameters to predict adsorption in the single- and multi-ligand kaolinite systems. The goodness-of-fit parameters (WSOS/DF values) for each system are presented in Table 7. The predicted vs.

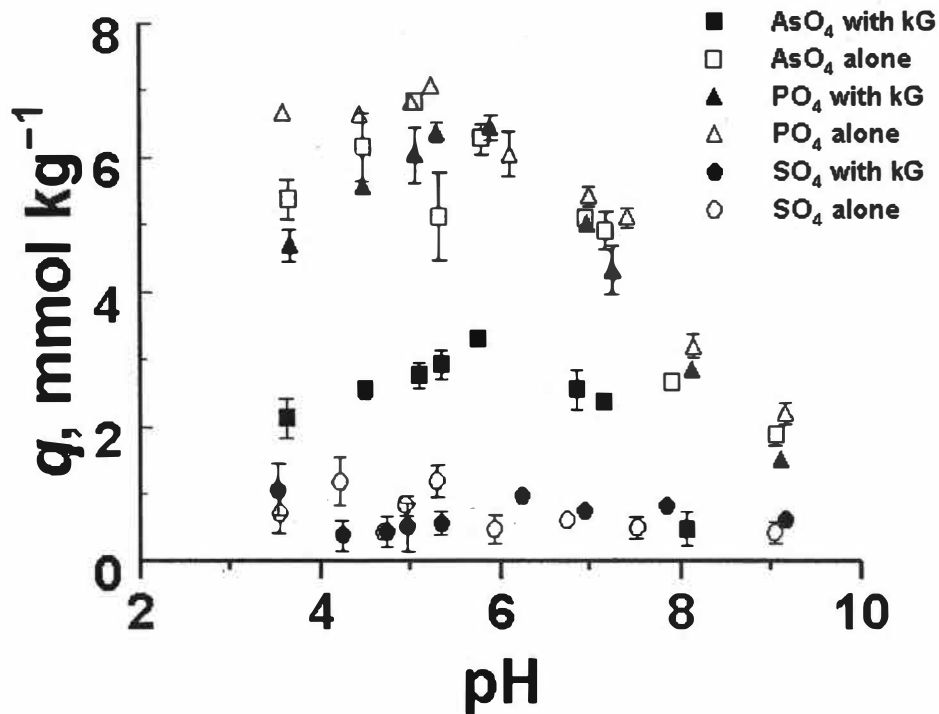


Figure 37. The effect of ketogluconate (kG) on the adsorption of AsO_4 , PO_4 , and SO_4 to kaolinite in 0.01 M NaCl. Error bars represent the standard error (Eq. [22]) of q . Where error bars cannot be seen, they are within the range of the marker.

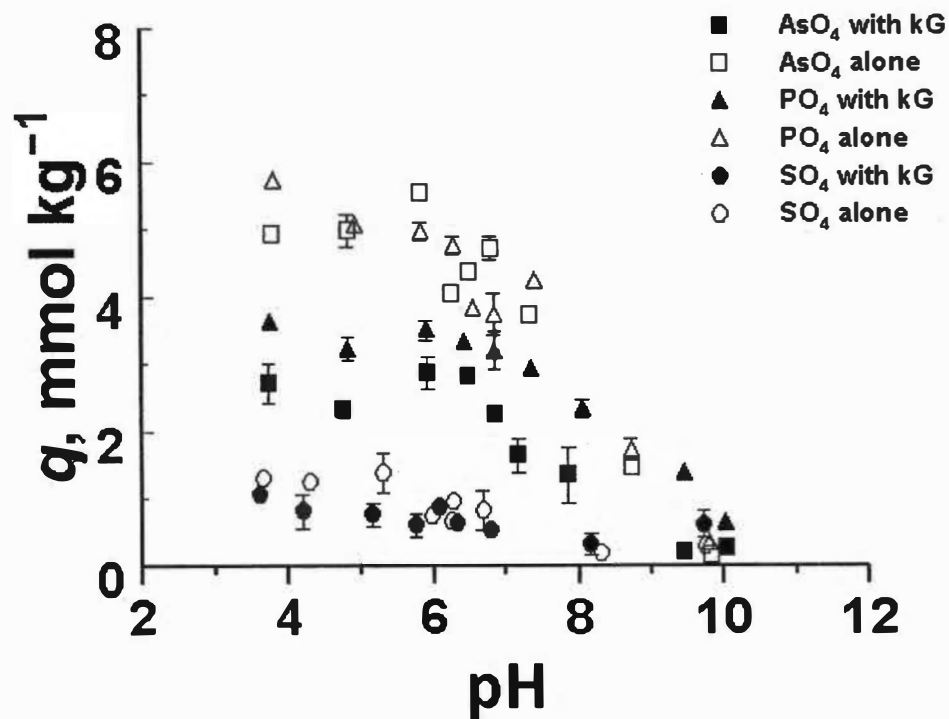


Figure 38. The effect of ketogluconate (kG) on the adsorption of AsO₄, PO₄, and SO₄ to kaolinite in 0.001 M NaCl. Error bars represent the standard error (Eq. [22]) of q . Where error bars cannot be seen, they are within the range of the marker.

Table 7. Goodness-of-fit parameters (WSOS/DF values) for ligand adsorption to kaolinite.

Adsorption system	Goodness-of-fit (WSOS/DF) values	
	0.001 M NaCl	0.01 M NaCl
2-Ketogluconate alone	NC	16.00
Phosphate alone	35.86	NC
Arsenate alone	21.88	329.88
Sulfate alone	5.79	9.99
2-Ketogluconate and phosphate	30.21	NC
2-Ketogluconate and arsenate	NC	NC
2-Ketogluconate and sulfate	23.10	32.18

NC = No convergence of the FITEQL program to the adsorption data.

experimental values of kG adsorption to kaolinite in 0.01 *M* NaCl is shown in Figure 39. In general, the chemical model predicts kG retention by kaolinite as a function of pH. This suggests that AsO₄ surface complexation models developed from the gibbsite adsorption data may not be correct. This is an indication that the chemical model and associated equilibrium values used in modeling kG adsorption to the ≡AlOH functional group on gibbsite may also be employed to describe kG adsorption by kaolinite. In the low ionic strength system (0.001 *M* NaCl), the chemical model used to describe kG adsorption to gibbsite did not converge due to mathematical instabilities in the FITEQL program.

The predicted vs. experimental values of PO₄ adsorption to kaolinite in 0.001 *M* NaCl is shown in Figure 40. Overall, the predicted model accurately describes PO₄ adsorption. This is an indication that the chemical model and associated equilibrium values used to model PO₄ adsorption by gibbsite at the low ionic strength may also be employed to describe the adsorption of PO₄ by kaolinite. As was observed with kG retention in the 0.001 *M* NaCl, the numerical algorithms in FITEQL did not converge, and PO₄ adsorption could not be predicted.

The predicted vs. experimental values of AsO₄ adsorption to kaolinite in the 0.001 *M* NaCl and 0.01 *M* NaCl systems is shown in Figures 41 and 42. The chemical models accurately describe AsO₄ adsorption. This is an indication that the chemical model and associated equilibrium values used in modeling AsO₄ adsorption to gibbsite in the high ionic strength system may accurately describe that of kaolinite adsorption. However, in the low ionic strength system, the predicted model under-predicts AsO₄ adsorption throughout the entire pH range of the study. This indicates that the chemical model and

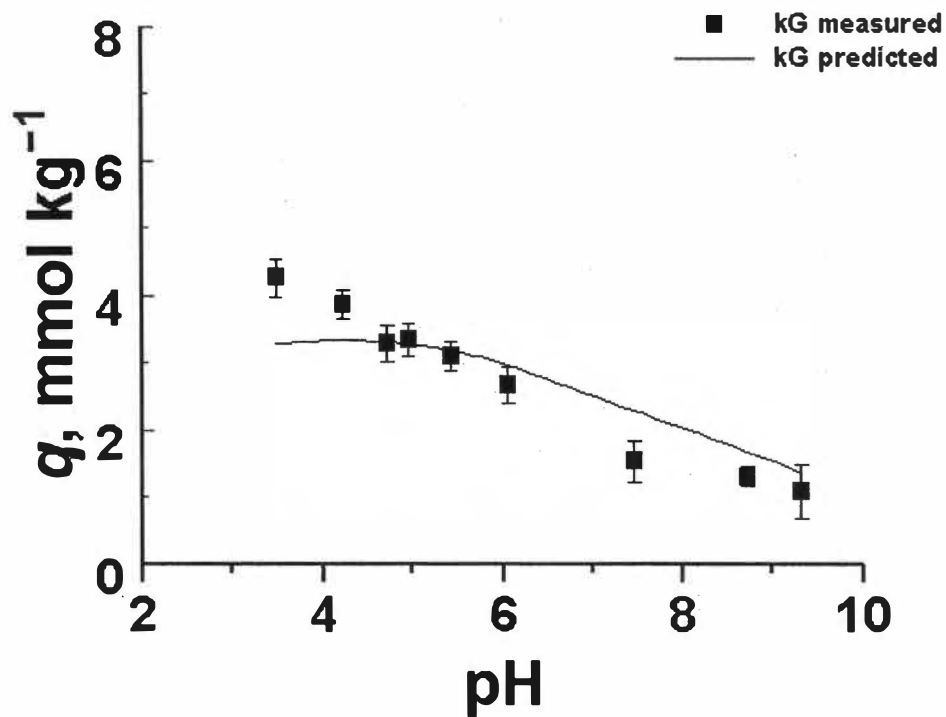


Figure 39. The predicted and experimentally-determined adsorption of ketogluconate (kG) by kaolinite in 0.01 M NaCl. The closed squares represent the experimental data, and the solid line represents predicted adsorption. Error bars represent the standard error (Eq. [22]) of q . Where error bars cannot be seen, they are within the range of the marker.

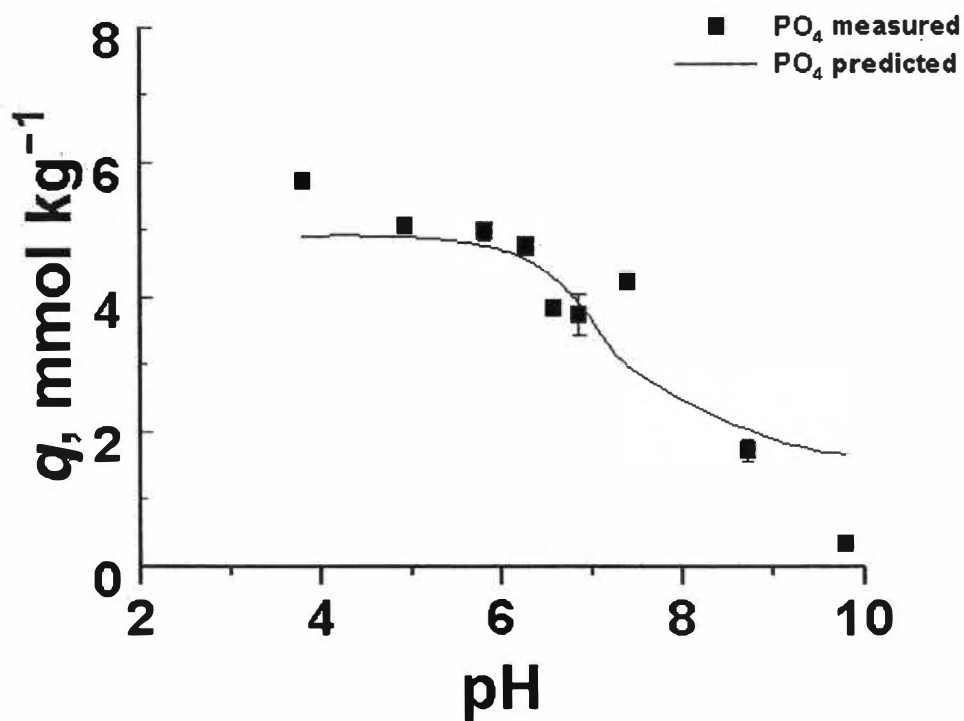


Figure 40. The predicted and experimentally-determined adsorption of phosphate (PO₄) by kaolinite in 0.001 M NaCl. The closed squares represent the experimental data, and the solid line represents predicted adsorption. Error bars represent the standard error (Eq. [22]) of q . Where error bars cannot be seen, they are within the range of the marker.

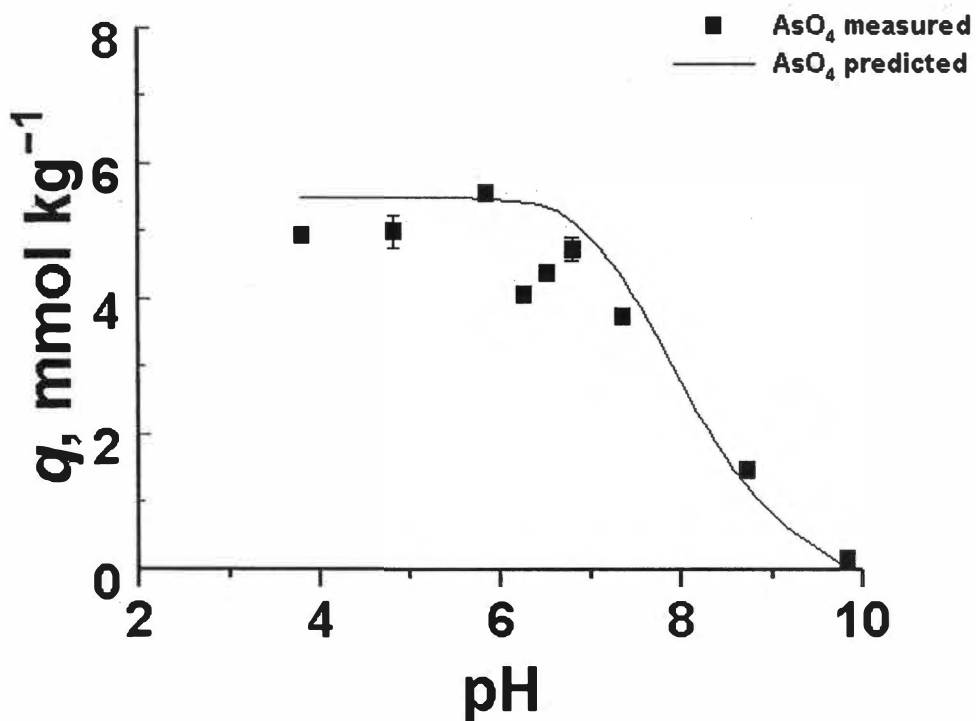


Figure 41. The predicted and experimentally-determined adsorption of arsenate (AsO_4) by kaolinite in 0.001 M NaCl . The closed squares represent the experimental data, and the solid line represents predicted adsorption. Error bars represent the standard error (Eq. [22]) of q . Where error bars cannot be seen, they are within the range of the marker.

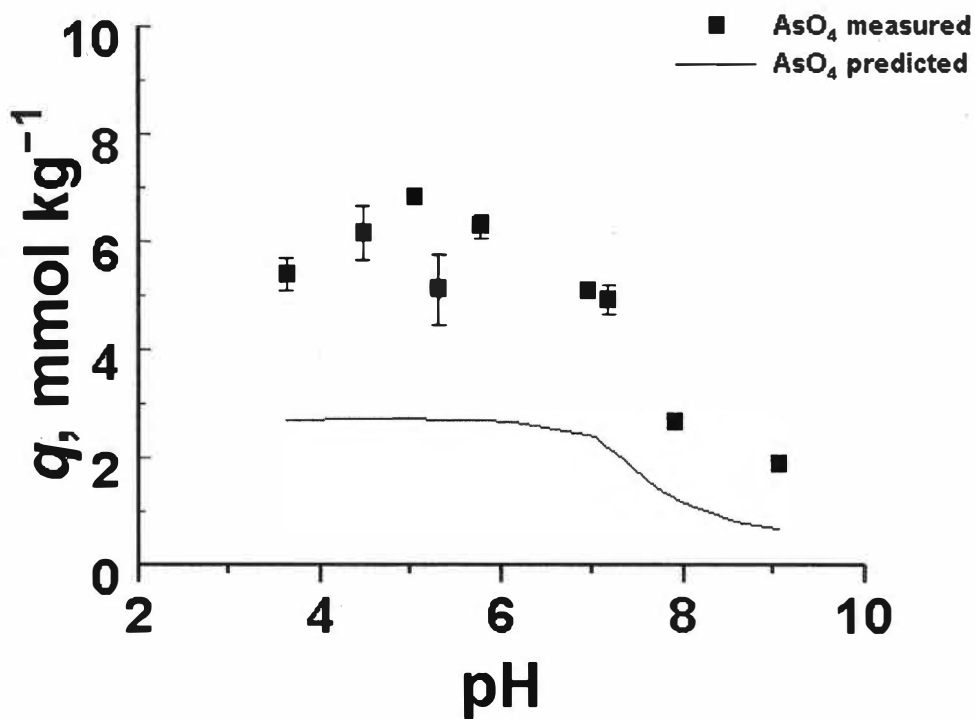


Figure 42. The predicted and experimentally-determined adsorption of arsenate (AsO_4) by kaolinite in 0.01 M NaCl . The closed squares represent the experimental data, and the solid line represents predicted adsorption. Error bars represent the standard error (Eq. [22]) of q . Where error bars cannot be seen, they are within the range of the marker.

associated equilibrium constants used in modeling AsO_4 adsorption to gibbsite at the low ionic strength does not accurately describe AsO_4 retention by kaolinite. This result suggests that AsO_4 surface complexation models developed from the gibbsite adsorption data may not be correct.

The predicted vs. experimental values of SO_4 adsorption to kaolinite in 0.001 *M* NaCl and 0.01 *M* NaCl is shown in Figures 43 and 44. Overall, the model predicts SO_4 adsorption throughout the entire pH range of the study. This is an indication that the chemical models and associated equilibrium constants used in modeling SO_4 adsorption to gibbsite can be used to accurately describe SO_4 retention by kaolinite. This result also substantiates the hypothesis that SO_4 is retained by electrostatic (outer-sphere) mechanisms.

The predicted vs. experimental values of kG and PO_4 adsorption to kaolinite in 0.001 *M* NaCl is shown in Figure 45. Overall, the model predicts kG and PO_4 adsorption throughout the entire pH range of the study. This is an indication that the chemical models and associated equilibrium constants used in modeling kG and PO_4 adsorption to gibbsite can be used to accurately describe kG and PO_4 retention by kaolinite. In the 0.01 *M* NaCl system, the numerical algorithms in FITEQL did not converge, and kG and PO_4 adsorption could not be predicted.

The predicted vs. experimental values of kG and SO_4 adsorption to kaolinite in 0.001 *M* NaCl and 0.01 *M* NaCl is shown in Figures 46 and 47. Overall, in both ionic strength systems, the model predicts kG adsorption throughout the entire pH range of the

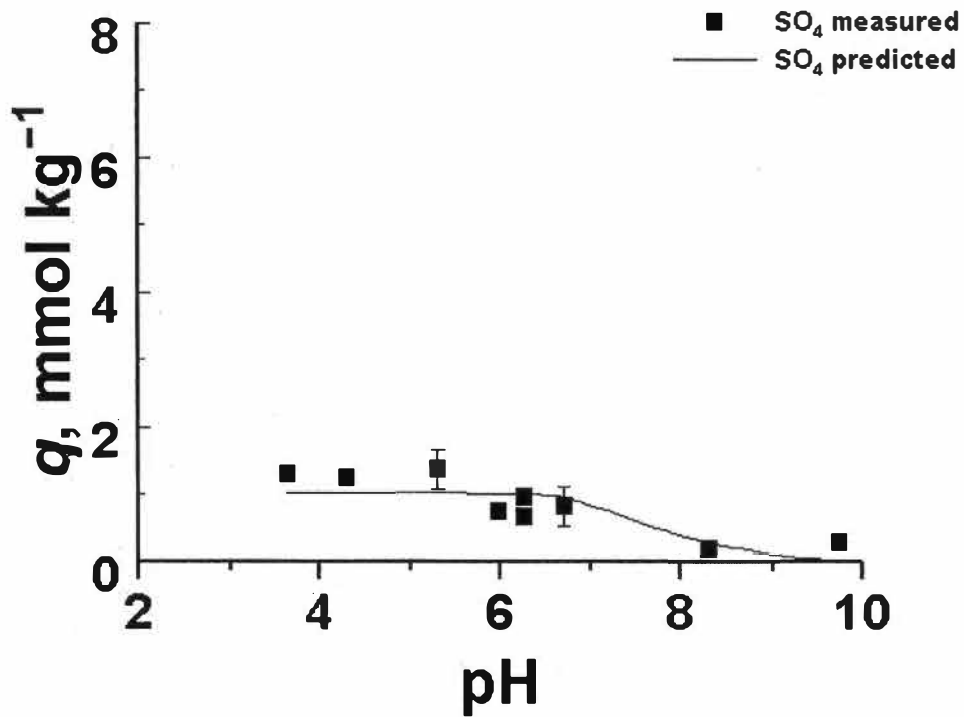


Figure 43. The predicted and experimentally-determined adsorption of sulfate (SO₄) by kaolinite in 0.001 M NaCl. The closed squares represent the experimental data, and the solid line represents predicted adsorption. Error bars represent the standard error (Eq. [22]) of q . Where error bars cannot be seen, they are within the range of the marker.

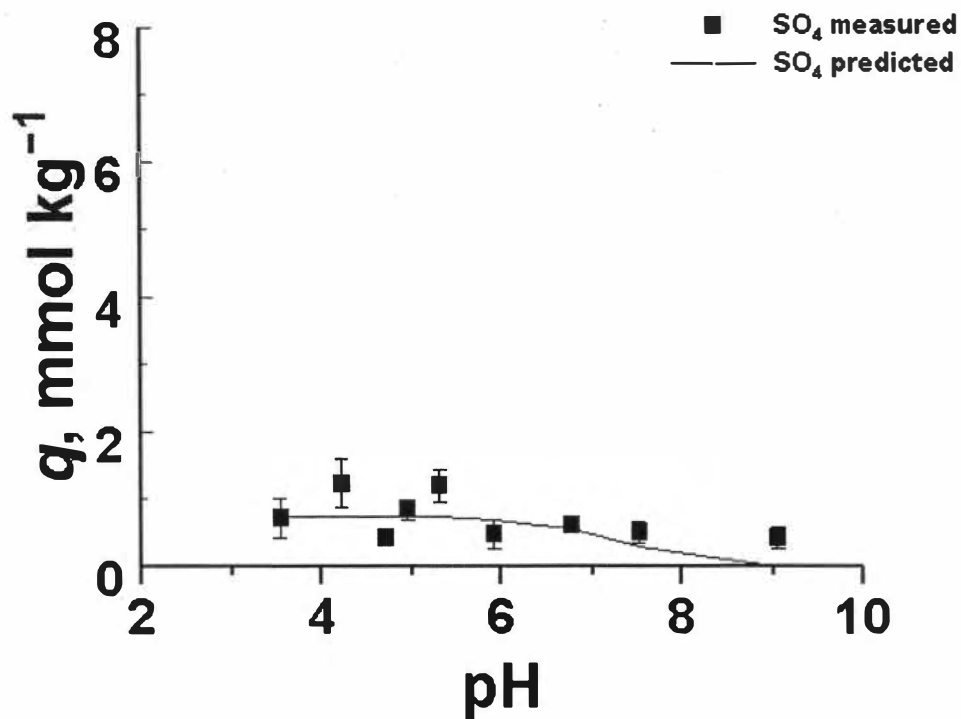


Figure 44. The predicted and experimentally-determined adsorption of sulfate (SO_4) by kaolinite in 0.01 M NaCl . The closed squares represent the experimental data, and the solid line represents predicted adsorption. Error bars represent the standard error (Eq. [22]) of q . Where error bars cannot be seen, they are within the range of the marker.

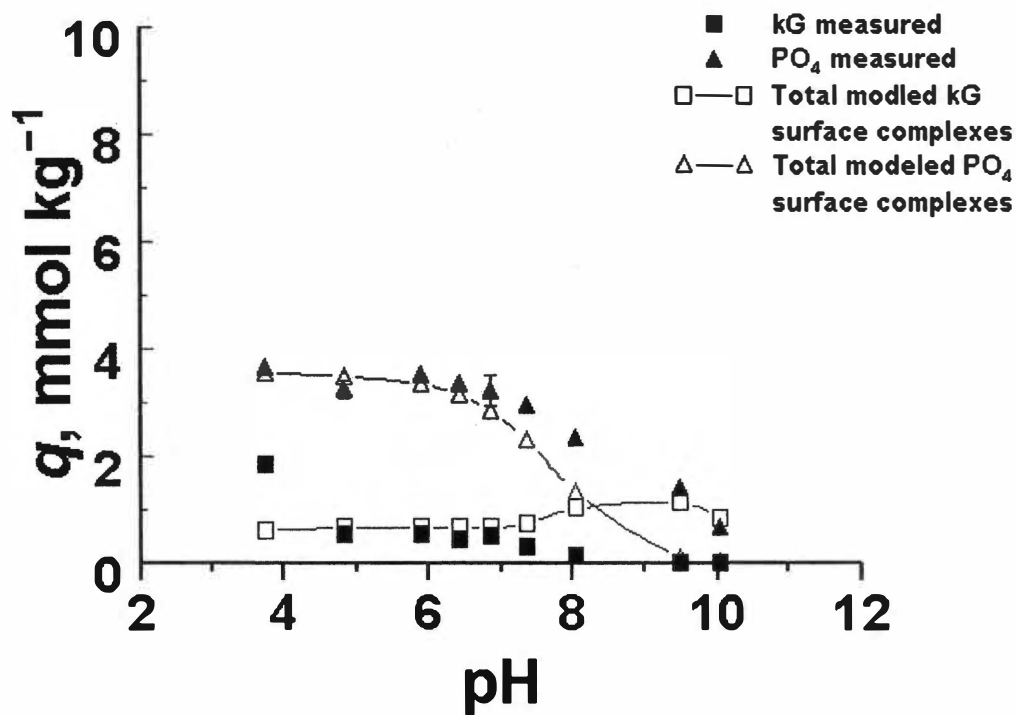


Figure 45. The predicted and experimentally-determined adsorption of 2-ketogluconate (kG) and phosphate (PO₄) by kaolinite in 0.001 M NaCl. The closed squares represent the experimental data, and the solid line represents predicted adsorption. Error bars represent the standard error (Eq. [22]) of q . Where error bars cannot be seen, they are within the range of the marker.

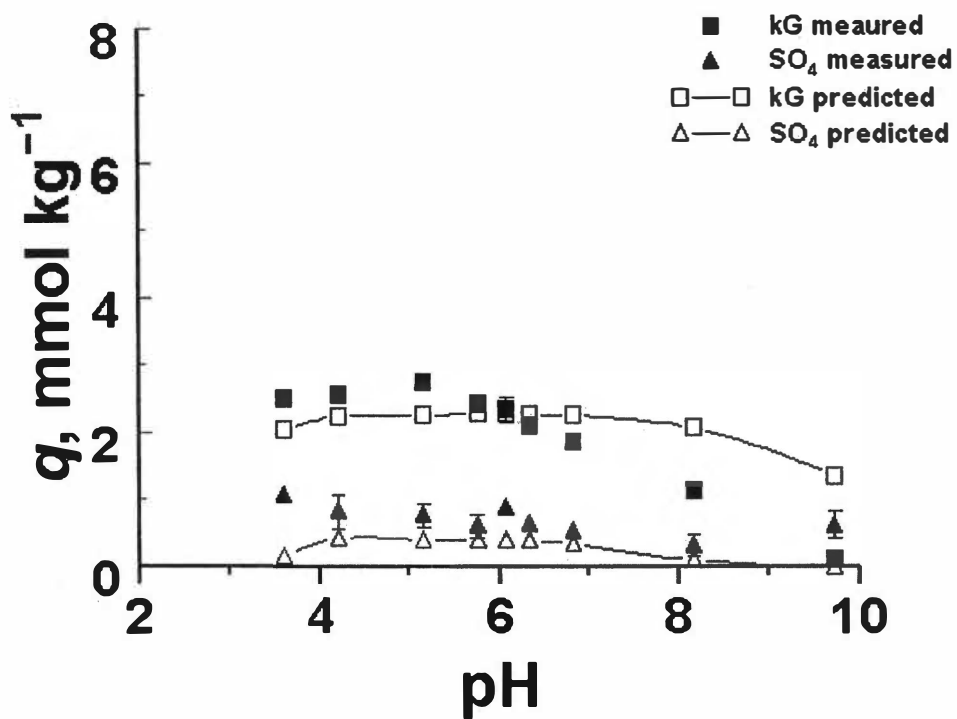


Figure 46. The predicted and experimentally-determined adsorption of 2-ketogluconate (kG) and sulfate (SO₄) by kaolinite in 0.001 M NaCl. The closed squares represent the experimental data, and the solid line represents predicted adsorption. Error bars represent the standard error (Eq. [22]) of q . Where error bars cannot be seen, they are within the range of the marker.

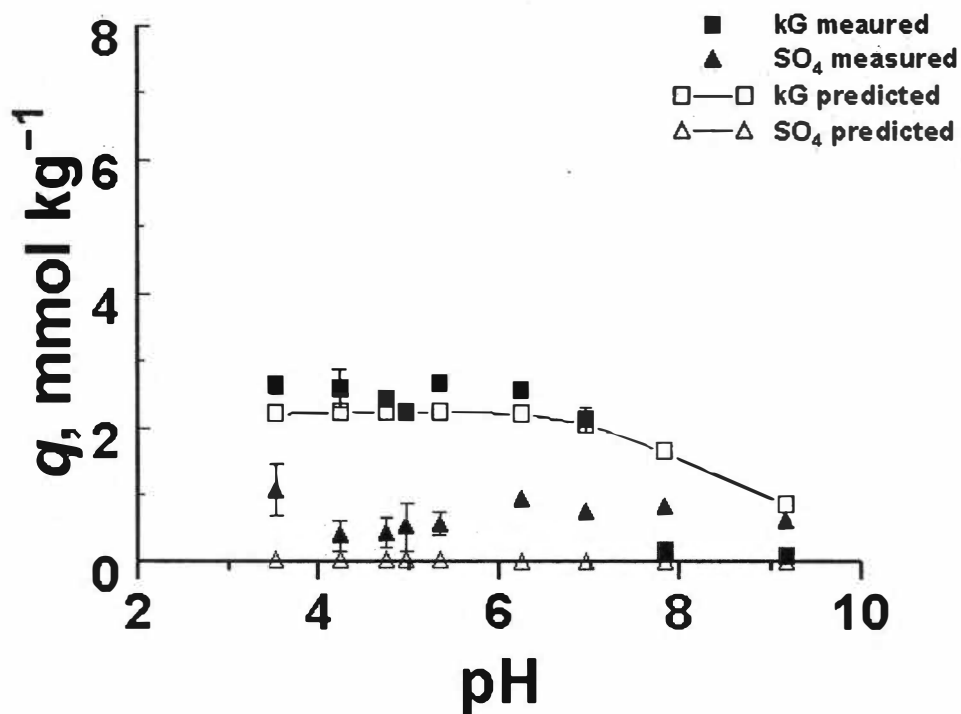


Figure 47. The predicted and experimentally-determined adsorption of 2-ketogluconate (kG) and sulfate (SO₄) by kaolinite in 0.01 M NaCl. The closed squares represent the experimental data, and the solid line represents predicted adsorption. Error bars represent the standard error (Eq. [22]) of q . Where error bars cannot be seen, they are within the range of the marker.

study. This is an indication that the chemical models and associated equilibrium constants used in modeling kG adsorption to gibbsite in the presence of SO_4 , in both ionic strength systems, can be used to accurately describe that in the kaolinite system. The model predicts SO_4 adsorption in the low ionic strength system, while SO_4 adsorption is under predicted in the high ionic strength system. This is an indication that the chemical models and associated equilibrium constants used in modeling SO_4 adsorption to gibbsite in the presence of kG in the low ionic strength system, can be used to model that in the kaolinite system.

For the kG and AsO_4 binary systems, the numerical algorithms in FITEQL did not converge, and kG and AsO_4 adsorption could not be predicted.

Goethite

Effects of pH and Ionic Strength

The adsorption of kG by goethite is a function of solution pH (Figure 48). The adsorption data for the 0.01 M NaCl and 0.001 M NaCl systems mirror each other throughout the studied pH range. Adsorption is at a maximum at pH values below approximately pH 6. Above pH 6, adsorption decreases with increasing pH, irrespective of the ionic strength conditions. In both 0.01 M and 0.001 M NaCl systems, an adsorption maximum of 7.2 mmol kg^{-1} occurs in the pH 3 to 5 range and a minimum adsorption of approximately 2.4 mmol kg^{-1} occurs at the highest pH studied. The pH_{50} values, the pH at which 50% of q_{max} is achieved, is approximately 9 for both the 0.01 and 0.001 M NaCl systems. The kG adsorption edges are similar to those of oxalate and citrate to goethite (Jara et al., 2006). As with the adsorption of kG to gibbsite, the observed kG adsorption edge to goethite may be interpreted as describing either anion exchange or ligand

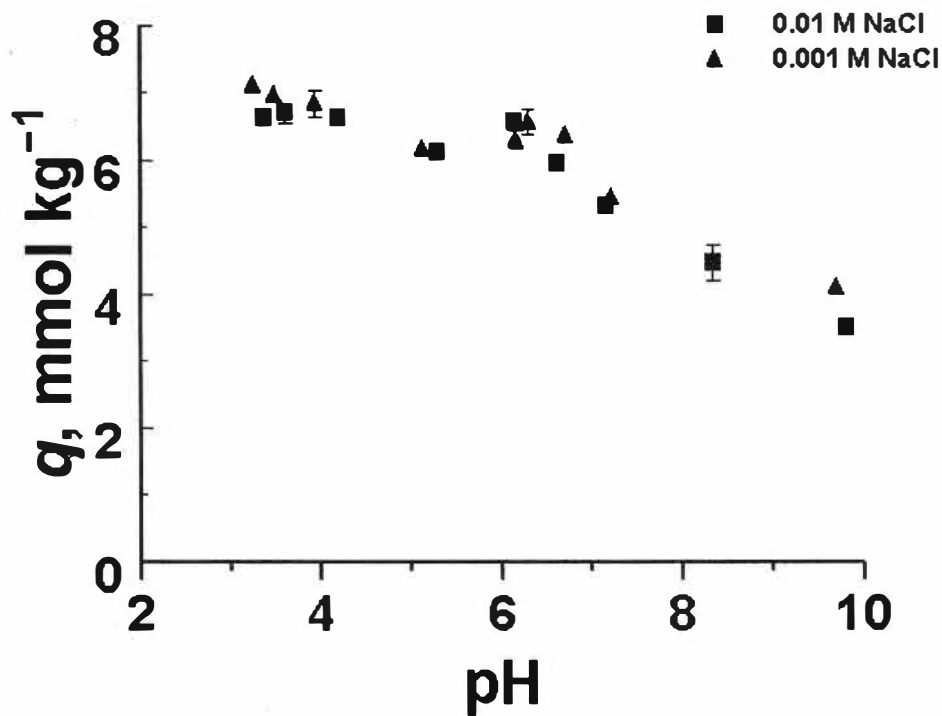


Figure 48. The adsorption edge of 2-ketogluconate (kG) on goethite in 0.01 and 0.001 *M* NaCl. Error bars represent the standard error (Eq. [22]) of *q*. Where error bars cannot be seen, they are within the range of the marker.

Effects of Inorganic Ligands on 2-Ketogluconate Adsorption

exchange. In general, the kG adsorption appears to mirror the expected reduction in $\equiv\text{FeOH}_2^{1/2+}$ concentration with increasing pH, suggesting that kG retention may be electrostatic; thus, participating in an anion exchange process (Eq. [23] substituting Fe for Al). However, as previously explained, the ligand exchange mechanism (Eq. [24]) is directly supported by the observation that kG adsorption by goethite is independent of ionic strength.

In general, the adsorption of kG by goethite was decreased in the presence of specifically adsorbed ligands (PO_4 and AsO_4), and was not significantly affected by the presence of SO_4 at pH values above 7 (Figures 49 and 50). In most cases, and at lower pH values (3 to 7), the adsorption of kG was decreased 50% or more in the presence of PO_4 and AsO_4 , while the difference in adsorption becomes minimal at higher pH values in the 7 to 10 range. In the 0.001 M NaCl systems, all ligands affected kG retention in the pH less than 7 systems. Arsenate had the greatest impact on kG adsorption, decreasing kG retention from 7 mmol kg^{-1} to less than 3 mmol kg^{-1} in the pH 3 to 5 range. Phosphate decreased kG maximum adsorption from 7 mmol kg^{-1} to approximately 5.0 mmol kg^{-1} and SO_4 decreased adsorption to 5.2 mmol kg^{-1} . The influence of AsO_4 on kG retention is also seen at higher pH values, while the impact of PO_4 on kG adsorption becomes minimal in the alkaline systems.

In the 0.01 M NaCl systems, a reduction in adsorbed kG in the presence of AsO_4 and PO_4 was observed into the alkaline pH range, even though the degree of the effect was not as substantial as was seen in the 0.001 M systems. The impact of SO_4 on kG

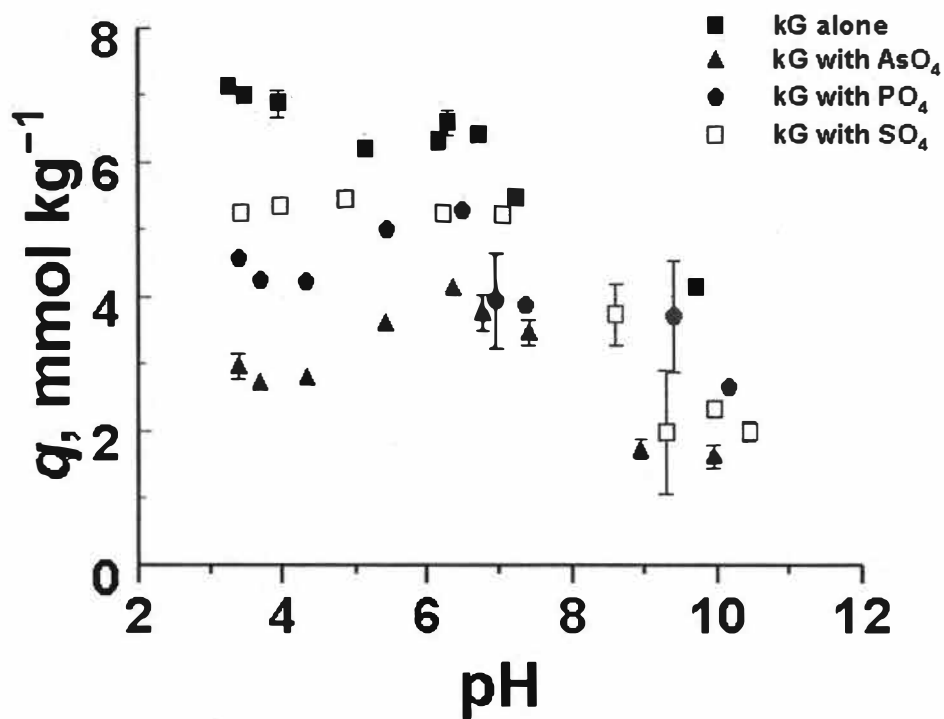


Figure 49. The adsorption of ketogluconate (kG) to goethite in 0.001 M NaCl in the presence and absence of AsO₄, PO₄, and SO₄. Error bars represent the standard error (Eq. [22]) of q . Where error bars cannot be seen, they are within the range of the marker.

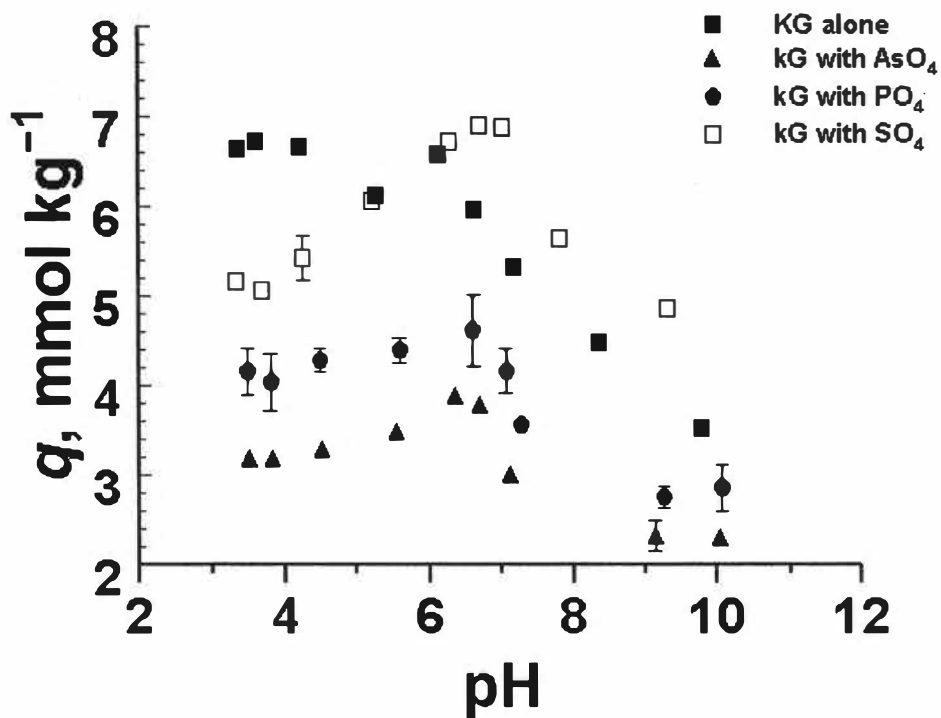
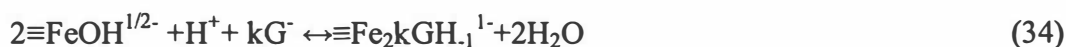


Figure 50. The adsorption of ketogluconate (kG) to goethite in 0.01 M NaCl in the presence and absence of AsO₄, PO₄, and SO₄. Error bars represent the standard error (Eq. [22]) of q . Where error bars cannot be seen, they are within the range of the marker.

adsorption is minimal and restricted to the pH 3 to 5 range. Further, kG retention is influenced by SO₄ only under acidic pH conditions, which corresponds to the pH conditions where SO₄ may be specifically retained; thus, competing with specifically retained kG. Ketogluconate adsorption was decreased to the greatest degree in the presence of AsO₄, and to a lesser degree in the presence of PO₄. This is in accordance with other studies that have concluded that AsO₄ is adsorbed to a greater extent than PO₄ to goethite surfaces (Gao and Mucci, 2001; Violante and Pigna, 2002). The decrease in kG adsorption in the presence of the specifically adsorbed ligands, particularly AsO₄ and PO₄, is further direct evidence that kG is adsorbed via specific mechanisms.

Surface Complexation Modeling

The adsorption of kG by goethite surfaces may be visualized to occur via a number of non-specific and specific mechanisms (Figure 17). Ligand adsorption to goethite was examined with the CD-MUSIC SCM model in conjunction with the FITEQL 4.0 computer code. Although numerous surface complexes were considered (Figure 17), the kG adsorption data in both the 0.001 M and 0.01 M NaCl systems were best described by assuming that kG forms both monodentate-mono-nuclear and monodentate-binuclear inner-sphere surface complexes according to the reactions (Figures 51 and 52):



These two surface species and the distribution of charge at the solid-solution interface are shown in Figure 17. The optimized adsorption constants and goodness-of-fit

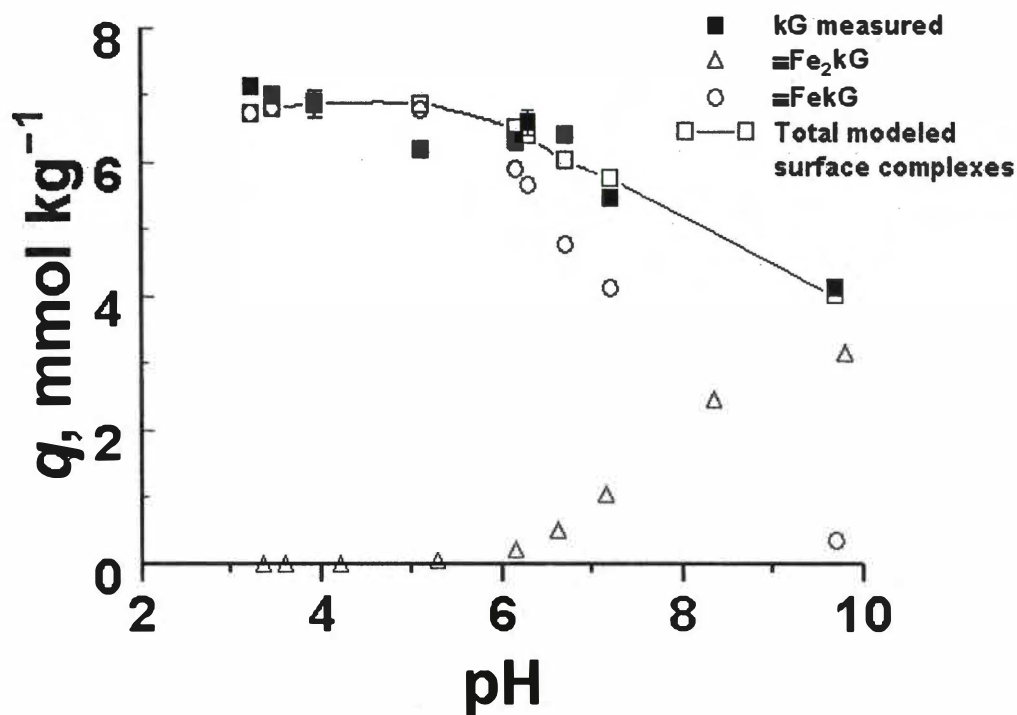


Figure 51. The predicted and experimentally-determined adsorption of ketogluconate (kG) by goethite in 0.001 M NaCl. The closed squares represent the experimental data; diamonds represent the predicted formation of $\equiv\text{FekG}^{1/2-}$ and open circles represent the predicted formation of $\equiv\text{Fe}_2\text{kGH}_1^{-}$. Error bars represent the standard error (Eq. [22]) of q . Where error bars cannot be seen, they are within the range of the marker.

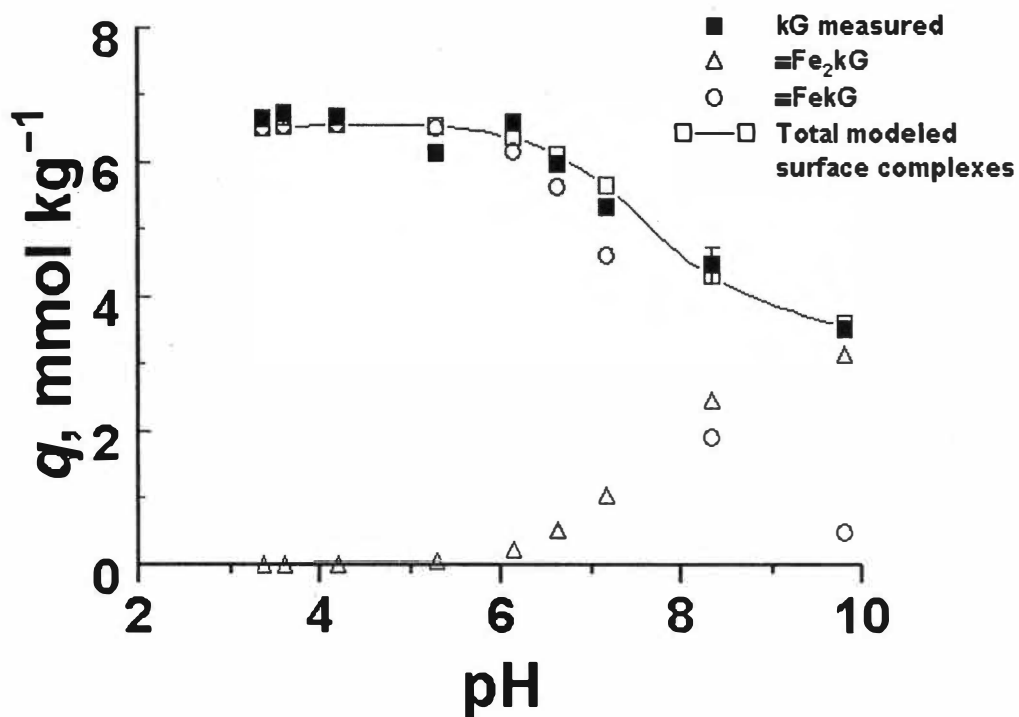


Figure 52. The predicted and experimentally-determined adsorption of ketogluconate (kG) by goethite in 0.01 M NaCl. The closed squares represent the experimental data; diamonds represent the predicted formation of $\equiv\text{FekG}^{1/2-}$ and open circles represent the predicted formation of $\equiv\text{Fe}_2\text{kGH}_1^{1-}$. Error bars represent the standard error (Eq. [22]) of q . Where error bars cannot be seen, they are within the range of the marker.

parameters (WSOS/SF) are shown in Table 8. At pH values that are less than the pK_a of $\equiv\text{FeOH}_2^{1/2+}$, the $\equiv\text{Fe}_2\text{kG}^{1/2-}$ species predominates as a result of Eq. [33]. As H_2O disappears from the goethite surface through the dissociation of $\equiv\text{FeOH}_2^{1/2+}$, the specific retention of kG is facilitated through the dissociation of the kG hydroxyl that is adjacent to the carbonyl group (Nelson and Essington, 2005). The dissociated proton then protonates $\equiv\text{FeOH}^{1/2-}$ sites to create H_2O on the surface (forming $\equiv\text{FeOH}_2^{1/2+}$), which then undergoes ligand exchange with the H_2kG^{2-} species to form the bidentate species $\equiv\text{Fe}_2\text{kGH}_2^{1-}$ (Eq. [33]). In both 0.01 M and 0.001 M NaCl, the chemical model involving the formation of the $\equiv\text{FeOH}_2^{1/2+}$, the $\equiv\text{Fe}_2\text{kG}^{1/2-}$ species accurately describes the adsorption of kG throughout the entire pH range of the study. This supports the conclusion that kG adsorbs to goethite via inner-sphere mechanisms.

Table 8. Goethite surface complexation reactions, FITEQL-optimized intrinsic equilibrium constants (log K values), and associated goodness-of-fit parameters (WSOS/DF values).

Reaction	Log K		WSOS/DF	
	0.001M	0.01M	0.001M	0.01M
	NaCl	NaCl	NaCl	NaCl
$kG^- + \equiv FeOH^{1/2-} + H^+ \Leftrightarrow \equiv Fe_kG^{1/2-} + H_2O$	14.76	15.29	6.00	3.73
$kG^- + 2 \equiv FeOH^{1/2-} + H^+ \Leftrightarrow Fe_2kGH_1^+ + 2H_2O$	22.13	22.76		

IV. Summary

In soils, low-molecular-mass-organic-acid (LMMOA) anions are comprised of a group of water-soluble non-humic substances with an arbitrary maximum molecular weight of approximately 300 to 500 D, and include such compounds as oxalate, formate, citrate, acetate, malate, and succinate. These compounds are principally plant root and microbial exudates (and their derivatives), which are concentrated in the soil rhizosphere and can be found in significant and sustained concentrations (0.1-100 μ M) in these soil solutions. Organic acid anions have been hypothesized to play a major role in many soil processes, including soil mineral solubilization, nutrient and metal mobility and bioavailability, metal detoxification, and in soil structural development. Both plant roots and soil microbes are capable of exuding elevated concentrations of LMMOA anions, and at elevated rates, when stressed for specific mineral nutrients (e.g., iron and phosphorous) and when soil aluminum concentrations reach potentially phytotoxic levels.

One mechanism by which LMMOA anions impact the chemistry of soil constituents is through adsorption reactions. Ligands in the soil solution can adsorb to constant-potential mineral surface sites through specific (inner-sphere or chemisorption) or non-specific (outer-sphere or physical adsorption) mechanisms. The adsorption of LMMOA anions by soil minerals has been investigated in a number of studies. These organic anions, mainly the di- and tri-carboxylates, have been shown to participate in ligand exchange reactions. As such, they may effectively compete with other specifically adsorbed ligands (e.g., PO₄ species) and subsequently increase the phytoavailability of the displaced species.

2-Ketogluconate (kG) is a LMMOA that is a microbial byproduct of glucose oxidation. It is produced by several microbial species known to exist in soils. 2-Ketogluconate has been isolated from the rhizosphere of common crops and it has been found in highest concentrations in well-drained agricultural soils and when P concentrations are limiting

Ketogluconate is diprotic. The carboxyl-group of kG is a relatively strong weak acid ($pK_a=3.00$), while an alcohol group dissociates in strongly alkaline solution ($pK_a = 11.98$) and may participate in metal complexation reactions. It has been shown that kG affects the solubility of calcium phosphates, as well as gibbsite and goethite, via aqueous metal complexation reactions. Determination of adsorption mechanisms of kG, as well as its ability to compete with other ligands for mineral surface sites, is required in order to understand and predict the impact of this ligand on rhizosphere processes.

The adsorption behavior of kG in the presence of arsenate (AsO_4), phosphate (PO_4), and sulfate (SO_4) may be used to infer the adsorption mechanisms of kG. It has been well established that PO_4 and AsO_4 are specifically adsorbed by hydrous metal oxide minerals, while SO_4 has been shown to principally participate in non-specific adsorption reactions. The comparison of kG adsorption behavior in the presence and absence of PO_4 , AsO_4 , and SO_4 can be used to determine the kG adsorption mechanism. Further, kG adsorption as a function of pH may be employed to develop chemical models of surface complexation.

Solution pH and ionic strength are two master variables that affect ligand retention to mineral surface. The pH dictates the ionization of mineral surfaces and ligand dissociation, and the ionic strength influences mineral surface potentials.

Background electrolytes that are known to participate entirely in outer-sphere adsorption (NaCl) affect the adsorption of ligands that participate in outer-sphere adsorption mechanisms. Therefore, adsorbates that display adsorption envelopes (q vs. pH) that are independent of ionic strength are interpreted to indicate relatively strongly bonded surface complexes and specific (nonelectrostatic) adsorption mechanisms. Also, ligand adsorption that exceeds the net positive charge created by the mineral surface, an adsorption maximum or an inflection in the adsorption envelope that occurs when the pH is close to the pK_a of the ligand adsorbate, and adsorption that is influenced by other specifically adsorbed species are all indicators of specific surface interactions.

The adsorption of kG was investigated by characterizing adsorption behavior as a function of pH by gibbsite, goethite, and kaolinite, at two different ionic strength conditions (0.001 M NaCl and 0.01 M NaCl) and in the presence or absence of PO_4 , AsO_4 , and SO_4 . The following adsorption systems were examined: kG alone, SO_4 alone, PO_4 alone, AsO_4 alone, kG with SO_4 , kG with PO_4 , and kG with AsO_4 , each under two ionic strength conditions (0.01 M and 0.001 M NaCl). To investigate the ability of kG to displace adsorbed PO_4 , kG was added to gibbsite systems containing preadsorbed PO_4 . Similarly, the ability PO_4 of to displace adsorbed kG was determined. For each adsorption experiment, ligand retention at nine different pH values in the 3 to 10 range (in triplicate) was characterized.

The adsorption data (q vs. pH) was employed to develop chemical adsorption models using the surface charge distribution multi-site complexation (CD-MUSIC) model. The CD-MUSIC model allows for metal and ligand adsorption by both inner-sphere and outer-sphere mechanisms. The acidity of the solid was assumed to be

controlled by the pK_a of the singly-coordinated $\equiv\text{XOH}$ (where X is Al for gibbsite and kaolinite, and Fe for goethite) functional group. The ligand surface complexation reactions established using the gibbsite single-ligand systems were used as non-adjustable parameters to predict adsorption in the single- and multi-ligand kaolinite systems and in multi-ligand gibbsite systems.

The adsorption of kG by gibbsite, goethite and kaolinite is a function of solution pH and independent of solution ionic strength. The kG adsorption edges are similar to those of oxalate and citrate on allophanes, two compounds known to adsorb via inner-sphere and multidentate mechanisms. Although the kG adsorption edge data can be interpreted to support either anion or ligand exchange, the ligand exchange mechanism is directly supported by the observation that kG adsorption by the constant potential minerals was not influenced by ionic strength. The adsorption of kG was decreased in the presence of specifically adsorbed ligands (PO_4 and AsO_4), and was not significantly affected by the presence of the non-specifically adsorbed SO_4 ligand at pH values above 6. In most cases and at lower pH values, the adsorption of kG was decreased 40% or more in the presence of PO_4 and AsO_4 , while the difference in adsorption becomes minimal at pH values in the 7 to 10 range. In the gibbsite systems PO_4 had the greatest impact on kG adsorption, while AsO_4 had the greatest impact on kG adsorption in the goethite systems. The impact of PO_4 and SO_4 on kG adsorption is similar to the observed impact of these ligands on oxalate and citrate adsorption by synthetic and natural allophanes. The decrease in kG adsorption in the presence of AsO_4 and PO_4 is further evidence that kG is adsorbed via specific mechanisms.

The adsorption of PO_4 , AsO_4 , and SO_4 ($\text{pH} < 6$) was affected by the presence of kG under both ionic strength conditions. The decrease in AsO_4 and PO_4 adsorption in the presence of kG is evidence that kG is effectively competing with these two ligands for mineral surface sites. This further supports the conclusion that kG adsorbs to mineral surface sites via inner-sphere mechanisms.

The adsorption edge experiments that were performed by adding equal concentrations of PO_4 and kG simultaneously resulted in lower adsorption of PO_4 compared to PO_4 adsorption in the absence kG. The addition of kG to gibbsite containing preadsorbed PO_4 did not result in PO_4 displacement, regardless of the concentration of kG. The addition of PO_4 to gibbsite containing preadsorbed kG resulted in the displacement of approximately 45% of the preadsorbed kG in pH 3 to 7 range. The adsorption of preadsorbed kG when PO_4 is added is greater than the adsorption of kG when added simultaneously with PO_4 . These results indicate that kG is not held as strongly as PO_4 to gibbsite surfaces, and that the ability of PO_4 to displace adsorbed kG is greater than the ability of kG to displace adsorbed PO_4 .

The kG adsorption data in both the 0.001 M and 0.01 M NaCl gibbsite systems were best described by assuming that kG forms two monodentate-mononuclear inner-sphere complexes: $\equiv\text{AlkG}^{1/2-}$ and $\equiv\text{AlkGH}_1^{3/2-}$. At pH values that are less than the pK_a of $\equiv\text{AlOH}_2^{1/2+}$, the $\equiv\text{AlkG}^{1/2-}$ species predominates. As H_2O disappears from the gibbsite surface through the dissociation of $\equiv\text{AlOH}_2^{1/2+}$, the specific retention of kG is facilitated through the dissociation of a kG hydroxyl. The dissociated proton then protonates $\equiv\text{AlOH}^{1/2-}$ sites to create H_2O on the surface (forming $\equiv\text{AlOH}_2^{1/2+}$), which then undergoes ligand exchange with the H_1kG^{2-} species to form $\equiv\text{AlkGH}_1^{3/2-}$. The surface-induced

deprotonation of the kG hydroxyl at pH values that are less than the pK_a can be envisioned to occur in a manner similar to that of the citrate hydroxyl.

The adsorption of PO_4 , AsO_4 , and SO_4 to gibbsite was also modeled using the adsorption edge data and the CD-MUSIC SCM. The model that best described PO_4 adsorption to gibbsite was a function of ionic strength. In the low ionic strength systems (0.001 M NaCl), the adsorption data was modeled using the two inner-sphere complexes: $\equiv AlOPO_3H^{3/2-}$ and $\equiv AlOPO_3H_2^{1/2-}$. Under the high ionic strength conditions (0.01 M NaCl), the PO_4 adsorption data was modeled using the two inner-sphere complexes: $\equiv AlOPO_3^{5/2-}$ and $\equiv AlOPO_3H_2^{1/2-}$. Arsenate adsorption data at both ionic strengths were modeled using the $\equiv AlOAsO_3^{5/2-}$ and $\equiv AlOAsO_3H_2^{1/2-}$ inner-sphere surface complexes.

Sulfate adsorption data at both ionic strength conditions were described using the outer-sphere $\equiv AlOH_2^{1/2+} \cdots SO_4^{2-}$ species. The adsorption of kG by goethite surfaces in both the 0.001 M and 0.01 M NaCl systems was best described by assuming that kG forms both monodentate-mononuclear and monodentate-binuclear inner-sphere surface complexes; $\equiv Fe_kG^{1/2-}$ and $\equiv Fe_2kGH_{.1}^1$. The chemical models and associated intrinsic equilibrium constants developed from the single ligand systems were employed to predict ligand retention in the binary systems. In general, predicted adsorption behavior did not adequately predict the experimental adsorption data in the gibbsite and kaolinite systems. This finding suggests that the inferred adsorption mechanisms may not have been the correct mechanisms.

It is evident from the adsorption envelopes that kG adsorbed to gibbsite, goethite, and kaolinite via inner-sphere mechanisms. Addition; albeit indirect evidence that kG

retention occurs through inner-sphere mechanisms is indicated by the surface complexation modeling results. Therefore, it is concluded that kG may potentially impact the phytoavailability of PO_4 and other specifically-retained ligands in the rhizosphere.

V. Conclusions

- 2-Ketogluconate forms inner-sphere complexes on gibbsite, kaolinite, and goethite surfaces.
- 2-Ketogluconate competes with PO_4 and AsO_4 for surface functional groups on gibbsite, kaolinite, and goethite.
- The adsorption of kG by gibbsite and kaolinite surfaces is described by the formation of the monodentate-mononuclear inner-sphere complexes: $\equiv\text{AlkG}^{1/2-}$ and $\equiv\text{AlkGH}_1^{3/2-}$.
- The adsorption of kG by goethite surfaces is described by the formation of monodentate-mononuclear and bidentate-binuclear inner-sphere surface complexes: $\equiv\text{FekG}^{1/2-}$ and $\equiv\text{Fe}_2\text{kGH}_1^{1-}$.
- Chemical models describing the specific retention of ligands (kG, PO_4 , and AsO_4) in single-adsorbate systems were not universally applicable.
- Different chemical models may better describe the adsorption data in the systems with relatively high WSOS/DF values, and when the FITEQL program did not converge.

References

- ✓Antelo, J., M. Avena, S. Fiol, R. López, and F. Arce. 2005. Effects of pH and ionic strength on the adsorption of phosphate and arsenate at the goethite–water interface. *J. Colloid Interface Sci.* 285:476-486.
- ✓Blake, R.E., and L.M. Walter. 1996. Effect of organic acids on the dissolution of orthoclase at 80°C and pH 6. *Chem. Geol.* 132:91-102.
- Bloom, P.R., and R.M. Weaver. 1982. Effect of the removal of reactive surface material on the solubility of synthetic gibbsite, *Clays Clay Miner.* 30:281-286.
- ✓Chen, R., B.W. Smith, J.D., Winefordner, M.S. Tu, G. Kertulis, and L.Q. Ma. 2004. Arsenic speciation in Chinese brake fern by ion-pair high-performance liquid chromatography-induced coupled plasma mass spectroscopy. *Anal. Chim. acta.* 504:199-207.
- ✓Dietzel, M., and G. Böhme. 2005. The dissolution rates of gibbsite in the presence of chloride, nitrate, silica, sulfate, and citrate in open and closed systems at 20°C. *Geochim. Cosmochim. Acta.* 69:1199-1211.
- Duff, R.B., and D.M. Webley. 1959. 2-Ketogluconic acid as a natural chelator produced by soil bacteria. *Chem. Ind. (London)* 1959: 1376-1377.
- Duff, R.B., D.M. Webley., and R.O. Scott. 1963. Solubilization of minerals and related material by 2-ketogluconic acid producing bacteria. *Soil Sci.* 95:105-114.
- van Duin, A.C.T., and S.R. Larter. 2001. Molecular investigation into the adsorption of organic compounds on kaolinite surfaces. *Org. Geochem.* 32:71-76.

- ✓ van Duin, A. C. T., and Steve R. Larter. 2001. Molecular dynamics investigation into the adsorption of organic compounds on kaolinite surfaces. *Organic Geochem.* 32:143-150.
- Essington, M.E. The complexity of aqueous complexations in the case of aluminum- and iron (III)- citrate. In A. Violante, P.M., Huang, and G.M. Gadd (eds.). *Biophysicochemical processes of heavy metals and metalloids in soil environments.* IUPAC, Research Triangle Park, NC. (in press).
- ✓ Essington, M.E. 2003. *Soil and water chemistry: An integrative approach.* CRC Press, Boca Raton, FL.
- ✓ Essington, M.E., J.B. Nelson, and W.L. Holden. 2005. Gibbsite and goethite solubility: the influence of 2-ketogluconate and citrate. *Soil Sci. Soc. Am. J.* 69:996-1008.
- ✓ Evanko, R. C., and A. D. Dzombak. 1998. Influence of structural features on sorption of NOM-analogue organic acids to goethite. *Environ. Sci. Technol.* 32: 2846-2855.
- ✓ Evanko, R. C., and A. D. Dzombak. 1999. Surface complexation modeling of organic acid sorption to goethite. *J. Colloid Interface Sci.* 214:189-206.
- ✓ Filius, D. J., T. Hiemstra, and H.W. Van Riemsdijk. 1997. Adsorption of small weak Organic acids on goethite: Modeling of mechanisms. *J. Colloid Interface Sci.* 195:368-380.

- ✓ Filius, J.D., J.C.L. Meeussen, and W.H. van Riemsdijk. 2001. Modeling the binding of Benzenecarboxylates by goethite: The ligand and charge distribution model. *J. Colloid Interface Sci.* 244:31-42
- ✓ Gao, Y, and A. Mucci. 2002. Acid base reactions, phosphate and arsenate complexation, and their competitive adsorption at the surface of goethite in 0.7 M NaCl solution. *Geochim. Cosmochim. Acta.* 14:2361-1378.
- ✓ Goldberg, S. 2005. Inconsistency in the triple layer model description of ionic strength dependent boron adsorption. *J. Colloid Interface Sci.* 285:509-517.
- Goldberg, S. 1992. Use of surface complexation models in soil chemical systems. p.233-329. In D.L. Sparks. *Advances in Agronomy.* Academic Press, Inc. San Diego.
- ✓ Goldberg, S., and G. Sposito. 1984. A chemical model of phosphate adsorption by soils: I. Reference oxide minerals. *Soil Sci. Am. J.* 48:772-778.
- Halder, A.K., and P.K. Chakrabarty. 1993. Solubilization of inorganic phosphate by *Rhizobium*. *Folia Microbiol.* 38:325-330.
- ✓ Hayes, K.F., and J.O. Leckie. 1987. Modeling ionic strength effects on cation adsorption at hydrous oxide/solution interfaces. *J. Colloid Interface Sci.* 115:564-572.
- ✓ Hayes, K.F., C. Papelis, and J.O. Leckie. 1988. Modeling ionic strength effects on anion adsorption at hydrous oxide/solution interfaces. *J. Colloid Interface Sci.* 125:717-726.

- Haynes, R.J., and M.S. Mokolobate. 2001. Amelioration of Al toxicity and P deficiency in acid soils by additions of organic residues: a critical review of the phenomenon and the mechanisms involved. *Nutrient Cycling Agroecosystems*. 59:47-63.
- He, L.M., L.W. Zelazny, V.C. Baligar, K.D. Rithney, and D.C. Martens. 1997. Ionic strength effects on sulfate adsorption on γ -alumina and kaolinite: triple-layer model. *Soil Sci. Am. J.* 61:784-793.
- He, Z., and J. Zhu. 1998. Microbial utilization and transformation of phosphate adsorbed by variable charged minerals. *Soil Biol. Biochem.* 30:17-923.
- Hees, P.A.W. van, U.S. Lundström, and R. Geisler. 1998. Low molecular weight organic acids and their Al-complexes in soil solution- composition, distribution and seasonal variation in three podzolized soils. *Geoderma*. 94:173-200.
- Hees, P.A.W. van. S.I. Vinogradoff, A.C. Edwards, D.L. Godbold, and D.L. Jones. 2003. Low molecular weight organic acid adsorption in forest soils: Effects on soil solution concentrations and biodegradation rates. *Soil Biol. Biochem.* 35:1015-1026.
- Hees, P.A.W. van. D.L. Jones, G. Jentschke, and D.L. Godbold. 2004. Organic acid concentrations in soil solution: effects of young coniferous trees and ectomycorrhizal fungi. *Soil Biol. Biochem.* 37:771-776.

- Herbelin, A.L., and J.C. Westall. 1999. A computer program for determination of chemical equilibrium constants from experimental data. Version 4.0. Report 99-01, Dept. of Chem., Oregon State Univ., Corvallis, OR.
- Hiemstra, T., H. Young, and W.H. Van Riemsdijk. 1999. Interfacial charging phenomena of alumina (hydr)oxides. *Langmuir*. 15:5942-5955.
- ✓ Hiemstra, T., and W.H. Van Riemsdijk. 1999. Surface structural ion adsorption modeling of competitive binding of oxyanions by metal (hydr)oxides. *J. Colloid Interface Sci.* 210:182-193.
- ✓ Horányi, G. 2002. Specific adsorption of simple organic acids on metal (hydr)oxides: A radiotracer approach. *J. Colloid Interface Sci.* 254:214-221.
- Hu, H. Q., J. Z. He, X. Y. Li, and F. Liu. 2001. Effect of several organic acids on phosphate adsorption by variable charge soils of central China. *Environ. Int.* 26:353-358.
- Huang, Q., Z. Zhao, and W. Chen. 2003. Effects of several low-molecular weight organic acids and phosphate on the adsorption of acid phosphatase by soil colloids and minerals. *Chemosphere*. 52:571-579.
- ✓ Ikhsan, J., J.D. Wells, B.B. Johnson, M.J. Angove. 2005. Surface complexation modeling of the sorption of Zn(II) by montmorillonite. *Colloids and Surfaces A*. 252:33-41

- Ioannou, A., and A. Dimirkou. 1997. Phosphate adsorption on hematite, kaolinite, and kaolinite–hematite (k–h) systems As described by a constant capacitance model. *J. Colloid Interface Sci.* 192:119-128.
- ✓ Jara, A.A., A. Violante, M. Pigna, and M. de la Luz Mora. 2006. Mutual interactions of sulfate, oxalate, citrate and phosphate on synthetic and natural allophanes. *Soil Sci. Am. J.* 70:337-346.
- Jiang, W., S. Zhang, X. Shan, M. Feng, Y. Zhu, and R.G. McLaren. 2005. Adsorption of arsenate on soils. Part 2. Modeling the relationship between adsorption capacity and soil physiochemical properties using 16 Chinese soils. *Environ. Pollut.* 138:285-289.
- ✓ Jones, D.L. 1998. Organic acids in the rhizosphere- A critical review. *Plant Soil.* 205:25-44.
- Jones, D.L., P.G. Dennis, A.G. Owen, and P.A.W. van Hees. 2002. Organic acid behavior in soils – Misconceptions and knowledge gaps. *Plant Soil.* 248:31-41.
- Klassen, R., S. Bringer-Meyer, and H. Sahm. 1992. Incapability of gluconobater to produce tartaric acid. *Biotechnol Bioeng.* 40:183-186.
- Kpombrekou-A, K., and M. A. Tabatabai. 2003. Effect of low-molecular weight organic acids on phosphorus release and phytoavailability of phosphorus in phosphate rocks added to soils. *Agric. Ecosystems & Environ.* 100:275-284.

- Kwong, K.F., and P.M. Huang. 1979. The relative influence of low-molecular-weight complexing organic acids on the hydrolysis and precipitation of aluminum. *Soil Sci.* 128:337-342.
- ✓ Lackovic, K., B. B. Johnson, J. M. Angrove, and D. J. Wells. 2003. Modeling the adsorption of citric acid onto Mulloorina illite and related clay minerals. *J. Colloid Interface Sci.* 267:49-59.
- ✓ Lackovic, K., J.D. Wells, B.B. Johnson, and M.J. Angove. 2004. Modeling the adsorption of Cd(II) onto kaolinite and Mulloorina illite in the presence of citric acid. *J. Colloid Interface Sci.* 270:86-93.
- ✓ Lenoble, V. O. Bouras, V. Deluchat, B. Serpaud, and J.-C. Bollinger. 2002. Arsenic adsorption onto pillared clays and iron oxides. *J. Colloid Interface Sci.* 255:52-58.
- ✓ Lützenkircken, J. 1999. The constant capacitance model and variable ionic strength: An evaluation of possible application and applicability. *J. Colloid Interface Sci.* 217:8-18.
- Martell, A.E., R.M. Smith, and R.J. Motekaitis. 2004. NIT critically selected stability constants of metal complexes. NIST Standard Reference Database 46, Version 8.0. NIST, Gaithersburg, MD.
- Moghimi, A., and M.E. Tate. 1978. Characterization of rhizosphere products especially 2-ketogluconic acid. *Soil Biol. Biochem.* 10:283-287.

Moghimi, A., M.E. Tate. 1978. Does 2-ketogluconate chelate calcium in the pH range 2.4 to 6.4? *Soil Biol. Biochem.* 10:289-292.

Neijssel, O.M., and D.W. Tempest. 1975. Production of gluconic acid and 2-ketogluconic acid by *Klebsiella aerogenes* NCTC 418. *Arch. Microbiol.*, 105:183-185.

Nelson J.B., and M.E. Essington. 2005. The association constants of H^+ and Ca^{2+} with 2-keto-D-gluconate in aqueous solutions. *J. Solution Chem.* 34:789-800.

Van Olphen, H., and J.J. Fripiat. 1979. Data handbook for clay minerals and other non-metallic minerals. Pergamon Press, Oxford England.

Quirk, J.P. and R.S. Murray. 1999. Appraisal of the ethylene glycol monoethyl ether method for measuring hydratable surface area of clays and soils. *Soil Sci. Soc. Am. J.* 63:839-849.

✓Rahnemaie, R., T. Hiemstra, and W.H. van Riemsdijk. 2005. A new surface structural approach to ion adsorption: Tracing the location of electrolyte ions. *J. Colloid Interface Sci.* in press.

✓Rahnemaie, R., T. Hiemstra, and W.H. van Riemsdijk. 2005. Inner- and outer-sphere complexation of ions at the goethite-water interface. *J. Colloid Interface Sci.* in press.

- Rosenqvist, J., K. Axe, S. Sjöberg, and P. Persson. 2003. Adsorption of dicarboxylates on nano-sized gibbsite particles: effects of ligand structure on bonding mechanisms. *Colloids and Surfaces A*. 220:91-104.
- ✓ Sakar, D., M.E. Essington, and K.C. Misra. 2000. Adsorption of mercury(II) by kaolinite. *Soil Sci. Soc. Am. J.* 64:1968-1975.
- Schwab, A.P., Y. He, and M.K. Banks. 2005. The influence of organic ligands on the retention of lead in soil. *Chemosphere*. 62:255-264.
- ✓ Srivastava, P. B. Singh, and M. Angove. 2005. Competitive adsorption behavior of heavy metals on kaolinite. *J. Colloid Interface Sci.* 290:28-38.
- ✓ Strobel, B.J. 2000. Influence of vegetation on low-molecular-weight carboxylic acids in soil solution: a review. *Geoderma*. 99:169-198.
- Sulyok, M., M. Miro, G. Stingeder, and G. Koellensperger. 2005. The potential of flow-through microdialysis for probing low-molecular weight organic anions in rhizosphere soil solution. *Anal. Chim. Acta.* 546:1-10.
- ✓ Tadanier, C.J., and M.J. Eick. 2002. Formulating the charge-distribution multisite surface complexation model using FITEQL. *Soil Sci. Soc. Am. J.* 66:1505-1517.
- ✓ Violante, A., and M. Pigna. 2002. Competitive sorption of arsenate and phosphate on different clay minerals and soils. *Soil Sci. Soc. Am. J.* 66:1788-1796.

- ✓ Wang, X., Q. Li, H. Hu, T. Zhang, and Y. Zhou. 2005. Dissolution of kaolinite induced by citric, oxalic, and malic acids. *J. Colloid Interface Sci.* 290:481-488.
- Webley, D.M., and R.B. Duff. 1965. The incidence, in soils and other habitats of microorganisms producing 2-ketogluconic acid. *Plant Soil.* 22:307-313.
- Weerasooriya, R., H.J. Tobschall, H.K.D.K. Wijesekara, E.K.I.A.U.K. Arachchige, and K.A.S. Pathirathne. 2003. On the mechanistic modeling of As(III) adsorption on gibbsite. *Chemosphere.* 51:1001-1013.
- Weerasooriya, R., H.J. Tobschall, H.K.D.K. Wijesekara, and A. Bandara. 2003. Macroscopic and vibration spectroscopic evidence for specific bonding of arsenate on gibbsite. *Chemosphere.* 55:1259-1270.
- Westall, J.C. 1980. *Am. Chem. Soc. Adv. Chem. Ser.* 189:33.
- Wijnja, H. and C.P. Schulthess. 2000. Interaction of carbonate and organic anions with sulfate and selenate adsorption on an aluminum oxide. *Soil Sci. Soc. Am. J.* 64:898-908.
- Wijnja, H., and C.P. Schulthess. 2002. Effect of carbonate on the adsorption of selenate and sulfate on goethite. *Soil Sci. Soc. Am. J.* 66:1190-1197.

VITA

Robert Maxwell Anderson III was born on January 7th, 1980 in Norfolk Virginia to Jane Jones Anderson and Robert Maxwell Anderson Jr. Rob grew up in Charleston, South Carolina, and received his high school diploma from St. Andrews High School in 1998. Rob attended Clemson University in Clemson SC, where he received his Bachelor of Science in Crop and Soil Environmental Science in May of 2003. He then went on to attend the University of Tennessee in Knoxville, TN, to receive a Master of Science in Soil and Environmental Science in May of 2006.

4583 4347 49

07/20/06

HFB

